Continuous Membrane Microbioreactor for Development of Integrated Pectin Modification and Separation Processes

Zainal Alam, Muhd Nazrul Hisham Bin; Gernaey, Krist V.

Publication date:
2011

Document Version
Early version, also known as pre-print

Technical University of Denmark

Muhd. Nazrul Hisham Zainal Alam

Continuous Membrane Microbioreactor for Development of Integrated Pectin Modification and Separation Processes

DTU Chemical Engineering
Department of Chemical and Biochemical Engineering

PhD Thesis, September 2010

Muhd. Nazrul Hisham Zainal Alam

Continuous Membrane Microbioreactor for Development of Integrated Pectin Modification and Separation Processes

PhD Thesis, September 2010

Continuous Membrane Microbioreactor for Development of Integrated Pectin Modification and Separation Processes

This thesis was prepared by
Muhd. Nazrul Hisham Zainal Alam

Supervisors

Krist V. Gernaey	Center for Process Engineering and Technology (PROCESS), Department of Chemical and Biochemical Engineering, DTU
Anne Meyer	Center for BioprocessEngineering (BioEng), Department of Chemical and Biochemical Engineering, DTU
Gunnar Jonsson	Computer Aided Process-Product Engineering Center (CAPEC), Department of Chemical and Biochemical Engineering, DTU

Center for Process Engineering and Technology (PROCESS)
Department of Chemical and Biochemical Engineering
Technical University of Denmark
Søltofts Plads, building 229
DK-2800 Kgs. Lyngby
Denmark

www.kt.dtu.dk
Tel: (+45) 45 25 35 00
Fax: (+45) 45 93 29 06
Email: kt@kt.dtu.dk

Release date: Date published
Category: (1) Public
Edition: First
Comments: This thesis is submitted in fulfillment of the requirements for the award of the degree of PhD in Chemical Engineering at the Technical University of Denmark.

Preface

This thesis is submitted as partial fulfillment of the requirements for Doctarate (PhD) degree at Technical University of Denmark (DTU - Denmark Tekniske Universitet), Kgs. Lyngby, Denmark. The PhD project started on the 1st of July 2007 and was carried out at Institute of Chemical and Biochemical Engineering (KT), DTU. It was funded by Universiti Teknologi Malaysia (UTM) and Malaysia Ministry of High Education. Associate Professor Krist Victor Gernaey was the principal supervisor for the project with Professor Anne Boye Strunge Meyer and Associate Professor Gunnar Eigil Jonsson as co-supervisors.

Core research activities - i.e. fabrication of membrane microbioreactor prototype, development of microbioreactor *on-line* measurements and process control apparatus, etc. - were conducted in microbioreactor lab at Center for Process Engineering and Technology (PROCESS), KT while analytical works - i.e. *off-line* analysis via micro titer plate reader and High Performance Liquid Chromatography (HPLC) of samples – were done at Center for Bioprocess Engineering (BioEng), KT.

It was truly a wonderful and rewarding experience working in this department and my staying here has been a tremendous educational value for me. I would like to take this opportunity to express my grateful thanks to those who has supported, inspired and contributed to the completion of this project. First, I am totally in debt and utmost grateful to all my supervisors, Krist, Anne and Gunnar for following this project from the very beginning to its completion. Thank you for your immense support and significant contributions to my needs during the long hours.

Secondly, I would also like to record my thanks to my parents for believing me and for their continuity support in these few years - without whom, I would not be at this point now. Also, special thanks to my fiancé, Raudhah Othman for her understanding, love and for always be there whenever needed be.

I had also received numerous helps and support from my fellow colleagues and friends from *PROCESS*, *BioEng*, *CAPEC* and *CHEC* group especially John, Mads Pedersen, Anis, Manuel, Daniel, Pär, Matthias, Nanna, Stuart, Albert, Lise, Anna, Michael, Marcel, Kamaruddin, Fazli, Nizam, Dayang, and Pavel for their assistances, support and sharing of their knowledge during this endeavor. For this, I am utmost grateful.

Last but not least, I would like to express my appreciation and thanks to staff in *KT workshop* – Ivan, Jens, Soren, Kristofer, Lars, Henning and Michael and also those from *DTU FOTONIK* – Karsten, Anders, Kamou, and Kirsten for all your supports.

Thanks all for all the jokes, stimulating discussions and for always make me feel welcome. I truly enjoyed our collaboration and hoped to continue working with you guys in the future.

Muhd Nazrul Hisham Zainal Alam, September 2010

Abstract

Microbioreactor technology has recently made significant progress, and has also demonstrated significant advantages for assessing biological processes over other low cost micro-scale devices such as microtiter plates, microtubes, etc. Microbioreactors (i.e. typical volume < 1 mL) are usually integrated with on-line sensors and actuators, and can often be designed such that they can mimic the events typically taking place in a bench-scale reactor system. In this work, a continuous membrane microbioreactor system was developed to facilitate integrated pectin modification and separation processes. The increasing need for high-throughput experimentation in novel 'biorefining' type of processes (e.g. enzyme-catalyzed degradation of complex biopolymers for obtainment of value-added oligosaccharides) justified the selection of the micro-scale reactor.

During the development of the membrane microbioreactor, relevant membrane microbioreactor design parameters i.e. reactor operating feature and size, reactor mechanics (materials, fabrication, membrane separation design, and mixing), reactor fluidics (connections, pumping mechanisms, and feeding strategy), process control of physical parameters (temperature, pH, and pressure) and detection methods for measuring the product concentration were carefully evaluated and implemented. Subsequently, hypotheses formulated for the thesis were tested one by one.

The membrane microbioreactor prototype developed here was realized as a loop reactor system to operate in *crossflow* filtration mode. It was also designed to work under bubble-free conditions with constant volume ($dV_r/dt = 0$). The reactor has outer dimensions of 35 mm (length) x 20 mm (width) x 8 mm (thickness) with an internal working volume of approximately 200 µL. A regenerated cellulose membrane was sandwiched between alternate poly(methylmethacrylate) (PMMA)-polydimethylsiloxane (PDMS) layers achieving a *clamp and play* reactor configuration. Mixing was accomplished with a magnetically actuated stir-bar combined with a high velocity recirculation flow in the loop delivered via a micro-gear pump. The quality of mixing was checked with a simple tracer test by using a fluorescence dye. Complete mixing (i.e. indicated by uniform colour spread of the fluorescent dye) at a system residence time of 1 hour was attained in about 3 minutes 15 seconds. Fluidic connections were established by using standard chromatography fittings, thus providing a *plug and play* fluidic connection design. The reactor has the capacity to operate either in continuous or semi-continuous (i.e. alternate substrate-buffer feeding strategy) mode, and the necessary pressure for the separation to occur was achieved via the feeding pump.

In addition, the prototype was equipped with an on/off temperature control loop where embedded resistance wires were used as the heating element. It was shown that integrated resistance wires coupled to a simple on/off controller result in accurate control of the temperature of the reactor ($\pm$ 0.1 ^{o}C of the set point value) and provide a good disturbance rejection capability (corrective action for a sudden temperature drop of 2.5 ^{o}C at an operating temperature of 50 ^{o}C takes less than 30 s). A gaseous pH control strategy was also evaluated where the dosing of CO_2 gas and an NH_3 (20 000 ppm) - N_2 gas mixture was used to respectively decrease and increase the pH of the reactor content.

Although the performance of the gaseous pH control method established was satisfactorily (i.e. accuracy of $\pm$ 0.1 pH units of the pH set point was achievable), implementation was impeded due to the limited dynamic measurement range of the pH optodes used (i.e. rather insensitive in the low pH range of 4 to 5). In the current membrane microbioreactor design, pH is therefore controlled by adding buffer to the medium.

The functionality of the membrane microbioreactor prototype was further evaluated in biologically relevant experimental work. Here, pectin lyase was employed to catalyze the sugar beet pectin (i.e. 60% methylated, 19% acetylated) degradation process. Results attained demonstrated the workability of the prototype for an extended enzymatic reaction – evaluated under different experimental conditions i.e. molecular weight cut-off (MWCO), reactor residence time, etc. – and showed its usefulness in obtaining real-time process data of the enzyme-catalyzed degradation of pectin. In the benchmarking step, it was shown that reaction conditions applied in the microbioreactor prototype can also be reproduced in the bench scale reactor system – evident by comparable process data (i.e. kinetic profiles) obtained in both scales.

The thesis is concluded with a brief discussion on the advantages and drawbacks of the continuous membrane microbioreactor system developed in this work. Future recommendations on how to further improve the reactor design are included as well, such that the technology can be pushed to meet satisfactorily industrial standards.

Dansk Resumé

Mikrobioreaktor teknologi er for nyligt blevet signifikant forbedret og har demonstreret signifikante fordele ved bedømmelse af biologiske processer i forhold til andre billige mikroskala apparater såsom mikrotiterplader, mikrotubes etc. Mikrobioreaktorer (typisk med volumen < 1 mL) er oftest integreret med online sensorer og aktuatorer og kan ofte designes sådan, at de kan efterligne de betingelser der findes i typiske laboratorie-reaktorsystemer. I dette arbejde er et kontinuert membran-mikrobioreaktor system blevet udviklet for at muliggøre enzymatisk nedbrydning af pektin integreret med separation af oligosaccharide rne (produktet). Det øgede behov for high-throughput eksperimenter med nye processer til raffinering af biologisk materiale (f.eks. enzymkatalyseret nedbrydning af komplekse biopolymerer til oligosaccharider) berettigede valget af en mikroskala reaktor.

Relevante membran-mikroreaktor designparametre, dvs. operationsfeature- og størrelse, reaktormekanik (materialer, fremstilling, membran separationsdesign og opblanding), fluidmekanik (forbindelser, pumpemekanismer, og fødestrategi), procesregulering af fysiske parameter (temperatur, pH og tryk) og detektionsmetoder til måling af produktkoncentrationen blev evalueret og implementeret under udviklingen af membran-mikrobioreaktoren. Hypoteser formuleret for denne afhandling blev derefter testet en efter en.

En membran-mikrobioreaktor prototype blev udviklet som et loop reaktorsystem med crossflow filtrering. Det blev designet til operation uden headspace, dvs med konstant volumen ($dV_r/dt = 0$). De ydre dimensioner af reaktoren er 34 mm (længde) x 20 mm (vidde) x 8 mm (tykkelse) med et indvendigt arbejdsvolumen på omkring 200 µL. En regenereret cellulose membran blev placeret mellem skiftevis poly(methylmethacrylate) (PMMA) og polydimethylsiloxane (PDMS) lag hvilket resulterede i en 'clamp and play' reaktorkonfiguration. Opblanding blev opnået vha. magnetiske omrørere kombineret med en høj hastighed af strømningen i recirkulationskanalen. Kvaliteten af opblandingen blev kontrolleret med en simpel spor-test vha et fluorescerende farvestof. Fuldstændig opblanding (indikeret ved en uniform spredning af det fluorescerende farvestof) blev opnået på omkring 3 minutter og 15 sekunder ved en opholdstid i reaktoren på 1 time. Brug af standard kromatografi-sammenkoblinger resulterede i et 'plug and play' sammenkoblingsdesign for væskestrømmene. Reaktoren kan operere enten kontinuert eller semi-kontinuert (dvs. med skiftevis substrat-buffer føde). Fødepumpen leverede det nødvendige tryk for membranseparationen.

Temperaturen blev kontrolleret vha. en til/fra reguleringssløjfe, hvor indstøbte metaltråde blev brugt som varmelement. Det blev vist at integrerede metaltråde kombineret med simpel til/fra regulering gav en nøjagtig regulering af temperaturen i reaktoren ($\pm$ 0,1 ^{o}C i forhold til reference værdien) og gav en tilfredsstillende afvisning af forstyrrelser (korrigerende handlinger ved et pludseligt fald i temperaturen på 2,5 ^{o}C ved en temperatur på 50 ^{o}C tog mindre en 30 s). Regulering af pH baseret på tilsætning af gas blev også evalueret. CO_2 og en NH_3 (20 000 ppm) – N_2 gas blanding blev tilsat for henholdsvist at sænke eller øge pH i reaktoren. Selvom den gas-baserede pH kontrol virkede tilfredsstillende (dvs. med en nøjagtighed på $\pm$ 0,1 pH enheder i forhold til reference

værdien), blev implementeringen hæmmet af det begrænsede dynamiske måleinterval af pH optoderne (optoderne var forholdsvist ufølsomme i pH intervallet mellem 4 og 5). I det nuværende reaktordesign bliver pH derfor kontrolleret ved tilsætning af buffer til mediet.

Funktionaliteten af membran-mikrobioreaktor prototypen bliver endvidere evalueret under biologisk relevant eksperimentelt arbejde. Pektin lyase blev brugt til at katalysere nedbrydningen af sukkerroe pektin (dvs. 60 % metyleret, 19 % acetyleret). Resultaterne demonstrerede brugbarheden af prototypen til en udvidet enzymatisk reaktion – evalueret under forskellige eksperimentelle betingelser som f.eks. afskæringsværdien for molekylevægten, opholdstiden i reaktoren osv. – og viste sig evnet til at opnå proces-data fra den enzymkatalyserede nedbrydning af pektin i realtid. Under den udførte benchmarking blev det vist at reaktionsbetingelserne i mikrobioreaktor prototypen kan reproduceres i et reaktorsystem i laboratorie-skala, hvilket fremgik af sammenlignelige procesdata (dvs. kinetiske profiler) opnået i begge skalaer.

Afhandlingen afsluttes med en kort diskussion om fordelene og ulemperne ved det kontinuerte membran-bioreaktor design udviklet i dette arbejde. Derudover gives anbefalinger for fremtidige forbedringer af reaktordesignet således at teknologien kan tilfredsstille industrielle standarder.

Contents

List of Figures

List of Tables

Nomenclature

Abbreviations:

NIR	near infra-red
HGA	Homogalacturonan
RG-I	rhamnogalacturonan I
RG-II	rhamnogalacturonan II
XGA	Xylogalacturonans
Rha	Rhamnose
GalA	D-galacturonic acid
PG	Polygalacturonase
PME	Pectinmethylesterase
PL	pectin lyase
PS	Polysulfone
UF	Ultrafiltration
MWCO	molecular weight cut-off
DM	degree of methylation
PE	pectin esterase
RC	regenerated cellulose
kDa	kiloDalton
PMMA	poly(methylmethacrylate)
PDMS	Polydimethylsiloxane
PEEK	Polyetheretherketone
PC	Polycarbonate
RTD	resistance temperature detector
optodes	optical sensors based on fluorescence sensor spots
ISFET	ion sensitive field effect transistor
OD	optical density
UV	ultra-violet
MBR	Microbioreactor
N/A	data not available
CNC	computer-numerical-controlled
PFA	Perfluoroalkoxy
NH_3	Ammonia
CO_2	carbon dioxide
ppm	parts per million
LED	light emitting diode
HCL	hydrochloric acid
NaOH	sodium hydroxide
H_2CO_3	carbonic acid
SO_2	sulfur dioxide
HCO_3^-	Bicarbonate
CO_3^{2-}	Carbonate

Symbols:

v_m	maximum reaction rates ($g.L^{-1}.hr^{-1}$)
K_m	Michaelis-Menten constant ($g.L^{-1}$)
τ	residence time (hr)
mL	Milliliter
µL	Microliter
nL	Nanoliter
S/V	surface area to working volume ratio
dV_r/dt	volume change over time ($L.hr^{-1}$)
F_{in}	volumetric feed inflow ($L.hr^{-1}$)
P_{out}/F_{out}	volumetric permeate outflow ($L.hr^{-1}$)
Re/N_{Re}	Reynolds number
U	average flow speed ($m.s^{-1}$)
D	characteristic dimensions (m)
ν	kinematic viscosity of fluid ($m^2.s^{-1}$)
Ω	stirrer bar rotational speed (rps)
ΔP	pressure drop (Pa)
η	liquid viscosity (Pa.s)
L	tube length (m)
Q	volumetric flow rate ($m^3.s^{-1}$)
R	radius of the capillary (m)
[E]	enzyme concentration (g/L)
[S]	substrate concentration (g/L)
Pt	platinum element
H/D	height to diameter
t_{90}	response time less than 90 s
µm	Micrometer
λ	specific chosen wavelength
I_o	excited light
l_{opt}	optical path length (cm)
I_t	transmitted (or reflected) light
A	absorbance measured
ε	extinction coefficient ($M^{-1}.cm^{-1}$)
C	concentration of measured sample (M)
T_{sp}	desired temperature set point value (^oC or K)
T_m	measured temperature value (^oC or K)
m_r	mass of water in the reactor chamber (kg)
c_p	specific heat capacity of water (4186 $J.kg^{-1}.K^{-1}$)
T	Corresponding temperature (K)
Q_{heat}	heat generated by applying a voltage to the resistance wires (W)
Q_w	heat absorbed due to water evaporation (W)
Q_f	heat transfer due to the inflow of water (W)
Q_{loss}	heat loss to the surroundings by convection (W)
V	voltage (Volt)
I	current (Ampere)
J_w	rate of mass loss due to the water evaporation through the membrane ($kg.s^{-1}$)
L_v	latent heat of water vaporization ($kJ.kg^{-1}$)
ρ_w	water density (1000 $kg.m^{-3}$)
θ_w	water evaporation rate in microbioreactors ($\mu L.hr^{-1}$)

T_f	feed temperature (^oC)
T_r	reactor temperature (^oC)
α_i	heat transfer coefficient ($W.m^{-2}.K^{-1}$)
A_i	heat transfer area (m^2)
$T_{amb,i}$	temperature of the surroundings (K)
P	power input by the heater (W)
E	energy generated (or dissipated) *(Joule)*
T	time (s or min or hr)
$\dot{m}_f$	feed flow rate ($\mu L.hr^{-1}$)
PL	pulse length (s)
H^+	hydrogen protons or ions
OH^-	hydroxyl ions
pH_{sp}	desired pH set point value
pH_m	measured pH value
pKa	acid dissociation constant
NH_4^+	ammonium ions
µg	Microgram
A_m	membrane area (m^2 or mm^2)
J	flux to the membrane on the retentate side ($L.hr^{-1}$)
J_p	permeate flux ($L.hr^{-1}$)
D	Diffusivity
x	distance between a point of the bulk solution and the membrane (m)
C_p	solute concentration in the permeate (g/L)
C_M	solute concentration on the surface of the membrane (g/L)

List of Publications

I Application of microbioreactors in fermentation process development: a review. (2009). Schäpper, D., **Zainal Alam, M. N. H.**, Szita, N., Lantz, A. E., and Gernaey, K. V. *Journal of Analytical and Bioanalytical Chemistry*. **395**: 679-695.

II Embedded resistance wire as heating element for temperature control in microbioreactors. (2010). **Zainal Alam, M. N. H.**, Schäpper, D., and Gernaey, K. V. *Journal of Micromechanics and Microengineering*. DOI: 10.1088/0960-1317/20/5 /055014.

III Establishment of a gaseous pH control concept in microbioreactors. **Zainal Alam, M. N. H.**, Schäpper, D., Bolic, A., and Gernaey, K. V. Manuscript in preparation and expected submission to *Journal of Micromechanics and Microengineering* in 2010.

IV A Continuous Membrane Microbioreactor system for Development of Integrated Pectin Modification and Separation Processes. **Zainal Alam, M. N. H.**, Pinelo, M., Samantha, K., Jonsson, G., Meyer, A., and Gernaey, K. V. Submitted to *Chemical Engineering Journal* in Mac 2010.

V Assessing enzymatic modification of pectin by application of a continuous membrane microbioreactor. **Zainal Alam, M. N. H.**, Pinelo, M., Arnuos, A., Jonsson, G., Meyer, S. A., and Gernaey, K. V. (2010). Submitted to *Journal of Biotechnology and Bioengineering* in August 2010.

CHAPTER 1

Introduction

CHAPTER 1

Introduction

1.1 General Introduction

At present, many laboratory studies on optimization of enzyme-based production processes or kinetic studies (e.g. determination of maximum reaction rates, v_m, and Michaelis-constant, K_m, product yield, etc.) and screening of new enzyme processes are done with the use of low cost micro-scale devices such as micro-tubes (1-1.5 mL) or microtiter plates (microwell format reactor with a typical working volume ranging from 50 to 1000 µL). Both require relatively low volumes of enzymes and substrates (normally µg or µL-nL range) [1-3]. Such small working volumes thus offer a significant cost reduction – relative to bench-scale bioreactors – in terms of obtaining sufficient enzyme and specific substrate stocks for assessing novel enzyme processes. Additionally, they are also easy to handle and can facilitate parallel experimentation under a range of relevant bioprocess conditions. This, as a result, not only accelerates throughput (number of experiments performed in one single run) but also keeps the running cost per experiment low [4-6].

Compared to bench-scale bioreactors, the attainable level of control and the flexibility in achievable operation modes of low cost micro-scale devices like micro-tubes and microtiter plates are rather limited. For example, in bench-scale bioreactors, reaction conditions such as temperature, pH, dissolved oxygen concentration (for reactions that consume oxygen as substrate), and pressure can often be tightly controlled. In micro-tubes and microtiter plates, temperature and pH (buffered) are typically the only controlled variables [5]. Secondly, the operating mode for micro-tubes and microtiter plates are limited to batch mode operation only. This is because control of liquid flow to or from each well or tube is rather difficult to install under shaking conditions [5-6]. Evaporation of the content of the well is also problematic (especially at high operating temperature) [5,7] and prohibits a longer operation. Finally, it is also not that evident to equip micro-tubes and microtiter plates with means for separation of products or inhibitory substances from the reaction mixture during an experiment. This is indeed a major limitation particularly for enzymatic hydrolysis processes of complex biopolymers where inhibitory low molecular weight products such as glucose, D-Galacturonic acid, etc. are normally produced as reaction by-products [8-9]. Enzymatic modification of pectins to produce oligosaccharides is an example of such a reaction [10-13].

Membrane bioreactors are gaining increasing attention in novel ‘biorefining’ type of processes which require either continuous separation of inhibitory products or selective removal of targeted oligosaccharides following partial hydrolysis of complex biopolymers [8] – a function that is not possible to achieve with traditional batch reactors. Advantages of membrane bioreactor systems include (1) ability to retain enzyme within the reactor system and thus, reduce the operating cost (reuse of enzymes); and (2) minimization of the

effect of end product inhibition and consequently increase of the reaction yield and rates [10-13]. The application of membrane bioreactor technology in bench-scale reactors, however, requires a considerably large amount of enzymes and substrates since the typical volume of bench-scale reactors is approximately 0.5 L or more. Low throughput limits its usefulness for screening purposes or for preliminary kinetic studies. Moreover, conducting experiments with bench-scale membrane bioreactors is laborious due to the efforts required for preparation and cleaning of the reactor.

In this respect, microbioreactor technology offers the prospect of circumventing these limitations and the possibility of fabricating a micro-scale bioreactor (typically with a working volume less than 1 mL [14-18]) to facilitate a specific application. For example, a miniature membrane bioreactor to accommodate enzyme-catalyzed degradation processes of complex biopolymers. Such a scaled-down version of a reactor would then emulate all the basic features of a typical bench-scale membrane bioreactor whilst retaining the low cost and easy handling features of microtiter plate operations. The fundamental idea underlying the microbioreactor concept is illustrated in Figure 1.1.

Microbioreactors offer a number of advantages for assessing enzyme-catalyzed reactions. First, microbioreactors can include a series of inlet and outlet micro-channels, thus allowing these microbioreactors to support continuous operation [14,19]. Secondly, they can also be included with built-in sensors and actuators to achieve a superior degree of control over key operational variables such as pH and temperature [17,18,20] compared to microtiter plates. Independent control for individual microbioreactor units operating in parallel can also be achieved [18,20]. Thirdly, the availability of technology for membrane integration into microfluidics devices [21] provides the means to fabricate membrane microbioreactors – an essential feature for studying enzymatic modification of biopolymers at micro-scale. Contrary to microwell format reactors where the whole reactor contents are forced into a turning motion [22-24], an active mixing scheme can be integrated in microbioreactors to provide a more intense local mixing [17-20]. By adapting technologies from polymeric bio-microsystems [25], microbioreactors can be made disposable to minimize reactor preparation efforts. Moreover, due to their reduced size and small footprint, microbioreactors can be scaled out to platforms of multiple reactors in parallel, thus greatly increasing experimental throughput [17,18,20]. Finally, microbioreactors have the capacity to acquire real-time experimental data which significantly increases the amount of information gained per experiment [17,18,20]. Optical fibers can for example be incorporated in the microbioreactor to facilitate spectroscopic measurement techniques (near infra-red (NIR), Raman spectroscopy, etc) for *on-line* detection of substrates, or product levels [26].

The development of microbioreactors is a topic of considerable interest due to the fact that these reactors have the promise of offering cheap experimentation under well-controlled conditions, a feature that is highly desirable in the bioprocess engineering field. An increasing demand for a cheap and yet versatile experimental tool elevates the motivation to further improve current microbioreactor technology. Microbioreactors are certainly potential substitutes for microtiter plates (or micro-tubes), and its widespread applications are beneficial particularly in generating relevant process-related information that could be applied for later up-scaling of novel enzyme-catalyzed processes.

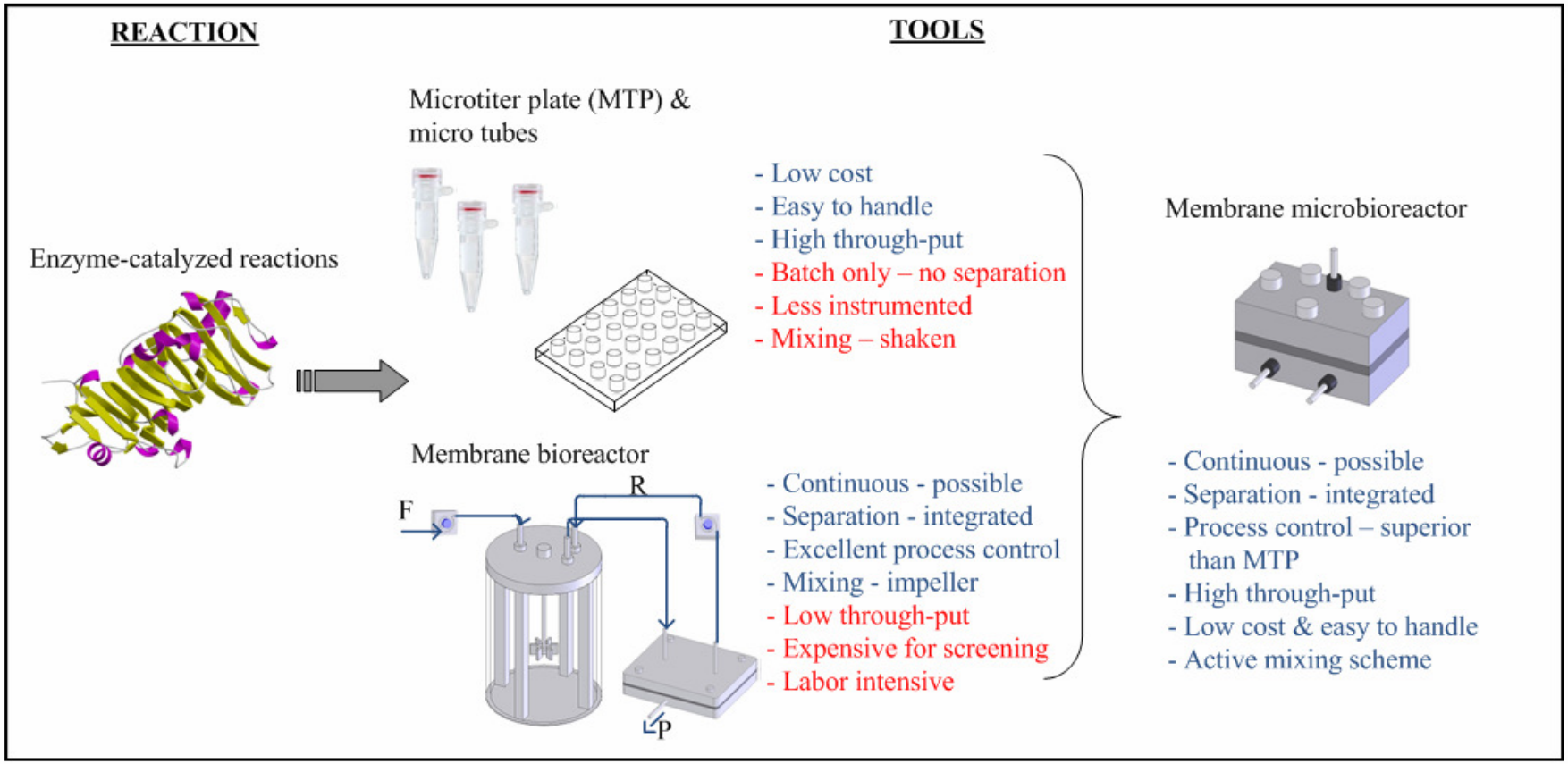

Figure 1.1. Illustration of the fundamental idea underlying the development of a membrane microbioreactor for processes involving enzyme-catalyzed degradation of biopolymers. The advantages (blue font) and limitations (red font) of the different systems are compared.

1.2 Research hypotheses

The basis for this PhD project is formed by the following hypotheses:

- It is possible to mimic events in bench-scale membrane reactors at reduced scale of operation, in this case in (membrane) microbioreactor systems. It is furthermore possible to design and build an appropriate (membrane) microbioreactor system to achieve this.

- It is possible to equip the microbioreactor prototype with the necessary sensors and actuators to establish a tight control over important reactor variables e.g. temperature and pH.

- The membrane microbioreactor prototype is capable of running an integrated reaction and separation process (e.g. enzyme-catalyzed modification of pectin) under well-controlled conditions with minimal amount of enzyme and substrate.

1.3 Research objectives and scope of work

The aims of this PhD project are:

- To develop feasible temperature and pH control strategies for a microbioreactor system.

- To develop a continuous membrane microbioreactor prototype for enzyme-catalyzed degradation of biopolymer.

- To demonstrate the operation of the continuous membrane microbioreactor for a specific bioprocess example, in this case the enzymatic degradation of pectin.

In the development work in the frame of this project, enzyme-catalyzed modification of pectin was used as a model system because of its industrial relevance [4,10-12,25]. Prototyping of the microbioreactor systems was done with three-dimensional (3D) computer-aided design (CAD) software, SolidWorks 2006, and micromachining. Development of the prototype also encompassed setting up of the necessary measurement apparatus and machinery to drive the microbioreactor systems. Programs for measurement and control routines were written in LabVIEW^{TM} v8.5 software (National Instruments, Austin, TX, USA), and were implemented by interfacing LabVIEW^{TM} with a data acquisition (DAQ) card (NI USB-6229, National Instruments, Austin, TX, USA) for data logging and sending signals to actuators. Further analysis of *on-line* measurement data (temperature, pressure, and pH) was done using Matlab v7.0 (The Mathworks, Natick, MA, USA).

Relevant design parameters to accommodate reactions for enzymatic modification of pectin were considered and realized. This includes reactor mechanics (materials, fabrications, membrane separation design, and mixing), fluidics (connections, pumping mechanisms, and feeding strategy), process control of physical parameters (temperature, pH, and pressure) and detection method or suitable assay to monitor the progress of the selected model system. The functionality and workability of the membrane

microbioreactor system were validated through a series of relevant experiments with enzyme-catalyzed degradation of pectin. Samples taken from the outlet of the microbioreactor were analyzed by means of microtiter plates and anionic chromatography methods (*off-line* analysis).

1.4 Thesis outline

The thesis was formulated according to the development steps of the continuous membrane microbioreactor prototype, and is structured into seven chapters. This chapter (*Chapter 1*) is the introductory chapter.

In *Chapter 2*, an overview on processes for enzymatic modification of pectin is presented. This chapter also includes a literature review on important design specifications as well as discussions on challenges for establishment of a continuous membrane microbioreactor. Part of this chapter is based on a review paper that I co-authored, and titled 'Application of microbioreactors in fermentation process development: a review', published in *Analytical and Bioanalytical Chemistry* in 2009 [14].

In *Chapter 3*, the technical realization of a low-cost temperature control method using a resistance wire as the heating element for the membrane microbioreactor prototype is presented. Design, basic functionality, and implementation of the method are discussed in detail. The basis for this chapter is a scientific paper entitled 'Embedded resistance wire as heating element for temperature control in microbioreactors', published in the *Journal of Micromechanics and Microengineering* in 2010 [27].

In *Chapter 4*, establishment of a gaseous pH control concept in microbioreactors is presented. The aim was to adapt the proposed gaseous pH control concept into the membrane microbioreactor prototype. This may lead to further improvement of pH control capability of the prototype, which thus far was operated as a buffered system. Design, basic functionality and limitations of the method are discussed in detail. Implementation, however, is hampered due to unavailability of a suitable cheap pH sensor spot for the system. The basis for this chapter is a scientific paper entitled 'Establishment of gaseous pH control concept in microbioreactors'. This particular manuscript is in preparation and is expected to be submitted to *Journal of Micromechanics and Microengineering* in 2010 [28].

In *Chapter 5*, a novel continuous membrane microbioreactor prototype is presented. Here, detailed design of the reactor with special emphasis on its mechanical features (materials used, fabrication methods applied, membrane integration and mixing) and its fluidics (connections, pumping mechanism and feeding strategy) are presented. Measurements and control concepts of the reactor (temperature, pressure, detection method and pH) are briefly discussed. The workability of the prototype was validated with results obtained in a bench-scale membrane bioreactor. The basis for this chapter is a scientific paper titled 'Continuous membrane microbioreactors for development of integrated pectin modification and separation processes', submitted to *Chemical Engineering Journal* in 2010 [29].

In *Chapter 6*, results obtained from enzyme-catalyzed degradation experiments of pectin performed in the membrane microbioreactor are presented and discussed. The experimental work in this chapter concludes the PhD project. The focus of the project has now shifted from microbioreactor technology development to demonstrating the usefulness of the membrane microbioreactors for investigation of enzymatic processes. The basis for this chapter is a scientific paper titled 'Assessing enzymatic modification of pectin by application of a continuous membrane microbioreactor', submitted to *Journal of Biotechnology and Bioengineering* in 2010 [30].

Finally in *Chapter 7*, overall conclusions are provided, and future perspectives of membrane microbioreactor technology are discussed in detail. Additionally, recommendations for future work and discussions on how the technology can be exploited are also presented.

1.5 References

[1] Rosgaard, L., Pedersen, S., Cherry, J. R., Harris, P., and Meyer, A. S. (2006). Efficiency of new fungal celllulase systems in boosting enzymatic degradation of barley straw lignocellulose. *Biotechnology Progress*, **22**: 493-498.

[2] Sørensen, H. R., Pedersen, S., and Meyer, A. S. (2007). Synergistic enzyme mechanisms and effects of sequential enzyme additions on degradation of water insoluble wheat arabinoxylan. *Enzyme Microbial Technology*, **40**: 908-918.

[3] Arnous, A., and Meyer, A. S. (2010). Discriminated release of phenolic substances from red wine grape skins (*Vitis vinifera L.*) by multicomponent enzymes treatment. *Biochemical Engineering*, **49**: 68-77.

[4] Doig, S. D., Pickering, S. C. R., Lye, G. J. and Woodley, J. M. (2002). The use of microscale processing technologies for quantification of biocatalytic Baeyer-Villiger oxidation kinetics. *Biotechnology and Bioengineering*. **80**: 42-49.

[5] Kumar, S., Wittmann, C. and Heinzle (2004). Minibioreactors. *Biotechnology Letters*. **26**: 1-10.

[6] Micheletti, M., Barret, T., Doig, S. D., Baganz, F. Levy, M. S., Woodley, J. M. and Lye, G. J. (2006). Fluid mixing in shaken bioreactors: Implications for scale-up predictions from microlitre-scale microbial and mammalian cell cultures. *Chemical Engineering Science*. **61**: 2939-2949.

[7] Zimmermann, H. F., John, G. T., Trauthwein, H., Dingerdissen, U., and Huthmacher, K. (2003). Rapid evaluation of oxygen and water permeation through microplate sealing tapes. *Biotechnology Progress*. **9**: 1061-1063.

[8] Pinelo, M., Jonsson, G., and Meyer, A. S. (2009). Membrane technology for purification of enzymatically produced oligosaccharides: Molecular and operational features affecting performance. *Separation and Purification Technology*. **70**: 1-11.

[9] Yadav, S., Yadav, P. K., Yadav, D., and Yadav, K. D. S. (2009). Pectin lyase: A review. *Process Biochemistry*. **44**: 1-10.

[10] Belafi-Bako, K., Eszterle, M., Kiss, K., Nemestothy, N., and Gubicza, L. (2007). Hydrolysis of pectin by *Aspergillus niger* polygalacturonase in a membrane bioreactor. *Food Engineering*. **78**: 438-442.

[11] Rodriquez-Nogales, J. M., Ortega, N. Perez-Mateos, and Busto, M. D. (2008). Pectin hydrolysis in free enzyme membrane reactor: An approach to the wine and juice clarification. *Food Chemistry*, **107**: 112-119.

[12] Olano-Martin, E., Mountzouris, K. C., Gibson, G. R., and Rastall, R. A. (2001). Continuous production of pectic oligosaccharides in an enzyme membrane reactor. *Food engineering and Physical Properties*. **66**: 966-971.

[13] Gallifuoco, A., Alfani, F., Cantarella, M., and Viparelli, P. (2001). Studying enzyme-catalyzed depolymerizations in continuous reactors. *Industrial and Engineering Chemistry Research*. **40**: 5184-5190.

[14] Schäpper, D., Zainal Alam, M. N. H., Szita, N., Lantz, A. E., Gernaey, K. V. (2009). Application of microbioreactors in fermentation process development: a review. *Analytical and Bioanalytical Chemistry*. **395**: 679-695.

[15] Betts, J. I., and Baganz, F. (2006). Miniature bioreactors: current practices and future opportunities. *Microbial Cell Factories*. **5**: 1-14.

[16] Urban, P. L., Goodall, D. M. and Bruce, C. B. (2006). Enzymatic microreactors in chemical analysis and kinetic studies. *Biotechnology Advances*. **24**: 42-57.

[17] Szita, N., Bocazzi, P., Zhang, Z., Boyle, P., Sinskey, A. J., and Jensen, K. F. (2005). Development of a multiplexed microbioreactor system for high-throughput bioprocessing. *Lab on a Chip*. **5**: 819-826.

[18] Lee, H. L., Bocazzi, P., Ram, R. J., and Sinskey, A. J. (2006). Microbioreactor arrays with integrated mixers and fluid injectors for high throughput experimentation with pH and dissolved oxygen control. *Lab on a Chip*. **6**: 1229-1235.

[19] Kee, S. and Gavriilidis, A. (2009). Design and performance of microstructured PEEK reactor for continuous Poly-L-leucine catalysed chalcone epoxidation. *Organic process Research and Development*. **13**: 941-951.

[20] Maharbiz, M. M., Holtz, W. J., Howe, R. T., and Keasling, J. D. (2004) Microbioreactor arrays with parametric control for high-throughput experimentation. *Biotechnology and Bioengineering*. **85**: 376-381.

[21] de Jong, J., Lammertink, G. H., and Wessling, M. (2006). Membranes and microfluidics: a review. *Lab on a Chip*. **6**:1125-1139.

[22] Büchs, J. (2001). Introduction to advantages and problems of shaken cultures. *Biochemical Engineering*. **7**: 91-98.

[23] Büchs, J., Lotter, S., and Milbradt, C. (2001). Out-of-phase operating conditions, a hitherto unknown phenomenon in shaking bioreactors. *Biochemical Engineering*. **7**: 135-141.

[24] Weiss, S., John G. T., Klimant, I., and Heinzle, E. (2002). Modeling of mixing in 96-well microplates observed with fluorescence indicators. *Biotechnology Progress*. **18**: 821-830.

[25] Betts, J. I., and Baganz, F. (2006). Miniature bioreactors: current practices and future opportunities. *Microbial Cell Factories*. **5** (21): 1-14.

[26] Pully, V. V., Lenferink, A., van Manen, H-J., Subramaniam, V., van Blitterswijk, C. A., and Otto, C. (2010). Microbioreactors for Raman microscopy of stromal cell differentiation. *Analytical Chemisty*. **82**: 1844-1850.

[27] Zainal Alam, M. N. H., Schäpper, D., and Gernaey, K. V. (2010). Embedded resistance wire as heating element for temperature control in microbioreactors. *Micromechanics and Microengineering*. DOI: 10.1088/0960-1317/20/5/055014.

[28] Zainal Alam, M. N. H., Schäpper, D., Andrijana, D., and Gernaey, K. V. (2010) Establishment of gaseous pH control concept in microbioreactors. *Micromechanics and Microengineering*. – manuscript in preparation.

[29] Zainal Alam, M. N. H., Pinelo, M., Samantha, K., Jonsson, G., Meyer, A., and Gernaey, K. V. (2010). Continuous membrane microbioreactors for development of integrated pectin modification and separation processes. *Chemical Engineering Journal* – submitted in March 2010.

[30] Zainal Alam, M. N. H., Pinelo, M., Arnuos, A., Jonsson, G., Meyer, S. A., and Gernaey, K. V. (2010). Assessing enzymatic modification of pectin by application of a continuous membrane microbioreactor. *Journal of Biotechnology and Bioengineering* – submitted in August 2010.

CHAPTER 2

Literature review

CHAPTER 2

Literature review

Abstract

This literature review chapter is subdivided into two main parts: In the first part of the chapter, a short overview on enzyme-catalyzed hydrolysis of pectin reactions is presented – focusing on the physical features of the pectin substrate, the enzymatic hydrolysis reaction of pectin as well as its industrial relevance. The application of membrane bioreactors for enzyme-catalyzed modification of pectin is also briefly explained. These are all relevant inputs for designing the continuous membrane microbioreactor prototype that will be developed and studied in the frame of this PhD thesis. In the second part of this literature review chapter, important design considerations as well as technical challenges for establishment of a continuous membrane microbioreactor to facilitate the targeted application (i.e. enzyme-catalyzed modification of pectin) are discussed. These include reactor operating feature and size, reactor mechanics (materials, fabrications, membrane separation design, and mixing), reactor fluidics (connections, pumping mechanisms, and feeding strategy), process control of physical parameters (temperature, pH, and pressure) and detection methods for measuring the product concentration.

Part of this chapter is based on a review paper: Schäpper, D., Zainal Alam, M. N. H., Szita, N., Lantz, A. E., and Gernaey, K. V. (2009). Application of microbioreactors in fermentation process development: a review. *Analytical and Bioanalytical Chemistry*. 395: 679-695.

2.1 Enzyme-catalyzed hydrolysis of pectin

Pectins are a complex biopolymers that occur as structural polysaccharides in the primary cell wall and middle lamella of plant cell walls. The primary structure of pectin consists of 'smooth' regions of homogalacturonan (HGA), and 'hairy or ramified' regions of rhamnogalacturonan I (RG-I) and substituted galacturonans. The latter includes rhamnogalacturonan II (RG-II) and xylogalacturonan (XGA) polysaccharides [1,2]. Although, the way in which these different types of polysaccharides are arranged is still not fully understood, it is suspected that these pectic polysaccharides may be covalently linked to each other forming the pectin macromolecule with a molecular weight in the range of 100 kDa [2]. A scheme of the model pectin structure is illustrated in Figure 2.1.

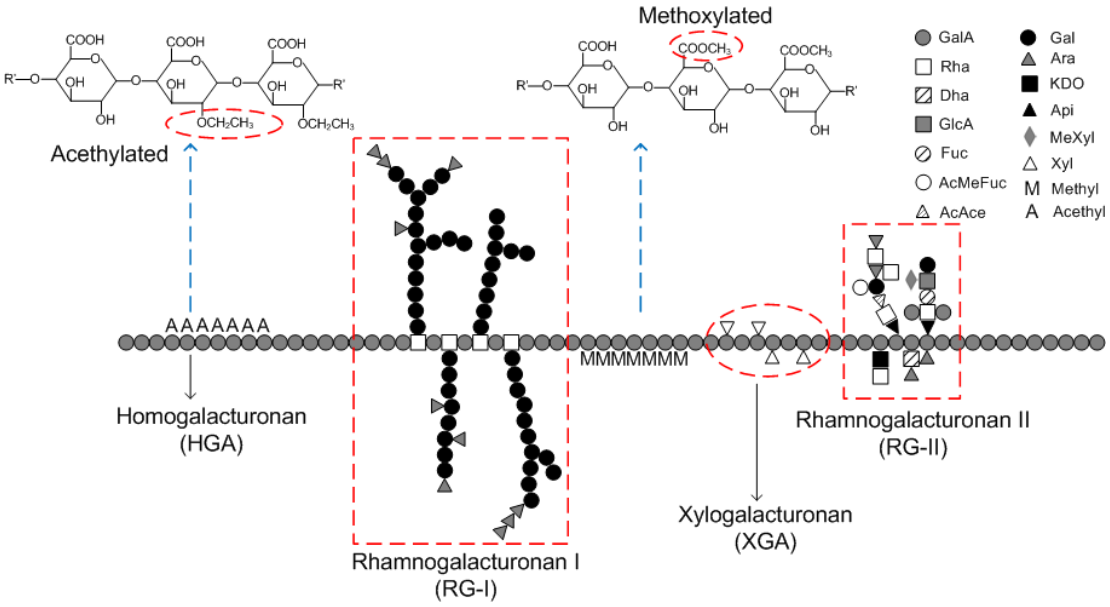

Figure 2.1. Sketch of the model pectin structure illustrating the homogalacturonan (HGA), rhamnogalacturonan I (RG-I), rhamnogalacturonan II (RG-II) and xylogalacturonan (XGA) polysaccharides. For simplicity, it is assumed that all pectic polysaccharides are covalently linked to each other. GalA: D-galacturonic acid; Rha: rhamnose; Dha: 2-keto-3-deoxy-D-*lyxo*-heptulosaric acid; GlcA: glucuronic acid; Fuc: fucose; Ac: acetyl; Me: methyl; Ace: aceric acid; Gal: galactose; Ara: arabinose; KDO: 2-keto-3-deoxy-D-*manno*-octulosonic acid; Api: apiose; Xyl: xylose. The structure was modified from the 'canonical' model structure by Perez *et al.* [2].

As shown in Figure 2.1, homogalacturonan (HGA) basically consists of a linear (i.e. unbranched) chain of α-1,4-linked D-galacturonic acid residues which forms the main backbone of pectin. A proportion of the D-galacturonic acid residues of HGA may be either methyl-esterified (i.e. methoxylation) at the C-6 position and/or *O*-acetylated (i.e. acetylation) at positions C-2 and/or C-3. The degree of methoxylation and acetylation varies depending on the pectin origin, extraction method and processing conditions. The term highly methoxylated pectin is often used for pectin with a degree of methoxylation greater than 50% [1,3].

Rhamnogalacturonan I (RG-I) is a long alternating backbone sequence (i.e. heteropolymeric backbone) consisting of the repeating disaccharide units of rhamnose and

D-galacturonic acid [(1→2)-α-L-Rha-(1→4)-β-D-GalA]. Similarly to HGA, The C-2 and/or C-3 positions of D-galacturonic acid residues may be *O*-acetylated to a certain extent depending on the pectin origin. Furthermore, the rhamnose residues may be substituted with neutral side-chains of galactan, arabinan and/or different arabino-galactan side-chains at the C-4 position [1,2]. The final components of the pectic polysaccharides are the rhamnogalacturonan II (RG-II) and xylogalacturonans (XGA). XGA is a linear backbone consisting of α-1,4-linked D-galacturonic acid residues with β-D-xylose substitutes at the C-3 position where else RG-II is a highly substituted and branched homogalacturonan (HGA) with distinct side-chains of a diversity of rare sugars. The former pectic polysaccharide (i.e. XGA) is only present in some reproductive plants, e.g. apple, carrot and cotton [1,2].

Pectic substances are abundant in agro-industrial waste streams particularly from sugar and potato starch production and juice processing [4,5]. In sugar beet pulp (by-product of a sugar refinery), pectic substances are accounting for more than 40% of the dry matter content [6]. Moreover, in apple pomace (solid residue from extraction of apple juice) [7], and potato pulp (waste generated from potato starch production) [8], pectin may constitute 14-17% of the dry matter content. Agro-industries are highly interested in converting these low-value waste streams into high value products, especially considering that these surplus pectic substances consist of suitable starting materials for obtaining bioactive carbohydrates with potential health benefits [4,9,10]. As an example; pectin-derived oligosaccharides have been reported to have applications as repressors of liver lipid accumulation in rats [11] and small oligomers of galacturonic acid are endogenous suppressors of disease resistance reactions in wheat leaves [12].

The conversion of pectin can be done through an enzymatic reaction catalyzed by pectinases [5,10,13]. Saccharification of pectin is also achievable via a chemical extraction method [14], but the use of enzymes is preferable as their usage has a number of advantages: relatively lower energy consumption of the enzyme-based process, no generation of waste chemicals, and enzymes are very selective [9]. Many different types of pectinases with various action sites within the pectin macromolecule have been identified [15], three of which are to be discussed here – polygalacturonase (PG), pectinmethylesterase (PME) and pectin lyase (PL). PG catalyzes the hydrolytic cleavage of the α-1,4-glycosidic bonds between unesterified D-galacturonic acid chains of the HGA region (i.e. depolymerization of pectin). Since PG only acts on unesterified D-galacturonic acid units, a low methoxylated and acetylated pectin substrate is preferable. The latter is achievable via the action of PME which catalyzes the de-esterification of pectin resulting in a product that subsequently is a substrate for PG. Thus, PME and PG are often combined to catalyze the degradation of pectin producing partially degraded fragments and methanol as by-product [5,15]. Contrary to the action mechanism of PME and PG enzymes, PL is capable of catalyzing the degradation of highly esterified pectin via a β-elimination mechanism producing a 4,5 unsaturated galacturonide residue with a double bond at its non-reducing end without generating any methanol as by-product [13,15]. *Endo*- and *exo*-acting enzymes are distinguished depending on the model of action of the pectinases [3]. The *exo*-acting enzymes cleave from the non-reducing end of the polymeric chain where else the *endo*-acting ones break the interior bonds of the polymer chain. PL, PG and PME action mechanisms and their various action sites on the pectin macromolecule are illustrated in Figure 2.2.

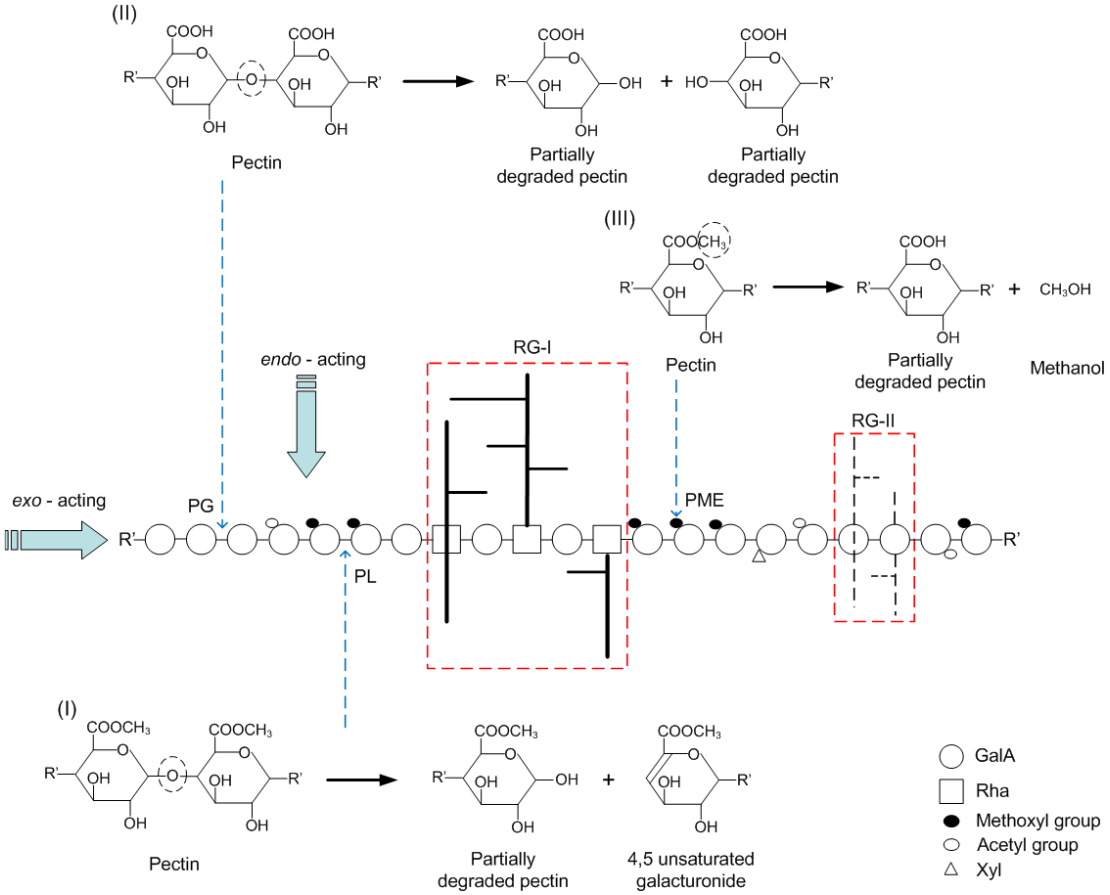

Figure 2.2. PL, PG and PME action mechanisms and their various acting sites on the pectin macromolecule [15]. (I) β-elimination mechanism via pectin lyase (PL). (II) De-polymerization of pectin via pectin galacturonase (PG). (III) De-esterification via pectin methyl esterase (PME). GalA: D-galacturonic acid, Rha: rhamnose, Xyl: Xylose.

Numerous research projects have successfully applied membrane bioreactors for studying enzyme modification of pectin (see Table 2.1 for details) [16-20]. Membrane bioreactors – thus far ultrafiltration membranes are mostly employed – are indeed quite advantageous for studying this type of processes for a number of reasons: (1) enzymes can be retained (i.e. typically as free and un-immobilized form) for a long continuous operation [17]; and (2) the membrane allows for *in situ* removal of the product [16-20]. The latter is indeed a useful feature for enzyme-catalyzed pectin modification processes where continuous removal of inhibitory products is necessary to minimize end product inhibition effects and thus, to achieve higher product yield and conversion rates [10]. An increase by 40% in hydrolysis specific productivity – compared to the traditional batch reactor – has been reported [19] when low molecular weight substances (e.g. D-galacturonic acid) produced from de-polymerization of pectin were continuously removed from the system. Furthermore, it was also claimed that a membrane reactor showed a good catalytic activity and may run stable for up to 15 days of continuous operation with the possibility to achieve a substrate conversion as high as 90% [21]. Membrane bioreactor systems also offer a

good as well as easy control over reactor operational variables such as pressure, temperature, feed flow rate, agitation, pH, etc. [10].

Table 2.1 Examples of the use of membrane reactors for enzyme-catalyzed hydrolysis of pectin

Ref.	[S]	[E]	Mode of operation	Conditions	Membrane specification
[16]	Sugar beet pulp, black currant, red currant & citrus pectin	PG	-Continuous feeding & separation *-cross flow*	T=50°C pH=4.1	Flat sheet, PS, UF, MWCO-45kDa
[17]	Apple pectin (DM=70-75%)	PG, PL	-Continuous feeding & separation *-cross flow*	T=48°C pH=4.8 P = 0.1-1.7 bar	Spiral wound, PS, UF, MWCO-10 & 50kDa
[18]	Citrus pectin (DM=60-66%) & apple pectin (DM=8%)	PG, PE	-Continuous feeding & separation *-dead end*	T=30°C pH=4	Flat sheet, RC, UF, MWCO-10 kDa
[19]	Pectic substrate (low esterified)	PG	-Continuous feeding & separation *-cross flow*	T=50°C pH=4.1	Flat sheet, RC, UF, MWCO-30 kDa
[20]	Polygalacturonic acid (MW_{ave}=30kDa)	PL, PE	-Batch feeding -continuous separation *-dead end*	T=25°C pH=5.6	Flat sheet, RC, UF, MWCO-30 kDa

DM=degree of methylation; PG=polygalacturonase; PL=pectin lyase; PE=pectin esterase; MWCO=molecular weight cut-off; T=temperature; P=pressure; RC= regenerated cellulose; UF= ultrafiltration; PS=polysulfone; [S]=Substrate; [E]=Enzyme.

Despite the obvious advantages, membrane bioreactor systems suffer from a minor setback – that is the build-up of unreacted substrates in the system [10,22]. In continuous operation, substrate (i.e. pectin) is continuously fed into the reactor (Figure 2.3). It is suspected that, at some intermediary state, the reaction medium may comprise of the following complex mixture:

- The enzyme (e.g. pectin lyase) and the newly fed substrate.
- Unreacted substrates presumably RG-I and RG-II polysaccharides if pectin lyase was utilized.
- Partially degraded substrate (i.e. pectin).

All the above-mentioned components of the reaction mixture have an average molecular weight greater than the membrane molecular weight cut-off, MWCO (e.g. > 10 kDa) applied.

Partially degraded substrate that is retained will undergo further hydrolysis whilst low molecular weight and shorter pectin fragments are continuously removed from the

membrane reactor system. It is also anticipated that the reactor output mixture (i.e. permeate solution) possibly will consist of 4,5 unsatured galacturonide residues with a broad molecular weight distribution range – monomers, dimers, trimers, etc. [13]. In contrast, the concentration of the unreacted substrates increases as reaction proceeds and they tend to accumulate on the surface of the membrane. The build-up of these un-reacted substrates – which also increases bulk phase viscosity and system pressure – aggravates the concentration polarization effect normally encountered in membrane separation systems. Severe membrane fouling caused from the concentration polarization effect is indeed a major limitation for a membrane reactor system [10,22].

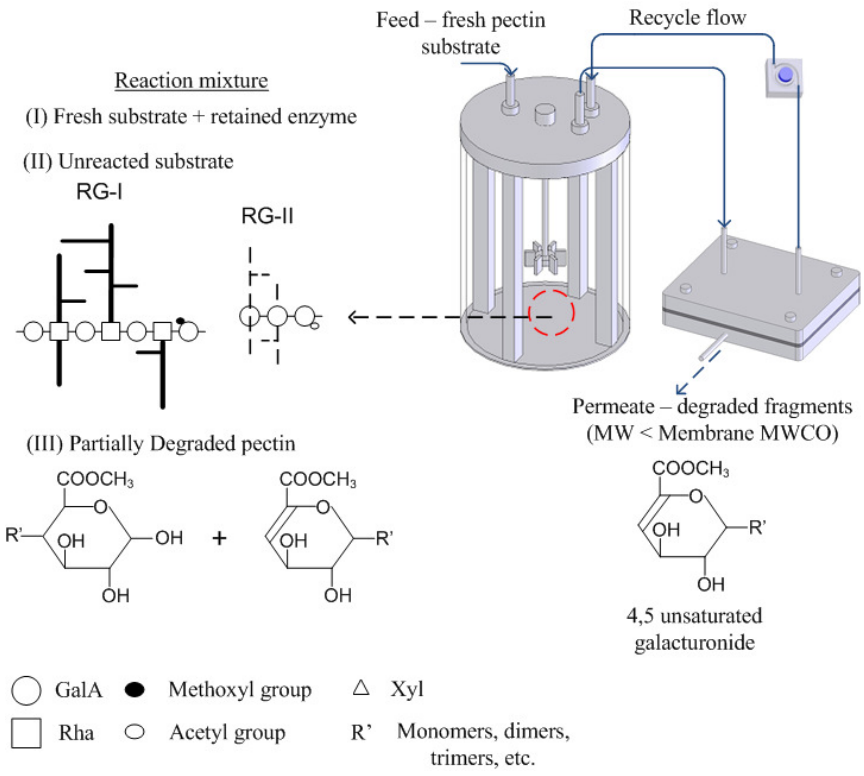

Figure 2.3. Example of the use of a continuous membrane bioreactor for enzyme-catalyzed modification of pectin. Assumptions: PL enzyme was used and the membrane molecular weight cut-off (MWCO) applied was below the average molecular mass of RG-I and RG-II.

Membrane reactor systems certainly have the potential to facilitate enzyme-catalyzed pectin hydrolysis reactions. Nevertheless, optimization of the membrane reactor systems is a rather challenging task as it is typically performed (1) to maximize product yield/rates and (2) to increase selectivity towards production of desired oligomers – all while minimizing the concentration polarization effect. This is indeed a complex task and it is a trade off between reaction rate (enzyme to substrate ratio, $[S]_o$, etc.), residence time, and appropriate choice for membrane MWCO [10,18,22]. Thus far, experimentation associated with investigation of an enzyme-catalyzed pectin hydrolysis reaction in a membrane reactor system has been carried out at laboratory scale [16-21] (i.e. working volume 0.5 L and upwards) which can be very costly, especially considering that a

multitude of experiments are normally performed when elucidating new enzyme-catalyzed production processes. In this respect, we believe that miniaturization or scaling down of the bench scale reactor systems could potentially resolve this issue and allow for relatively cheap experimentation.

2.2 Development of a continuous membrane microbioreactor system: Design considerations and challenges

Typical bench-scale membrane reactors consist of a mechanically agitated and jacketed tank with membrane assembly counterpart [10,22]. Such a bench-scale reactor design, however, cannot be scaled down to fit into an appropriate form for miniature scale reactors because of the fundamental differences introduced by altering the system size. Additionally, there are a number of specific design considerations which need to be evaluated carefully. To design a continuous membrane microbioreactor system, one must consider the design of the entire system that drives the reactor and not just restrict the design only to the mechanical aspects of the reactor. Important design considerations for a complete membrane microbioreactor system include reactor operating feature and size, reactor mechanics (materials, membrane separation design, and mixing), reactor fluidics (connections, pumping mechanisms, and feeding strategy), process control of physical parameters (temperature, pH, and pressure) and detection methods for measuring the product concentration. Each and every one of these design components need to be established whilst minimizing working volume, fabrication cost, and if it's possible at all, system complexity [23,24].

In this part of the literature review chapter, technical solutions that have been implemented in the microbioreactor world for each of the above mentioned design components are reviewed. Technical challenges as well as the necessary engineering compromises are also discussed. The scope of the review is only limited to (1) continuous microbioreactor systems, and therefore microwell format reactors are excluded as they in general do not support continuous operation; (2) free and un-immobilized form enzyme systems though in exceptional cases, microbial cell-based microbioreactors are referred to as examples as well. Our targeted application is enzymatic hydrolysis of polymeric substrates (e.g. pectic substances). These native biopolymers (i.e. pectic substances) exhibit unfavorable mixing conditions in the laminar flow regime of microfluidic systems. They produce a highly viscous solution due to the extent of branching and high degree of methyl-esterified and acetylated substitutes [10]. Such reaction medium may cause severe mass transfer limitation for an immobilized enzyme system [22,25] which justifies why a free and un-immobilized enzyme system is preferable.

2.2.1 Reactor operating feature and size

Microbioreactors are generally designed to work under bubble-free conditions with constant volume (no head space) [24,26-31]. This means that, during operation, the reactor will be completely filled with liquid and there is no increase in volume ($dV_r/dt = 0$). Bubbles are not desirable as their relatively large size – compared to the size of the microbioreactor channels – would easily clog the microchannels or even block fluidic ports. Due to the high surface tension in micro-scale systems, bubbles that are trapped inside a microfluidics chip tend to bond with the inner surface of the microchannels [32].

Small air bubbles are also problematic as they have a high tendency to coalesce and accumulate. This is often evident in a loop type reactor system where recirculation of fluid at high flow rate promotes the coalescing of bubbles in the system [31,32]. Large bubbles – as they are not breakable – may occupy a large volume of a microbioreactor reaction chamber [33]. For a microbioreactor design consisting of a reaction chamber and relying on a magnetic stirrer bar for mixing [29,33], the presence of bubbles in the reactor chamber might perturb the stirring motion of the magnetic stirrer bar. This certainly affects the mixing efficiency of the system. Furthermore, gas bubbles that appear in the system could also disturb any *on-line* measurements in microbioreactors – consequently, rendering them useless [24]. Formation/presence of air bubbles is indeed a major obstacle for successful microbioreactor operation, and it is crucial that they are either removed (via an integrated bubble-trap [32]), prevented from entering the system (via a passive bubble filter [34]) or purged out of the system before initiating the experiment [31].

The microbioreactor size is governed by the working volume which is normally less than 1 mL (i.e. characteristic dimensions are in a range of 10-1000 μm) [24,35]. On the one hand, working with small volumes (in the order of a few μL) generally leads to fast-response systems (e.g. faster mass and heat transfer rates) because of the high surface area to working volume ratio (*S/V*) of microsystems [24]. On the other hand, as size decreases, the less instrumented the reactor will be [36]. This is due to the limited ability to manipulate essential reactor variables within a small working volume. In some applications, the reactor volume is kept between 100 and 200 μL [26,27,29,31]; one of the reasons for that is that such a volume is typically needed if one needs to perform *off-line* analysis of the microbioreactor content (e.g. at the end of the experiment) [29]. Moreover, a minimum volume is required to be able to obtain sufficient space to place sensors for *on-line* measurements (e.g. temperature, pH, dissolved oxygen, etc.). The possibility to perform *on-line* measurements allows for continuous monitoring of the state of the reaction [26,27,29], and thus increases the amount of information gained from the system. It is also important to keep the size of the reactor relatively small to maintain its small footprint characteristic. This is an important consideration as it will ease later scaling-out step to increase experimental throughput – compared to a bulky microbioreactor design [26,27].

2.2.2 Reactor mechanics

This section focuses on the mechanical design of the reactor. It includes an overview on commonly used materials for microbioreactor fabrication, mechanics for integration of the membrane separation counterpart and suitable mixing schemes in microbioreactor systems.

Materials

The suitability of materials for fabrication of microbioreactor prototypes is depending on the compatibility of the selected material with the targeted application. Material selection is also often associated with the fabrication steps required to produce the entire chip. The degree of difficulty to fabricate a single microbioreactor prototype must be minimal to allow future mass production of the chip. Microbioreactor prototypes are typically made from polymethylmethacrylate (PMMA) and polydimethylsiloxane (PDMS) [26,27,29,33,37]. These are the most commonly used substrates for fabrication of microbioreactor prototypes due to their low material costs, easy handling, biocompatibility, non-toxicities, good solvent and chemical compatibilities, and durabilities. Additionally,

they also exhibit high optimal transmission in the visible wavelength range, which facilitates optical measurements [38,39]. Moreover, using PMMA and PDMS substrates, it is possible to fabricate two- or three-dimensional (2D or 3D) microfluidics geometries using a rather straightforward and relatively cheap micromachining process [40,41]. Whilst the bonding (or structuring) of multiple layers of PMMA is normally done using replication methods like injection molding or hot embossing [40,41], the fabrication of PDMS-based reactors merely involves a few casting and curing steps [40,42]. Pressing a PDMS slab between two PMMA layers with metal screws or clamps is an alternative way to ensure watertight seals in multilayered reactors consisting of PMMA-PDMS substrates [37]. The use of screws to compress the layers together has the advantage that the screws can also be used as a guide to ensure all layers are properly aligned. A slight mis-alignment would indeed compromise the leak-free operation of the reactor. The low material cost of PMMA and PDMS coupled with their cheap fabrication processes are ideal characteristics for low-cost mass production and rapid prototyping. This also allows for the fabrication of disposable reactors to prevent sample contamination and reduces efforts involved in reactor preparation significantly.

An important advantage of PDMS substrates over other thermoplastic polymers like PMMA, polyetheretherketone (PEEK) or polycarbonate (PC) is that PDMS enables the integration of microfluidics devices such as microvalves, micropumps, and mixers as an integral part of the reactor [27,43]. While the integration of microfluidics devices may complicate the reactor design, it – more importantly – decreases the cost of the entire microbioreactor setup because fewer macroscale devices are needed to drive the system. Despite of these advantages, PDMS also suffers from several drawbacks. One drawback is that the gas permeability of PDMS can lead to unwanted levels of evaporation [37,40]. The evaporation rate in a microbioreactor system via a PDMS layer has been reported to be in the order of 5 $\mu L\ hr^{-1}$ (for water at 37^{o}C [29]). This is however not really a concern because in a continuous operation system, the reactor can often be operated at a relatively high input feeding rate, e.g. 100 or 200 $\mu L\ hr^{-1}$. At such feeding rate, the water evaporation level is negligible or can easily be replenished by the high input feeding rate of the system. Another limitation of PDMS material is that it also swells in most organic solvents [40]. Specifically for enzymatic hydrolysis of pectin, this is not an issue as most of the substrate solution is prepared by using water as a solvent. Additionally, pectin or saccharide molecules are water-soluble, or at least suspendable in water – up to a certain concentration level – and not soluble in organic solvents [10].

Silicon and glass can also be used as substrates for the fabrication of microbioreactors, but these materials are rather difficult to work with. Moreover, the fabrication techniques used for these substrates are expensive, time consuming, and require access to clean-room facilities [42].

Membrane separation design

The integrated membrane counterpart serves as a selective barrier, typically allowing only low molecular weight hydrolysis products (i.e. smaller than membrane pore size) to diffuse through it, and separation occurs by a pressure difference. When designing the membrane separation feature for a membrane microbioreactor system, one should take into account the following considerations:

- Selection of membrane

It is crucial to apply a membrane (i.e. material and type) that best fits the targeted application. Membrane properties differ from one membrane to another and they greatly affect the overall membrane separation efficiency. As an example, in purification/concentration and/or separation of saccharides by ultra- or nanofiltration membranes, cellulosic membranes (i.e. an organic membrane) are normally employed – relative to ceramic type membranes – as they are hydrophilic and exhibiting a low protein adsorption [10]. Hydrophilic membranes are advantageous in this particular case because they allow the penetration of solvent and solute into the membrane surface and further diffusion through the membrane (i.e. in accordance to a solution-diffusion model). Thus, hydrophilic membranes limit the adsorption of protein on the membrane surface and decrease the fouling on the membrane [10]. The membrane can either be directly purchased from a commercial supplier (e.g. Millipore, Sigma, etc.) or prepared in-house [44]. The typical selection criteria include membrane hydrophobicity, operation variables e.g. allowable pH, temperature or pressure, MWCO, and finally the type of membrane used (i.e. flat sheet or hollow-fiber) [44]. Membrane pore-size or molecular weight cut-off is also a key factor in separation where it may influence the selectivity of the separation process [10,44]. A rule of thumb for a good membrane rejection is that the membrane pore size should be in the order of one-third or one-fifth of the size of the compound to be retained. This is however not entirely true because in practice, the rejection characteristic of a membrane is often a function of concentration polarization, heteroporosity of the membrane, and system operating variables (pH, temperature and pressure or flux) [10,44,45].

- Membrane integration

Different approaches have been used to integrate a membrane into microfluidic devices. Thus far, direct incorporation of a flat sheet membrane is the most commonly employed method for fabrication of micro membrane enzyme reactors [31,44-51]. Direct incorporation of a membrane is advantageous due to its easy-handling in terms of membrane assembly. Most importantly, it offers the 'clamp-and-play' chip design where a broad range of applications can be made possible by merely changing the type of membrane [44]. A flat sheet membrane can be integrated into a microfluidics device, simply by clamping, fitting or pressing it (i.e. sandwiched) in between two polymer pieces [31,44,48-51]. Figure 2.4 presents the schematics of typical approaches for direct incorporation of flat sheet membranes in between thermoplastic polymers such as PMMA, PEEK, PC etc. and/or PDMS substrates – standard materials used for microbioreactor fabrication. For integration of a membrane in between thermoplastic polymers, water-tight sealing is achieved by pressing all layers together by a metal clamp or with metal screws (see Figure 2.4a) [31,44,51]. This is however unnecessary if the membrane is squeezed in between PDMS substrates as bonding is possible by 'gluing' in place with pre-polymer PDMS solution. Tight sealing can be sufficiently created at least as long as there is no excessive pressure build-up from within the system (see Figure 2.4b) [44,48]. Precautions have to be taken to avoid any overflow of the pre-polymer solution that may clog the microchannels during bonding. The membrane can also be assembled in between PDMS and thermoplastic polymers where an additional layer of polymer is required such that all layers can be pressed together via metal screws to create a water-tight sealing (see Figure 2.4c) [50]. Flat sheet membranes can also be arranged in a stack. For example, Xiang *et al.* [51] microfabricated a dual-microdialysis system where two pieces of polymeric membranes with different molecular weight cut-offs (i.e. low and high) were alternatingly

sandwiched between three polycarbonate plates containing four serpent-like microchannels for mixing. Such a microsystem allows for fractionation of a mixture with a broad molecular weight distribution range.

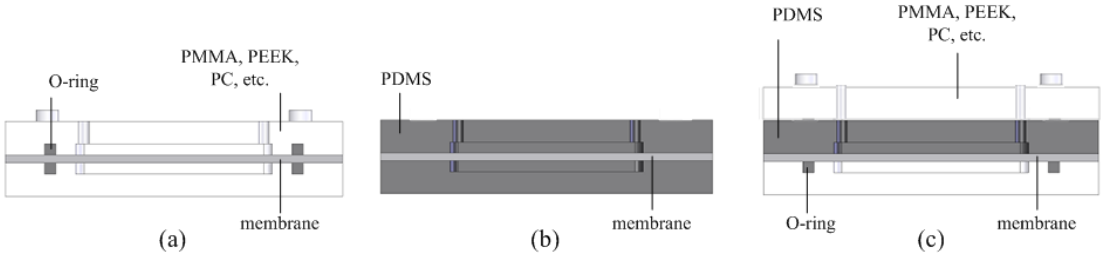

Figure 2.4. Schematics of typical approaches for direct incorporation of flat sheet membranes into microfluidics devices. (a) in between thermoplastic polymers such as PMMA, PEEK, PC etc. [31,44,51] (b) in between PDMS substrates [44,48] (c) in between PDMS and thermoplastic polymers [50].

- Operation mode (e.g. *dead-end* or *cross-flow*)

There are two distinct modes of operation for a membrane system; i.e. a *dead-end* or a *cross-flow* filtration and one ought to decide which one of these modes of operation best suits the specific application. In a *dead-end* filtration, feed solution is pumped directly towards the membrane and forced through the membrane by the applied pressure [44,46,47,49]. Posthuma-Trumpie *et al.* [49] devised a *dead-end* micro enzyme membrane reactor where enzyme was coated on the surface of a polyether sulfone (PES) filter (or confined in between the filters) and feed solution was continuously perfused through the membrane. Another example of a *dead-end* system is the trypsin membrane microreactor design by Gao *et al.* [47]. The enzyme was adsorbed within the porous structure of a poly(vinylidene fluoride) membrane that was sealed in between PDMS substrates. The protein solution was pre-concentrated and separated on the membrane as it was continuously pushed into the system. The problem with a *dead-end* system – despite being simple and easy to operate – is that retained particles continuously accumulate on the membrane surface leading to a severe concentration polarization effect.

Contrary to the *dead-end* filtration mode, the concentration polarization problem is reduced in a *cross-flow* system because the bulk liquid phase flows parallel to the membrane surface and thus sweeps any retained particles. During every pass across the membrane surface, the applied pressure pushes a portion of the bulk phase through the membrane into the permeate stream [31,44,46,50]. A *cross-flow* filtration mode of operation can easily be realized in a loop-type reactor system. A loop reactor system has a good residence time distribution and was reported to show identical flow behavior to ideal continuously stirred tank reactors (CSTR) [31,50]. In the simplest configuration, a loop reactor may be integrated with a filtration chip consisting of a narrow microchannel to establish a membrane microbioreactor system (see Figure 2.5a) [31]. Alternatively, a separate microreactor and filtration chip can also be placed in/on a housing or chip holder which then serves as the main component in the loop-type reactor system. A rather bulky reactor design usually results, but it provides room for integration of sensors and actuators (see Figure 2.5b). Another option is to integrate a hybrid reactor-filtration chip into the loop – a more compact design which has the advantage of a small reactor footprint (see

Figure 2.5c) [50].

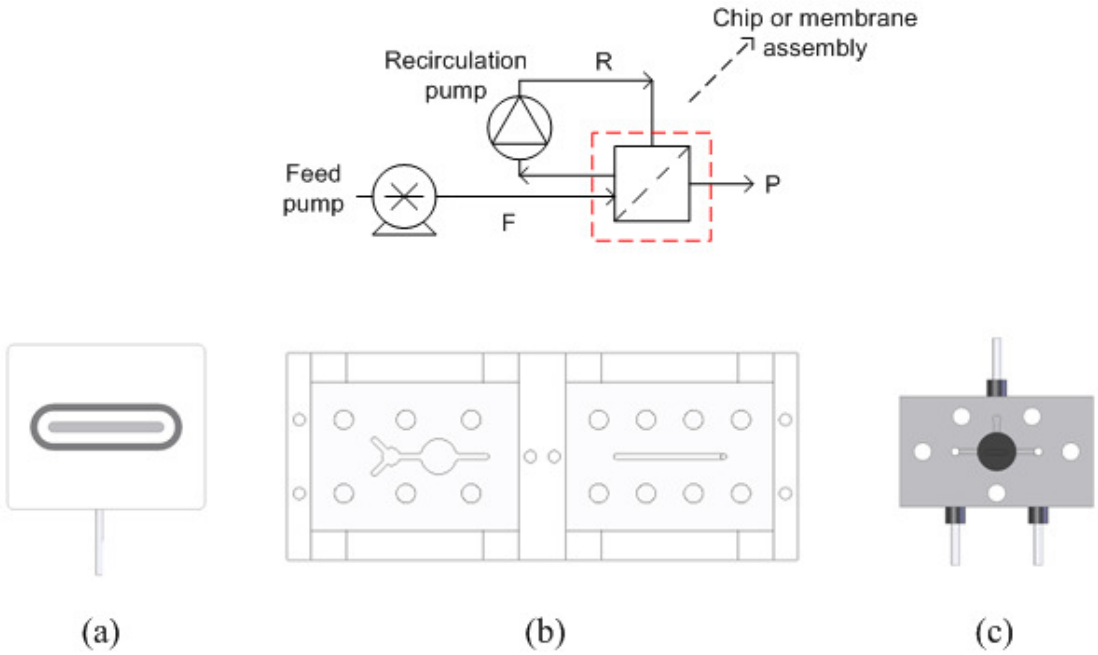

Figure 2.5. (*top*) Basic schematic for a loop-type reactor system. (*bottom*) Different types of membrane chips that can be fit into the loop-type reactor system (a) Chip with a narrow microchannel [31]. (b) Microfluidics housing consisting of separate reactor (*left*) and filtration (*right*) chips. (c) A hybrid reactor-filtration chip [50].

- Pressure for separation

For microbioreactors (or microfluidic devices) with constant working volume where bubbles are not desirable and nitrogen purging is therefore not feasible, the necessary pressure for separation to occur is normally created by the feeding pump [31,47-50]. Continuous pumping increases the system pressure and hence, forces the liquid to diffuse through the membrane. Since there is no volume change in the system ($dV_r/dt = 0$), a constant permeate flux is guaranteed because the volumetric feed inflow, F into the reactor is equivalent to the volumetric permeate outflow, P as illustrated in Figure 2.5.

Mixing

A good mixing scheme is crucial for microbioreactor operation and it is important for a variety of applications. For example, in enzymatic reactions; mixing is required for homogenization of solutions of substrates, enzymes or any reagents used, for recirculation of the reactor content (i.e. *cross-flow* system) and to promote a uniform temperature distribution throughout the reactor. All those factors have a direct influence on the reaction rates and separation performance of a membrane microbioreactor system (e.g. increasing enzymes-substrates contact times, reducing particle deposition on membrane surface, good mass and heat transfer, etc.) [24,31,50]. Mixing in a microfluidic system is however very challenging because it is governed by diffusion rather than turbulence – a condition that is often associated with good mixing – due to the low Reynolds number typical for the micro-scale. This can often be explained by the small characteristic dimensions of the microfluidic system (e.g. $Re=UD/\nu$ (flow in microchannel) [52] and $Re=\Omega D^2/\nu$ (stirrer bar

in microchamber) [29] < 100; where U is the average flow velocity ($m.s^{-1}$), Ω is the stirrer bar rotational speed (rps), D is the characteristic dimension (m) and ν is the kinematic viscosity of the fluid ($m^2.s^{-1}$). Mixing under the laminar flow regime on micro-scale is indeed very slow and inefficient. Therefore, alternatives for micromixing are generally aimed at increasing the contact/interfacial area and/or reduce the diffusion lengths between two or more fluids [52,53].

Mixing in microbioreactors can be achieved by either passive mixing and/or active mixing schemes [54,55]. Passive (or static) mixing schemes are achievable without any moving parts and can be categorized into molecular diffusion and chaotic advection. In molecular diffusion, natural Brownian motion of molecules is exploited and good mixing is attained with large interfacial areas, longer contact times, large gradients and high molecular diffusion coefficients [24]. Nevertheless, diffusive mixing is slow compared with the convection of material along the microchannel, and the required microchannel lengths for mixing can be excessively long in order to sufficiently homogenize the unmixed volumes [28]. Though, this can be compensated by operating at high flow velocity in the channel. Chaotic advection mixing further accelerates diffusive mixing operation by stretching, folding and dispersing the fluid streams. This is achieved by forcing motion transverse to the flow direction upon the fluid, for instance by machining well-structured grooves that are placed in the microchannel. The drawback of this type of mixer is that to develop a strong chaotic advection mixing, it's necessary to realize complex three-dimensional microstructures which can be difficult to fabricate e.g. the staggered herringbone mixer [52]. The mixing efficiency of passive mixers can also be increased by increasing the interfacial area which for example is done through repeated split-and-combine of flows in microchannels. Passive mixers are generally integrated on a chip-type or microchannel enzyme reactor (see Figure 2.6a for example). Swarts *et al.* [30] utilized a Y shaped mixer to mix substrate and enzyme solution that were injected into the chip from two separate inlets. Moreover, Jung *et al.* [56] and Kee and Gavriilidis [28] both combined different passive mixers in series on the same chip i.e. a Y shaped mixer and the staggered herringbone mixer machined inside a serpent like microchannel to ensure that diffusion time is faster than the catalyzed reaction time during a continuous mode operation.

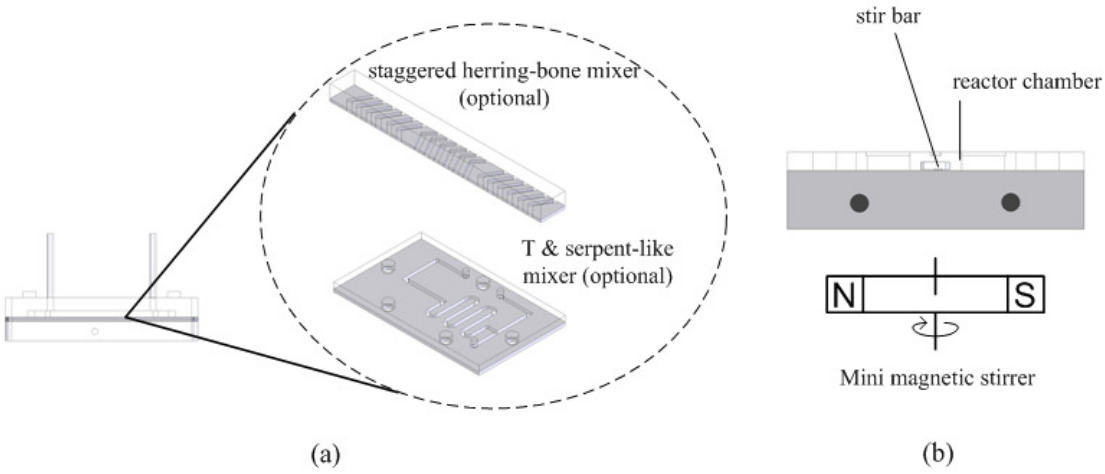

Figure 2.6. (a) Chip type microbioreactor design with integrated passive mixers – T shaped mixer, serpent-like channel and the staggered herringbone mixer [28,52,56]. (b) Active mixing scheme i.e. magnetically actuated stirrer bar, applied in microbioreactor designs consisting of a cylindrically shaped reaction chamber [26,29,57,58].

In active mixing schemes, moving parts (e.g. variable-frequency pumps off-chip, moving component on chip i.e. stirrer bar, etc.) are utilized to periodically perturb the flow field creating transverse flows within the designated cross-sectional area [52,54,55]. Active mixing schemes can be activated on demand and are commonly deployed to induce mixing inside a reaction chamber (i.e. cylindrical shape chamber) of microbioreactors. One of the examples of such mixing scheme is the magnetically actuated stirrer bar – an active mixing scheme that often is utilized in microbial cell-based microbioreactors [26,29,57,58] (see Figure 2.6b for example). The use of a stirrer bar is advantageous as it provides more interfacial area for mixing. Specifically for a microbial fermentation, the stirrer bar also provides the necessary updraft lifting force to keep the microbial cells in suspension [24]. In the microbioreactor design of Zhang *et al.* [29], a ring-shape magnetic stirrer bar (6 mm arm length, 0.5 mm diameter) was fabricated and mounted on a hub (i.e. a rigid vertical post) for a steady mixing on a fixed rotational axis. Whilst this system creates defined liquid movement in the reaction chamber volume, it suffers from a couple of drawbacks as well. First, both the stirrer bar as well as the hub needed to mount the impeller require a precise fabrication which can be complicated and secondly, it cannot guarantee that there are no dead zones in the reactor: the corners between the vertical walls and the horizontal floor are typically the most critical point [24]. An alternative solution and perhaps a simpler approach is to use a commercially available micro magnetic stirrer bar [57,58]. Schäpper *et al.* [57] and Zainal Alam *et al.* [58] used a micro magnetic stirrer bar (3 mm length, 1.2 mm diameter, Sigma) and actuated it above this magnetic stirrer platform – reactor was positioned slightly off the center of the platform – to create a random chaotic motion inside the reactor chamber. Thus, this eliminates any possible dead zones whilst keeping the microbial cells in suspension. Another type of active mixing approach involves moving of the reactor boundaries. Lee *et al.* [27] assembled a series of inflatable air cushions in the ceiling of the reactor chamber. Periodic inflation of these air cushions generated peristaltic movement of the liquid in the reactor chamber. Furthermore, Li *et al.* [59] employed a recycle flow mixing strategy where external syringe pumps coupled with multi-ports valves were used to pump liquid back and forth between serially connected reactors. Since the recirculation flow was operated at a high flow velocity, fluid motion is

no longer laminar but approaches transition phase conditions. Hence, they created a convection flow that increases the concentration gradient (i.e. reduces diffusion length) for faster diffusion.

2.2.3 Reactor fluidics

The term reactor fluidics refers to the fluidic-handling capacity of microbioreactors and it encompasses the establishment of reliable macro-to-micro fluidic interconnects, pumping mechanisms for different modes of operation (i.e. preferably continuous mode) and feasible substrate and enzyme feeding strategies for running enzymatic reaction.

Connections

A microbioreactor system requires carefully designed fluidic interconnects to reliably interface the system to macro world devices (e.g. pumps). Reliable fluidic interconnects are highly desirable as they are required for delivery of liquids to and from the reactor internal microfluidic network and/or the reaction chamber of the microbioreactor. Various types of fluidic interconnects have been applied to provide a satisfactory solution for microbioreactor system macro-to-micro fluidics interfacing. This includes needle-diaphragm interconnects [57], gluing a tube into fluidic ports [58,60], metal ferrule-O ring interconnects [61] and the standard tube-nut assembly [31,50].

In the needle-diaphragm interconnects, fluidic connections are made by piercing a needle into the reactor side wall (i.e. made of PDMS) and all the way through a self-sealing septum (i.e. diaphragm) that could either be embedded inside or attached on the outside of the reactor walls (Figure 2.7a) [57]. The enclosing PDMS walls that surround the needle ensure adequate tightness – exploiting the elastic properties of PDMS – where else the embedded diaphragm provides a leak-proof connection. A certain minimum PDMS layer thickness may be required to guarantee sufficiently tight sealing, and such interconnects may only be feasible for a PDMS-based reactor. Despite offering an easy-to-use and cheap solution for the microbioreactor system, it has several drawbacks. First, although the fluidic connection offers a reversible connection, the needle can only few times be removed and inserted back into the reactor before the embedded diaphragm starts to leak. Secondly, the alignment is a problem, where a slight mishandling may compromise the leak-free operation of the reactor. This is however solvable by creating a small microchannel to guide the needle in.

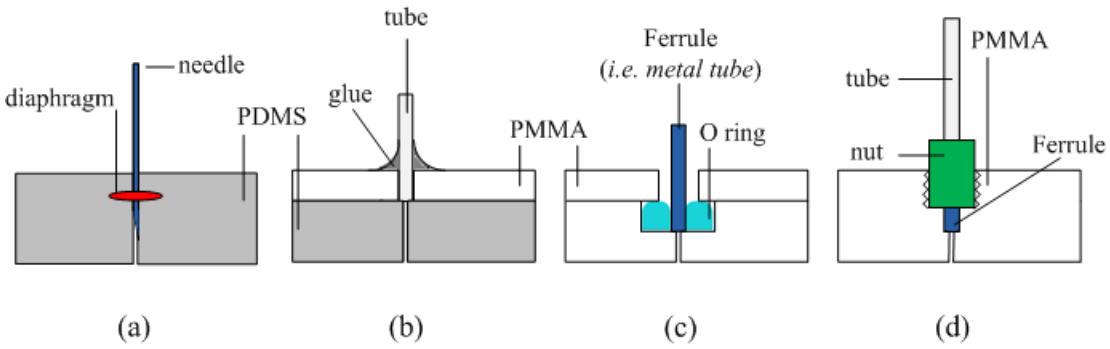

Figure 2.7. Various types of fluidics interconnects that have been applied to establish microbioreactor macro-to-micro fluidics interface. (a) Needle-diaphragm interconnects (*top view*) [57]. (b) By gluing a tube into fluidic ports [58,60]. (c) Metal ferrule-O ring interconnects [61]. (d) A standard tube-nut assembly [31,50].

Gluing a tube into a fluidic port is in theory the simplest approach to establish fluidic connections on thermoplastic polymer substrates (e.g PMMA) [58,60]. Standard size chromatography tubing can simply be glued into fluidic ports or holes that have been fabricated on a microbioreactor interface and are connected to the internal fluidic network (Figure 2.7b). The size of the drilled hole is typically fabricated to have an inner diameter that is one-tenth smaller than the outer diameter of the tube to ensure a tight connection (i.e. rule of thumb). A certain minimum depth is also required for a steady connection, and thus preventing the tube from disconnecting during an experiment. During fabrication, often there is a mismatch between the shape/size of the drilled hole and the tube which normally results in a gap. To avoid any leakages, adhesives (i.e. glue or epoxy) are mainly used for bonding. The use of adhesives can however be very risky as the glue (or the epoxy) may seep into the gap due to capillary forces and clog the microchannel [62]. Despite its simplicity, and despite the fact that it can be useful for a chip used for proof-of-concept experiments, this type of connection is unreliable, and the connection established is irreversible (i.e. permanent connection). Moreover, the spatial extent of the glue cone that forms around the connected tube limits the minimum distance between adjacent fluidic ports. However, more viscous glue can be used to overcome this problem but the complexity of the gluing process makes it uneconomical if many connections have to be made [62].

A more versatile approach is to connect rigid tubes or metal ferrules into connection holes that have been fabricated on a microbioreactor interface with the use of a soft intermediate element, e.g. O rings in combination with mechanical stress to ensure a tightly sealed connection (Figure 2.7c) [61]. The connecting tubes typically stand normal to the substrate plane and tightness is ensured by two sealing interconnects: the surface between the ferrule and the O ring (mostly defined by how oversized the tube is), and that between the O ring and the device itself (largely defined by the axial or radial space into which the O ring is pressed) [63]. Concentric shape grooves can be fabricated around the connection holes to facilitate proper alignment of the O ring. To reduce the number of fabrication steps for each reactor and also for ease of operation, the metal ferrule-O ring interconnects can also be established on a chip holder where compression of the surface-contact gaskets (i.e. O rings) between the holder and the microfabricated chip tightly seals the fluidic connections. Though this type of interconnects has the advantage that they allow for repeated unplugging and plugging of the connection in an easy manner (i.e. reversible

connection); nonetheless, it requires a precise fabrication of the O ring as well as for bonding of the corresponding polymer substrates (e.g. PMMA) and thus trained fabrication personnel.

Reliable microbioreactor fluidic connections can also be established with the use of commercially available chromatography fittings. Threaded ports can be fabricated on a microbioreactor interface to fit specialized connectors (e.g. from Upchurch Scientific, Vici Jour, etc.) for a standard tube-nut assembly (Figure 2.7d) [31,50] – fluidic interconnects that are normally achieved on thermoplastic polymer substrates (e.g. PEEK, PMMA, etc.). This type of interconnects has a low dead volume, is leak-proof over a wide operating pressure range and could provide a plug-and-play solution for fluidic connections of microbioreactor systems. They are however, relatively costly and occupy a large area when mounted.

Ideally, satisfactorily fluidic interconnects for microbioreactor systems – at least for a laboratory work environment – should encompass the following requirements; low dead volume, leak-proof over a wide pressure range, inert (i.e. does not react with the reactor content), good solvent resistivity, easy to use (i.e. 'plug-and-play' fluidic ports), simple design and cheap fabrication [24,62,63]. These requirements nonetheless are difficult to meet and thus far, feasible solutions are often a compromise between easy handling, cost and specific system requirements.

Pumping mechanism

The pump is an important component in a continuous membrane microbioreactor system. It is utilized generally for (1) supply/transport of liquids to the reactor from the feed reservoir, (2) recirculation (or mixing) of the reactor content e.g. in the loop reactor system, and (3) to create the necessary pressure for separation to occur. In most microbioreactor systems, external syringe pumps (i.e. positive displacement pumps) are employed [28,30,31,50,58-61]. Syringe pumps produce a highly accurate flow and they do not require any specialized tubing connection for operation (i.e. macro-micro-world fluidic interface is relatively easy). With syringe pumps, the syringe itself serves as the feed reservoir which is sized based on reactor operating flow conditions. For example, a microbioreactor system is designed with a working volume of about 200 µL, and is set to work at a residence time of 1 hr, for a total operation time of approximately 6 hours. To meet these requirements, the pump should operate at a flow rate of 200 $\mu L.hr^{-1}$ with a syringe that has a volume capacity larger than 1.2 mL. Else, the syringe will run low of feeding solution and thus halt the entire experiment. Refilling the syringe in the middle of an experiment will only increase the risk for introducing bubbles into the system when reconnecting the fluidic connections.

In a loop-type membrane reactor system or in a *crossflow* membrane filtration operation, a recirculation line (i.e. consists of a recycle pump and tubing connecting the pump to the reactor) is often integrated [31,50]. This is necessary especially to recirculate the reactor content (i.e. retained enzymes and the substrate solution) whilst minimizing the concentration polarization effects. Sufficient mixing is provided by operating at high recirculation to feed flow ratio. An important factor to consider when designing the recirculation line is the pressure drop within the capillary tube. Pressure-drop in the capillary tube can be estimated from the Hagen-Poiseuille equation i.e. $\Delta P = 8\eta lQ/\pi r^4$ [64], where ΔP is the pressure drop (Pa), η is liquid viscosity (Pa.s), l is the tube length

(m), Q is volumetric flow rate ($m^3.s^{-1}$) and r is the radius of the capillary (m). Based on the equation, pressure drop can be reduced if shorter tube length, l is used. Muller *et al.* [31] deployed a micro-gear pump as a recirculation pump in their loop reactor system. The micro-gear pump employed has the capacity to dispense volumes as low as 0.25 µL with an operating flow rate ranging between 0.15 to 300 $mL.min^{-1}$. The micro-gear pump used – i.e. connected via standard chromatography fittings – also ensures a steady flow rate and low shear stress effect.

Interfacing a microbioreactor system with external pumps (e.g. syringe pumps, micro-gear pumps, etc.) is a very straightforward way for transporting fluids into/within the system but these pumps have a considerably large footprint – compared to the size of a microfluidic chip – and are very costly. Such a solution is perhaps only limited to testing the workability of newly designed single reactor system prototypes. Liquid handling for parallel operation is rather complex (i.e. requires a defined flow splitting system) and operation-wise, is not very flexible (e.g. equal input flow rates for every chip) [24]. A typical arrangement for these pumps in a loop-type reactor system is illustrated in Figure 2.8a.

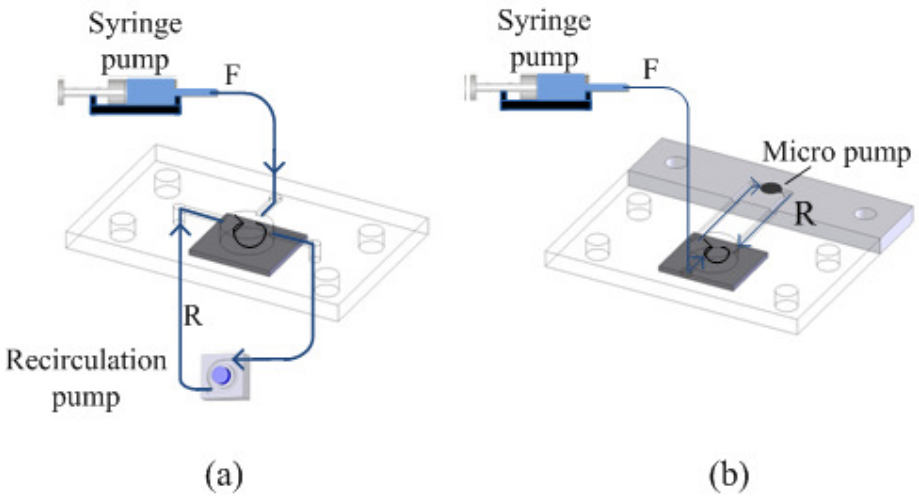

Figure 2.8. (a) Typical arrangement of external syringe and recirculation pumps in a loop-type reactor system [31,50]. (b) Integrated micropump as an alternative to a relatively larger external recirculation pump [65].

An alternative solution is to integrate the reactor system with onboard micropumps and microvalves e.g. a micro pneumatic pump [65]. In such a micropump, the fluid flow is facilitated by peristaltic motion of the pumping chamber (i.e. pneumatic tank) which squeezes the fluid into the desired direction. Individual flow rates to/from the reaction chamber can be realized although this will require a series of air chambers with reciprocating membrane, active valves and properly structured internal fluidic network [65,66]. This adds on to the complexity of the system with respect to fabrication and installation difficulty. Such a system, thus far, has only been evident in perfusion reactor systems; nevertheless implementation to other types of microbioreactor systems (e.g. enzyme or microbial cell-based system) can also be made possible [67]. A similar onboard micropump design was also applied by Lee *et al.* [27] where minute amounts of acid/base was injected into the reaction chamber for pH control of their microbioreactor system. Micropumps can also be integrated into a microbioreactor system as a driving mechanism

for recirculation flow and therefore eliminate the need for a larger and expensive external recirculation pump (see Figure 2.8b for an example). Integrated micropumps and microvalves are indeed potential substitutes for transportation of fluids to/from or within microbioreactor systems. Furthermore, they also keep the small footprint characteristic of the microbioreactor and ease the process of multiplexing microbioreactor systems [24,68] – all while maintaining fabrication cost at a reasonable level.

Feeding strategy

The continuous mode of operation normally entails a continuous feeding of substrate solution into the reactor system. Since continuous pumping also provides the necessary pressure for separation to occur, this technically rules out any possibility of operating the system in batch mode operation. However, by integrating a multi-ports valve at the feeding line, a batch-wise loading of substrate solution with subsequent flushing step with inert solution (e.g. buffer) – a semi-continuous mode of operation – can be facilitated [50]. Such a substrate feeding strategy can be very useful (1) for washing out hydrolysis product residues during an experiment, and (2) for achieving a high conversion rate, since a low substrate concentration (i.e. high [E]/[S] ratio) can be maintained in the reactor system. The use of multi-ports valves also prevents any formation of bubbles during re-distribution of liquids. Switching of port connections can be done either manually or automatically (i.e. similar to a typical analytical chromatography column system). Another important consideration is the location of the inlet fluidic port for the feeding solution. Ideally, it should be as close as possible to the main reaction zone (e.g. reaction chamber or microchannels embedded with passive mixers [28-31,50]). This is specifically to promote a good mixing between fresh substrate and reaction medium.

In larger reactor systems (e.g. milliliter scale and upwards), the enzyme solution can be directly injected into the reactor. This method however is not feasible for a reactor with a fixed working volume that operates under bubble-free conditions because direct injection (e.g. with needles) will also introduce bubbles into the system. Therefore, a different enzyme feeding strategy needs to be pursued. Various types of enzyme feeding strategies are available for micro scale enzyme reactors. The first is based on the use of a commercially available sample loop. A sample loop containing a defined enzyme solution (i.e. loop volume is available from 10 µL and upwards, Upchurch scientific) is normally integrated into a multi-ports valve that is placed in between the feed reservoir and the reactor fluidic inlet port. The enzyme solution is then pushed into the reactor system as substrate feeding is initiated (Figure 2.9a) [31]. In a chip-type reactor system, the enzyme solution is pumped into the reactor through a separate inlet [28,30]. To implement such technique in a loop-type reactor system is however not so straightforward. A microvalve may have to be utilized to stop the flow of the enzyme solution before substrate feeding can take place. As the reactor has a fixed volume, the same amount of reactor content will be pushed out of the system during the addition of the enzyme solution (Figure 2.9b). A simpler approach is to first fill the reactor (adapter is mounted to disconnect and reconnect the loop) with enzyme solution before initiating the reaction with subsequent substrate feeding (Figure 2.9c). In this manner, reactor preparation efforts are reduced, and simpler reactor design eases the fabrication process [50].

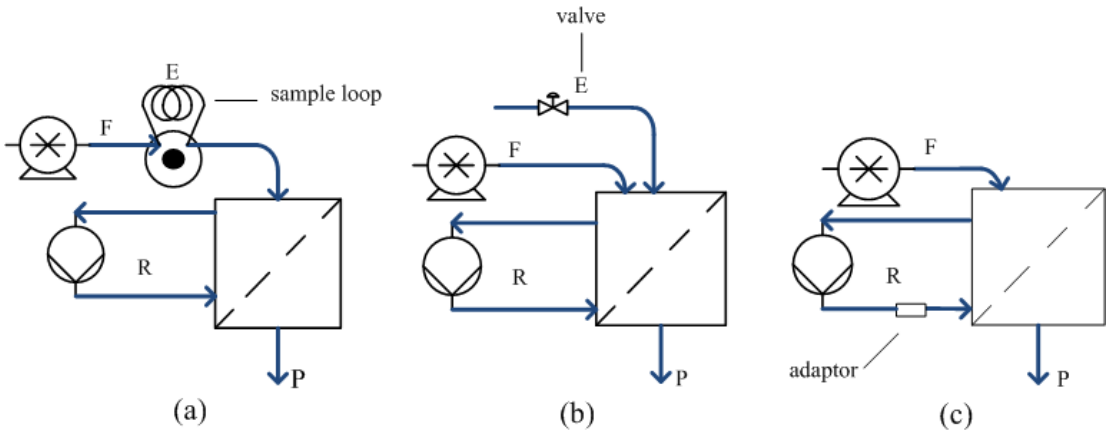

Figure 2.9. Various options for addition of enzyme into a microbioreactor system. (a) With the use a of sample loop [31]. (b) Through a separate inlet [28,30]. (c) Fill the reactor with enzyme solution first before initiating the reaction with subsequent substrate feeding [50].

2.2.4 Measurement and process control

On-line process monitoring and control is often a requirement for a standard microbioreactor design as they are a necessity in order to obtain meaningful experimental results. Temperature, pH and pressure are key physical variables in running enzymatic reactions in membrane bioreactors. This part of the review thus focuses on state-of-the-art sensing and control of the aforementioned physical variables in microbioreactor systems. Measurement techniques that may be useful for monitoring the progress of the enzymatic reaction (i.e. potential detection methods) in membrane microbioreactors are reviewed as well.

Temperature

In microbioreactors, temperature is typically measured by means of thermistors or resistance temperature detectors (RTDs) [27,59,69,70]. Thermocouples are used in some setups [26,29,33,71]. RTDs are sensors with resistance varying according to the temperature; RTDs made up from a platinum element are preferably used (e.g. Pt 100 or Pt 1000 sensors; both have a nominal resistance of 100 and 1000 Ohm at 0^{o}C, respectively) [72]. RTDs are very cheap and commercially available in bulk quantity. Since they are mass-fabricated for many industries in relatively small sizes (e.g. 5x2x1.3 mm), this type of sensors can easily be embedded into the microbioreactors for a precise temperature measurement of the microbioreactor content [58,70]. They are fairly accurate (~0.1^{o}C) [73] and able to operate reliably for a long period of time [70]. Moreover, RTDs can also be connected to an external circuit with connecting lead wires or wire bonded onto a printed circuit board for on-line temperature measurement and control [69,73]. Such features are crucial for parallel operation at various operating temperatures. Ideally, for a precise temperature measurement, the temperature sensor should be located close to the microbioreactor chamber. However in several cases it was reported that temperature was measured on other parts of the setup. Lee *et al.* [27] controlled the temperature of the microbioreactor by measuring the temperature of the base plate holding the microbioreactors. Vervliet-Scheebaum *et al.* [73] integrated the Pt 100 sensor in a flow-through measuring device to measure the temperature of the liquid that was circulating in

the microbioreactor system. Zanzotto *et al*. [33], Szita *et al*. [26], Boccazzi *et al*. [71], and Zhang *et al*. [60] measured the temperature of the circulated heated water that was used to control the temperature of the microbioreactors or of the enclosing chamber.

Whilst temperature measurement is relatively easy to establish in microbioreactors, temperature control on the other hand is a rather challenging task due to the high surface area to working volume ratio (*S/V*). For instance, a conventional bench-scale bioreactor with a height to diameter (*H/D*) ratio of 2 would have an *S/V* ratio of about 0.9 [75]. In contrast, microbioreactors with a chamber diameter of 10 mm and height of about 2 mm would give an *S/V* ratio of about 1500 [29]. This implies that heat transfer in microbioreactor systems is large and very rapid compared to conventional systems. One also needs to bear in mind that heat loss by natural convection is significant and inevitable when working at such a small scale. Another factor affecting the efficiency of temperature control in microbioreactors is the location of the heating element. It is crucial to place the heating element so that it will not create a large temperature gradient [70]. This is particularly important for microbioreactors fabricated from PMMA and PDMS because these materials have a very low thermal conductivity, about 0.2 $W.m^{-1}.K^{-1}$ [76] and 0.17 $W.m^{-1}.K^{-1}$ [77] for PMMA and PDMS, respectively.

Temperature uniformity in the microbioreactor chamber is also a critical issue in establishing a good temperature control system for a microbioreactor. There are several techniques that can potentially be used to probe temperature uniformity in the reactor chamber. First, one could place several temperature sensors at different spots within the reactor chamber to evaluate the temperature distribution. Secondly, thermal distribution patterns in the reactor chamber can also be examined by monitoring heat images by using a thermo or infra-red camera [78,79]. Finally, based on a model describing mass and heat transfer in a microbioreactor one could also opt for simulating a three-dimensional (3D) temperature distribution profile in the reactor chamber using e.g. the finite element method [29,70], which is now a standard engineering tool implemented in several software packages.

Several alternatives are available to efficiently control the microbioreactor temperature. The simplest method is to conduct the experiment in a temperature controlled room [74], water bath [30] or in an incubator [31,80]. Vervliet-Scheebaum *et al*. [74] reported that the temperature variation can be kept within 1.5^{o}C of the desired set point in a temperature controlled room. Although temperature can be accurately controlled with this method, and it also allows for the operation of many microbioreactors in the same space at the same temperature, it is of course not feasible for parallel operation of microbioreactors at different operating temperatures, such as when screening for the optimal temperature of an enzymatic reaction. Another option is to link the device to a water bath and circulate thermostated water through the microbioreactor chamber base [26,29,33,71]. The main drawback of this method is the limitation it imposes on the parallel operation of reactors at different temperatures. Also, the additional fluidic system increases the risk of a liquid leak leading to failure of the temperature control system. Temperature control in microbioreactors may also be accomplished by integrating electrical micro-heaters [27,69,70,73]. Maharbiz *et al*. [69] and Krommenhoek *et al*. [73] incorporated a micro-heater on a printed circuit board that was adhered to the base of the microbioreactors. The micro-heater was positioned next to the thermistors such that tight temperature control of the microbioreactor content could be achieved. Lee *et al*. [27] implemented a commercially available on-off controller (Minco, Minneapolis U.S.A., CT325TF1A5) to control the

temperature of the base plate that served as the microbioreactor holder. The microbioreactor temperature was controlled by maintaining the temperature of the copper base plate by using a foil heater. Petronis *et al.* [70] embedded two electrode heaters in the side walls of the microbioreactor chamber to create an even heat distribution across the chamber. Having an integrated heater in the microbioreactor setup is by far the most preferable method for temperature control in microbioreactors as it is simple, cheap and allows for parallel operation at different temperatures, provided some thermal insulation preventing thermal cross-talk is in place. However, as the reactor chamber is not thermally insulated, the high *S/V* ratio makes a well-functioning temperature control loop necessary.

pH

Standard pH probes are too bulky and not feasible for use in microbioreactors. The most commonly applied miniature pH sensors are optical sensors based on fluorescence sensor spots or 'optodes' [26,27,29,71,82] and solid state, ion sensitive, field effect transistor (ISFET) pH sensor chips [37,69,73,83]. Many microbioreactor operators seem to prefer the optical sensors owing to their non-invasive feature and easiness of integration [26,27,29,33,61,71,84]. Since optodes do not require any reference element to perform pH measurements and are relatively cheap (about EUR 15 per piece) they are good alternatives for disposable microbioreactors [26,29,33,71]. Optical sensing is performed either through fluorescence intensity or fluorescence lifetime measurements [26,29,33,71,84]. The fluorescence sensor spots however, suffer from the photo bleaching effect, reducing their lifetimes, and have a rather narrow dynamic pH range, typically 2-4 pH units [84]. Lifetime would not be an issue for single-use reactors as the reactor packaging could be lightproof and the reaction itself typically does not run long enough for this to be an issue. Optical pH sensors have a measurement accuracy of about 0.01 pH unit with a response time (t_{90}) less than 90 s. Furthermore, the operating temperature for optodes ranges from 0 to 50^{o}C. Most pH sensor spots have a measurement range from pH 4 to 9, and a nonlinear response [84]. This nonlinearity is apparent as a low sensitivity of the sensor signal to pH changes at both ends of the measurement range, which makes accurate pH control there very difficult. In the middle of the measuring range the sensor spots have a nearly linear response with a sensitivity of around 10 degrees phase angle per pH unit. In contrast, the ISFET pH sensors cover a wider pH range (typically from pH 2-12 [85]) and have a linear response similarly to that of a standard pH probe (Nernstian sensitivity of about 58.2 mV per pH unit at 20 °C [85]). ISFET pH sensors have a measurement accuracy of about 0.01 pH unit with response time (t_{90}) less than a second. They can also work under a wide temperature range (-45^{o}C to 120^{o}C). Though ISFET pH sensors have a broader dynamic measurement range and greater sensitivity than the pH sensor spots, the ISFET pH sensors have also some drawbacks. This includes measurement drift (linear and reproducible in due course, thus allowing for compensation of data) and sensitivity to surrounding light [37,69,85]. Moreover, the ISFET pH sensor chip requires a reference electrode (i.e. Ag/AgCl reference electrode) to perform the pH measurement [37,69,73], meaning that the microbioreactors have to be designed such that the part with the integrated ISFET pH chip is reusable to keep the cost per microbioreactor at an acceptable level. Practically, this is typically done by encapsulating the ISFET pH sensor chip on a printed circuit board before integrating the pH sensor into the microbioreactor [37,69,73]. Despite some limitations, both sensors have been proven to provide a rapid and precise pH measurement over a long period of time [26,27,29,33,37,61,69,71,73,82-84]. It can thus be concluded that a real time pH measurement in microbioreactors, similar to the pH monitoring feature of the lab-scale bioreactors, is fully feasible.

While a number of reliable pH sensors are available for *on-line* monitoring of pH, pH control in microbioreactors is still in the developing phase. Early attempts to control pH in microbioreactors were accomplished by either a buffered system [26,29,33,71,74] or by intermittently injecting base or acid [27,61,67,75,86]. The use of buffer to control pH in microbioreactors is the simplest way of controlling pH. Nevertheless, the use of a buffered system is not always sufficient to maintain a constant pH level: pH buffers have a limited buffering capacity, and can only compensate for a certain number of ions before losing the resistance towards pH changes. This limitation was apparent in a stirred, membrane-aerated microbioreactor study where the pH dropped by nearly 2 pH units due to the acidification during the fermentation process [33]. The limit on the buffer capacity can however be extended in a continuous microbioreactor reaction system. Wu *et al.* [87] showed in a perfusion reactor system that continuous feeding of a freshly buffered nutrient medium enabled the reactor pH to be kept constant to within ± 0.02 pH units. It is to be expected that a similar effect would be visible in any continuous microbioreactor system, assuming that the buffer strength is adapted to the substrate concentration.

Intermittently injecting base or acid is another alternative approach to pH control in microbioreactors. It is a direct adaptation of a bench-scale bioreactor pH control method. Zhang *et al.* [61] and Lee *et al.* [27] showed that the decrease of the pH value due to the metabolic activity of the growing microorganisms can be compensated by intermittent injection of a base solution. Lee *et al.* [27] managed to reach higher cell densities when pH was maintained longer at the desired set point. However, this method is limited by the microbioreactor chamber volume. The addition of an excessive volume of acid or base dilutes the culture broth which leads to uncertainties in concentration measurements [86]. A strong base (or acid) can be used to reduce the added volumes, however, this may lead to local high (or low) pH values, particularly if mixing is poor. Such pH deviations can deactivate enzymes, leading to lower average conversion rates for the enzymatic reaction that is studied. A solution to this problem would be gaseous pH control, the practical feasibility of which has been proven by Isett *et al.* [81] and it has been implemented in an industrial system [88] in a 24-well 4-6 mL plate where NH_3/CO_2 are sparged through the individual wells. Maharbiz *et al.* [69] developed an in situ electrolytic gas generation where CO_2 gas can be precisely dosed from underneath the reactor chamber through a thin, semi-permeable silicone membrane. However, Maharbiz *et al.* [69] have yet to test the effectiveness of CO_2 gas generation for pH control with a real culture. The method applied seems promising but formation of bubbles due to gas diffusion is not desirable in microbioreactors. De Jong [37] demonstrated that the pH of a *Saccharomyces cerevisiae* fermentation can be controlled by dosing of CO_2 gas and NH_3 vapor. However, this method needs further development as the microbioreactor that was fabricated had poor mixing and the response time with respect to pH control was rather slow (the pH took several hours to return back to its desired set point). Although both Maharbiz *et al.* [69] and De Jong [37] have yet to optimize their methods, they have certainly underlined the potential of introducing gases through a membrane to control pH in microbioreactors.

Pressure

A miniaturized pressure transducer is generally used to measure pressure changes in micro membrane reactors. It can be mounted on a T junction connector, and is normally connected in between the feed reservoir and the inlet fluidic port [31,50,64,80]. The voltage output signal of these miniature pressure sensors can be correlated to standard

pressure readings (e.g. bar, Pa, psi, etc.), and often a linear relation is obtained. Measurement could be attained either as an absolute pressure or as relative pressure values (i.e. the pressure difference between system pressure and the atmospheric pressure) [50,64,80]. In a continuous membrane microbioreactor system, the necessary pressure for separation is created by the feeding pump. The feeding pump may be exploited as an actuator to regulate the system pressure, but the drawback is that altering the feed flow rate will perturb the reaction residence time (i.e. conversion rate) as well as the product removal rate. Consequently, this might result in an unsteady state condition due to variation of substrate feeding rate. Moreover, tuning of the feeding rate to meet the desired operating pressure is difficult as pressure might also increase due to accumulation of unreacted substrates that are retained in the system during continuous operation. This type of accumulation is uncontrollable.

Detection methods

In most microbioreactor experiments, sampling is not possible due to the small working volumes of the reactor, and monitoring of the concentration dynamics typically relies on *on-line* optical measurement systems, e.g. optical density (OD) measurements [26,27,29,33,60,61]. However, in a membrane microbioreactor system, under pressurized conditions, reaction products (e.g. low molecular weight substances) can be continuously removed from the reaction system in the permeate flow. The ability to filter out the reaction products continuously from the microbioreactor system allows for (1) collection and fractionation of reaction products (e.g. in small sample vials) to monitor the progress of the reaction, and (2) obtaining a clean/pure hydrolysis product that is free of contaminants (i.e. enzyme, unreacted substrates, etc.) [22]. The latter is indeed an added advantage of membrane microbioreactor systems as many different types of analytical techniques (e.g. gas chromatography [31], mass spectrometry [47], etc.) or assays can now be applied to analyze reaction products (i.e. hydrolysis products). The amount of sample generated may be very low but this is not an issue as the sample can be diluted to produce the desired amount of sample for further analysis.

The permeate stream can also be readily interfaced with a microfluidic chip [89] to enable *on-line* monitoring via optical probes. In the simplest microfluidic detection chip design, it may consist of a single inlet and outlet fluidic port joined together with a microchannel. The chip also comprises of grooves for the placement of optical fibers. These grooves are typically aligned perpendicular to the position of the microchannel inside the chip. The gap between the grooves and the microchannel can be fabricated to be as short as 50 μm [89] and the microchannel width is defined by the desired path length for *on-line* measurement. Light emitted from the light source is guided into the microfluidic chip with optical fibers (or probes), sent through the microchannel, and then guided back to a photodetector (i.e. either as transmitted or reflected signal) [24]. Most optical measurement techniques are sensitive to ambient light, thus to avoid any measurement interference from the ambient light, the microfluidic chip can be confined in a lightproof box. Mounting the optical probes via a microfluidic detection chip at the permeate stream instead of inserting the optical probes into the microbioreactor system has the advantage that the measured signal will have less interferences from bubbles and chaotic motion of the spinning magnetic stirrer bar, and will have greater selectivity as the desired product is filtered out from a complex reaction medium. This approach offers the possibility to facilitate various types of *on-line* optical measurement systems such as ultra-violet (UV) absorption, Near-infrared (NIR) spectroscopy, Raman spectroscopy, etc. for measuring the

product concentration [90,91].

The UV absorption method is a simple transmission measurement system and is commonly applied in microbial cell-based microbioreactors to measure, e.g. optical density (OD) of cells [26,27,29,33,60,61,91]. When light at a specific chosen wavelength, λ is excited, I_o through a space (i.e. containing a sample) with defined optical path length, l, part of the light is selectively absorbed by the sample while the remaining light may be transmitted (or reflected) back, I_t. The absorbance measured (i.e. $A = log\ I_o/I_t$) is then correlated in accordance to the Beer-Lambert law (i.e. $A = \varepsilon\ c\ l$, where A is sample absorbance, ε is the extinction coefficient ($M^{-1}.cm^{-1}$), l is the optical path length (cm) and c is the concentration of the measured sample (M) [92]) to estimate the concentration of product of interest. For example, pectin lyase (PL) catalyzed de-polymerization of a pectin macromolecule structure via a β-elimination mechanism produces relatively shorter saccharides with a double-bond on their non-reducing ends [5,13]. These double-bonds readily absorb light at a wavelength, λ, of 235 nm and can be exploited to estimate the concentration of saccharides (mono, dimers, trimers, etc.) resulting from the hydrolysis reaction [50]. It is important to note that UV absorption only measures the total amount of saccharides produced per volume and it cannot distinguish shorter fragments from the long ones.

Spectroscopy (e.g. NIR [91,92], Raman spectroscopy [90,91], etc.) is also a viable *on-line* optical measurement method and may offer means to simultaneously measure, e.g. concentration changes of various analytes. These systems scan a whole wavelength spectrum in one single measurement. Measurements could be based on transmission or on diffuse reflectance measurements, or a combination of both (transflectance). Evaluation of spectral data is however not so straightforward. It requires a feasible signal processing in combination with the use of chemometric models to estimate the desired analyte concentrations. Each of these measurement systems has its own merits and limitations and one must first carefully evaluate them before implementation. For example, NIR is less expensive and simpler to implement than Raman spectroscopy, but suffers from significant signal interference from water. On the contrary, Raman spectroscopy offers more flexibility in choice of wavelength and provides excellent spectra in aqueous systems (i.e. the Raman spectrum of a specific analyte is often not affected by weak scattering of the water band), but strong fluorescence activity of many biological molecules often overlaps Raman scattering bonds [91]. The latter can make measurements very difficult.

2.3 Conclusion

Microbioreactors, and especially the combination of a membrane separation with a microbioreactor – a so-called membrane microbioreactor – are promising tools for performing enzymatic hydrolysis experiments with high-molecular organic biopolymers. However, a successful membrane microbioreactor design will depend on the implementation of relatively simple – to keep reactor fabrication cost low – but reliable engineering solutions for every single important reactor design aspect that is to be considered in the frame of the targeted applications. A concrete understanding of the properties and the complexity/nature of the used substrates (solubility, viscosity, etc.), and in addition to that knowledge of the reaction kinetics in the targeted operating range (temperature, pH, residence time, etc.), are all valuable inputs that will support the design process. The design of a membrane microbioreactor system can be divided into two parts:

the design of individual reactor components (i.e. pumps, mixing, controllers, etc.) and the integration of individual reactor components in the membrane microbioreactor system. Whilst development of each of the individual reactor components is important for the construction of the reactor, the real challenge however lies in combining all these components together in order to obtain a complete workable membrane microbioreactor system. Due to technical differences as well as the need to integrate them on a very small microbioreactor footprint (i.e. working volume < 1 mL), these individual components may not easily fit together, and a compromise might be necessary to resolve the mismatch. Indeed, there is often not a single 'ideal' solution, and every design solution normally has specific merits and drawbacks. Therefore, in the final microbioreactor design, one must carefully balance between the reactor limitations and important specific process requirements.

2.4 References

[1] Wong, D. (2008). Enzymatic Deconstruction of backbone structures of the ramified regions in pectins, *Protein journal*. **27**: 30-42.

[2] Perez, S., Rodriguez-Carvajal, M. A. and Doco, T. (2003). A complex plant cell wall polysaccharide: rhamnogalacturonan II. A structure in quest of a function, *Biochimie*. **85**: 109-121.

[3] Todisco, S., Calabro, V., and Iorio, G. (1994). A kinetic model for the pectin hydrolysis using an *endo*-acting pectinase from *Rhizopus*, *Molecular Catalysis*. **92**: 333-346.

[4] Martinez, M., Gullon, B., Yanez, R., Alonso, J. L. and Parajo, J. C. (2009). Direct enzymatic production of oligosaccharides mixture from sugar beet pulp: Experimental evaluation and mathematical modeling, *Agricultural and Food Chemistry*. **57**: 5510-5517.

[5] Jayani, R. S., Saxena, S. and Gupta, R. (2005). Microbial pectinolytic enzymes: A review, *Process Biochemistry*. **40**: 2931-2944.

[6] Aksu, Z. and Isoglu, I. A. (2006). Use of agricultural waste sugar beet pulp for the removal of Gemazol turquoise blue-G reactive dye from aqueous solution, *Journal of Hazardous Materials*. **B137**: 418-430.

[7] Bhushan, S., Kalia, K., Sharma, M., Singh, B. and Ahuja, P. S. (2008). Processing of apple pomace for bioactive molecules, *Critical Reviews in Biotechnology*. **28**: 285-296.

[8] Mayer, F. and Hillebrandt, J.-O. (1997). Potato pulp: microbial characterization, physical modification, and application of this agricultural waste product, *Applied Microbiology and Biotechnology*. **48**: 435-440.

[9] Molnar, E., Eszterle, M., Kiss, K., Nemesthoty, N., Fekete, J. and Belafi-Bako, K. (2009). Utilization of electrodialysis for galacturonic acid recovery, *Desalination*. **241**: 81-85.

[10] Pinelo, M., Jonsson, G., and Meyer, A. S. (2009). Membrane technology for purification of enzymatically produced oligosaccharides: Molecular and operational features affecting performance, *Separation and Purification Technology*. **70**: 1-11.

[11] Yamaguchi, F. Shimizu, N. and Hatanaka, C. (1994). Preparation and physiological effect of low-molecular-weight pectin, *Bioscience, Biotechnology and Biochemistry*. **58**: 679-682.

[12] Moerschbacher, B. M., Mierau, M., Graeβner, B., Noll, U. and Mort, A. J. (1999). Small oligomers of galacturonic acid are endogenous suppressors of disease

resistance reactions in wheat leaves, *Journal of Experimental Botany*. **50**: 605-612.

[13] Yadav, S., Yadav, P. K., Yadav, D., and Yadav, K. D. S. (2009). Pectin lyase: A review, *Process Biochemistry*. **44**: 1-10.

[14] Round, A. N., Rigby, N. M., Macdougall, A. J. and Morris, V. J. (2009). A new view of pectin structure revealed by acid hydrolysis and atomic force microscopy, Carbohydrate Research. **345**: 387-397.

[15] Pedrolli, D. B., Monteiro, A. C., Gomes, E. and Carmona, E. C. (2009). Pectin and Pectinases: Production, characterization and industrial application of microbial pectinolytic enzymes, *The Open Biotechnology Journal*. **3**: 9-18.

[16] Kiss, K., Nemestothy, N., Gubicza, L. and Belafi-Bako, K. (2009). Vacuum assisted membrane bioreactor for enzymatic hydrolysis of pectin from various agro-wastes, *Desalination*. **241**: 29-33.

[17] Rodriquez-Nogales, J. M., Ortega, N. Perez-Mateos, and Busto, M. D. (2008). Pectin hydrolysis in free enzyme membrane reactor: An approach to the wine and juice clarification, *Food Chemistry*, **107**: 112-119.

[18] Olano-Martin, E., Mountzouris, K. C., Gibson, G. R., and Rastall, R. A. (2001). Continuous production of pectic oligosaccharides in an enzyme membrane reactor, *Food engineering and Physical Properties*. **66**: 966-971.

[19] Belafi-Bako, K., Eszterle, M., Kiss, K., Nemestothy, N., and Gubicza, L. (2007). Hydrolysis of pectin by *Aspergillus niger* polygalacturonase in a membrane bioreactor, *Food Engineering*. **78**: 438-442.

[20] Gallifuoco, A., Alfani, F., Cantarella, M., and Viparelli, P. (2001). Studying enzyme-catalyzed depolymerizations in continuous reactors, *Industrial and Engineering Chemistry Research*. **40**: 5184-5190.

[21] Rodriquez-Nogales, J. M., Ortega, N. Perez-Mateos, and Busto, M. D. (2008). Operational stability ad kinetic study of a membrane reactor with pectinases from *Aspergillus niger*, *Food Science*. **70**: 104-108.

[22] Andric, P., Meyer, A. S., Jensen, P. A. and Johansen, K. D. (2010). Reactor design for minimizing product inhibition during enzymatic lignocellulose hydrolysis II. Quantification of inhibition and suitability of membrane reactors, *Biotechnology Advances*, **28**: 407-425.

[23] Zhu, X., Bersano-Begey, T., Kamotani, Y., and Takayama, S. (2006). *Encyclopedia of Medical Devices and Instrumentation*, 2nd Edition. John Wiley & Sons, Inc., New York: 383-400.

[24] Schäpper, D., Zainal Alam, M. N. H., Szita, N., Lantz, A. E., Gernaey, K. V. (2009). Application of microbioreactors in fermentation process development: a review, *Analytical and Bioanalytical Chemistry*. **395**: 679-695.

[25] Diano, N., Grimaldi, T., Bianco, M., Rossi, S., Gabrovska, K., Yordanova, G., Godjevargova, T., Grano, V., Nicolucci, C., Mita, L., Bencivenga, U., Canciglia, P. and Mita, D. G. (2008). Apple juice clarification by immobilized pectolytic enzymes in packed or fluidized bed reactors, *Agricultural and Food Chemistry*. **56**: 11471-11477.

[26] Szita, N., Bocazzi, P., Zhang, Z., Boyle, P., Sinskey, A. J., and Jensen, K. F. (2005). Development of a multiplexed microbioreactor system for high-throughput bioprocessing, *Lab on a Chip*. **5**: 819-826.

[27] Lee, H. L., Bocazzi, P., Ram, R. J., and Sinskey, A. J. (2006). Microbioreactor arrays with integrated mixers and fluid injectors for high throughput experimentation with pH and dissolved oxygen control, *Lab on a Chip*. **6**: 1229-1235.

[28] Kee, S. and Gavriilidis, A. (2009). Design and performance of microstructured

PEEK reactor for continuous Poly-L-leucine catalysed chalcone epoxidation, *Organic process Research and Development*. **13**: 941-951.

[29] Zhang, Z., Szita, N., Boccazzi, G., Sinskey, A. J. and Jensen, K. F. (2005). A well-mixed, polymer-based microbioreactor with integrated optical measurements, *Biotechnology and Bioengineering*. **93**: 287-296.

[30] Swarts, J. W., Vossenberg, P., Meerman, M. H., Janssen, A. E. M. and Boom, R. M. (2008). Comparison of two-phase lipase-catalyzed esterification on micro and bench scale, *Biotechnology and Bioengineering*. **99**: 855-861.

[31] Muller, D. H., Liauw, M. A. and Greiner, L. (2005). Microreaction technology in education: Miniaturized enzyme membrane reactor, *Chemical Engineering Technology* **28**: 1569-1571.

[32] Sung, J. H. and Shuler, M. L. (2009). Prevention of air bubble formation in a microfluidic perfusion ell culture system using a microscale bubble trap, *Biomedical Microdevices*. **11**: 731-738.

[33] Zanzotto, A., Szita, N., Boccazzi, P., Lessard, P., Sinskey, A. J. and Jensen, K. F. (2004). Membrane-aerated microbioreactor for high-throughput bioprocessing, *Biotechnology and Bioengineering*. **87**: 243:254.

[34] Tsai, J. and Lin, L. (2002). Active microfluidic mixer and gas bubble filter driven by thermal bubble micropump, *Sensors and Actuators A*. **97-98**: 665-671.

[35] Fernandes, P. (2009). Miniaturization in biocatalyst, *International Journal of Molecular Science*. **11**: 858-879.

[36] Betts, J. I. and Baganz, F. (2006). Miniature bioreactors: current practices and future opportunities, *Microbial Cell Factories*. **5**:21.

[37] De Jong, J. (2008). Application of membrane technology in microfluidic devices (*Ph.D. thesis*), University of Twente, Twente.

[38] Zhao, Y. G., Lu, W. K., Kim, S. S., Ho, S. T. and Marks, T. J. (2000). Polymer waveguides useful over a very wide wavelength range from the ultraviolet to infrared, *Applied Physic Letter*. **77**: 2961-2963.

[39] Fleger, M. and Neyer, A. (2006). PDMS microfluidic chip with integrated waveguides for optical detection, *Microelectronic Engineering*. **83**: 1291-1293.

[40] Becker, H. and Gärtner, C. (2008). Polymer microfabrication technologies for microfluidic systems, *Analytical and Bioanalytical Chemistry*. **390**: 89-111.

[41] Tsao, C. W. and Devoe, D. L. (2009). Bonding of thermoplastic polymer microfluidics, *Microfluidics and Nanofluidics*. **6**: 1-16.

[42] Mcdonald, J. C. and Whitesides, G. M. (2002). Poly(dimethylsiloxane) as a material for fabricating microfluidic devices, *Accounts of Chemical Research*. **35**: 491-499.

[43] Huang, C-W. And Lee, G-B. (2007). A microfluidic system for automatic cell culture, *Micromechanics and Microengineering.* **17**: 1266-1274.

[44] De Jong, J., Lammertink, G. H., and Wessling, M. (2006). Membranes and microfluidics: a review, *Lab on a Chip*. **6**: 1125-1139.

[45] Jonsson, G. (1985). Molecular weight cut-off curves for ultrafiltration membranes of varying pore sizes, *Desalination*. **53**: 3-10.

[46] Wang, P-C., Devoe D. L. and Lee, C. S. (2001). Integration of polymeric membranes with microfluidic networks for bioanalytical applications, *Electrophoresis*. **22**: 3857-3867.

[47] Gao, J., Xu, J., Locascio, L. E. and Lee, C. S. (2001). Integrated microfluidic system enabling protein digestion, peptide separation and protein identification, *Analytical Chemistry*. **73**: 2648-2655.

[48] Jiang, Y. and Lee, C. S. (2001). On-line coupling of micro-enzyme reactor with micro-membrane chromatography for protein digestion, peptide separation and

protein identification using electrospray ionization mass spectrometry, *Chromatography A*. **924**: 315-322.

[49] Posthuma-Trumpie, G. A., Venema, K., van Berkel, W. J. H. and Korf, J. (2007). A low perfusin rate microreactor for continuous monitoring of enzyme characteristic: application to glucose oxidase. *Analytical and Bioanalytical Chemistry*. 389: 2029-2033.

[50] Zainal Alam, M. N. H., Pinelo, M., Samantha, K., Jonsson, G., Meyer, A. M. and Gernaey, K. V. (2010). A continuous membrane microbioreactor system for integrated pectin modification and separation processes, *Submitted to Chemical Engineering Journal – March 2010.*

[51] Xiang, F., Lin, Y., Wen, J., Matson, D. W. and Smith, R. D. (1999). An integrated microfabricated device for dual microdialysis and on-line ESI-ion trap mass spectrometry for analysis of complex biological samples, *Analytical Chemistry*. 71: 1485-1490.

[52] Strook, A. D., Dertinger, S. K. W., Ajdari, A., Mezić, I., Stone, H. A. and Whitesides, G. M. (2002). Chaotic mixer for microchannels, *Science*. **295**:647-651.

[53] Ryu, K. S., Shaikh, K., Goluch, E., Fan, Z. and Liu, C. (2004). Micro magnetic stir-bar mixer integrated with parylene microfluidic channels, *Lab on a Chip*. **4**: 608-613.

[54] Hessel, V., Löwe H. and Schönfeld, F. (2005). Micromixers – A review on active and passive mixing principles, *Chemical Engineering Science*. **60**: 2479-2501.

[55] Lu, L-H., Ryu, K. S. and Liu, C. (2002). A magnetic microstirrer and array for microfluidic mixing, *Microelectromechanical systems*. **11**: 462-469.

[56] Jung, S-Y., Liu, Y. and Collier, P. (2008). Fast mixing and reaction initiation control of single-enzyme kinetics in confined volumes, *Langmuir*. **24**: 4439-4442.

[57] Schäpper, D., Stocks, S. M., Szita, N., Lantz, A. E. and Gernaey, K. V. (2010) Development of single-use microbioreactor for cultivation of microorganisms, *Chemical Engineering* DOI: 10.1016/j.cej.2010.02.038.

[58] Zainal Alam, M. N. H., Schäpper, D. and Gernaey, K. V. (2010). Embedded resistance wire as heating element for temperature control in microbioreactors, *Micromechanics and Microengineering*. DOI: 10.1088/0960-1317/20/5/055014.

[59] Li, X., van der Steen, G., van Dedem, G. W. K., van der Wielen, L. A. M., van Leeuwen, M., van Gulik, W. M., Heijnen, J. J., Krommenhoek, E. E., Gardeniers, J. G. E., van den Berg, A. and Ottens, M. (2008). Improving mixing in microbioreactors, *Chemical Engineering Science*. **63**: 3036-3046.

[60] Zhang, Z., Boccazzi, P., Choi, H., Perozziello, G., Sinskey, A. J. and Jensen, K. F. (2006). Microchemostat – microbial continuous culture in a polymer-based instrumented microbioreactor, *Lab on a chip*. **6**: 906-913.

[61] Zhang, Z., Perozziello, G., Boccazzi, P., Sinskey, A. J., Geschke, O. and Jensen, K. F. (2007). Microbioreactors for bioprocess development, *Association for Laboratory Automation*. **12**: 143-151.

[62] Snakenborg, D., Perozziello, G., Geschke, O. And Kutter, J. P. (2007). A fast and reliable way to establish fluidic connections to planar microchips, *Micromechanics and Microengineering*. **17**: 98-103.

[63] Perozziello, G., Bundgaard, F. and Geschke, O. (2008). Fluidic interconnections for microfluidic systems: A new integrated fluidic interconnection allowing *plug'n'play* functionality, *Sensors and Actuators B*. **130**: 947-953.

[64] van Leeuwen, M., Buijs, N. A. A., Canelas, A. B., Oudshoorn, A., Heijnen, J. J. and van Gulik W. M. (2009). The Hagen-Poiseuille pump for parallel fed-batch cultivations in microbioreactors, *Chemical Engineering Science*. **64**: 1877-1884.

[65] Wu, M-H., Huang, S-B., Cui, Z., Cui, Z. and Lee, G-B. A high-throughput perfusion-based microbioreactor platform integrated with pneumatic micropumps for three-dimensional cell culture, *Biomedical Microdevices*. **10**: 309-319.

[66] Nguyen, N-T., Huang, X. and Chuan, T. K. (2002). MEMS-Micropumps: A review, *Fluids Engineering*. **124**: 384-392

[67] Funke, M., Buchenauer, A., Schnakenberg, U., Mokwa, W., Diederichs, S., Mertens, A., Muller, C., Kensy, F., and Buchs, J. (2010). Microfluidic Biolector – microfluidic bioprocess control in microtiter plates, *Biotechnology and Bioengineering.* DOI: 10.1002/bit.22825.

[68] Melin, J. and Quake, S. R. (2007). Microfludic large-scale integration: The evolution of design rules for biological automation, *Annual Review of Biophysics and Biomolecular Structure*. **36**: 213-231.

[69] Maharbiz, M. M., Holtz, W. J., Howe, R. T. and Keasling, J. D. (2004). Microbioreactor arrays with parametric control for high-throughput experimentation, *Biotechnology and Bioengineering.* **85**:376-381.

[70] Petronis, S., Stangegaard, M., Christensen, C. B. V. and Dufva, M. (2006). Transparent polymeric cell culture chip with integrated temperature control and uniform media perfusion, *BioTechniques.* **40:** 368-376

[71] Boccazzi, P., Zhang, Z., Kurosawa, K., Szita, N., Bhattacharya, S., Jensen, K. F. and Sinskey, A. J. (2006) Differential gene expression profiles and real-time measurements of growth parameters in *Saccharomyces cerevisiae* grown in microliter-scale bioreactors equipped with internal stirring, *Biotechnology Progress.* **22:** 710-717.

[72] Maiti, T. K. (2006). A novel lead-wire-resistance compensation technique using two-wire resistance temperature detector, *IEEE Sensors.* **6**: 1454-1458.

[73] Krommenhoek, E. E., van Leeuwen, M., Gardeniers, H., van Gulik, W. M., van den Berg, A., Li, X., Ottens, M., van der Wielen, L. A. M. and Heijnen, J. J. (2008). Lab-Scale fermentation tests of microchip with integrated electrochemical sensors for pH, temperature, dissolved oxygen and viable biomass concentration, *Biotechnology and Bioengineering.* **99**: 884 – 892.

[74] Vervliet-Scheebaum, M., Ritzenthaler, R., Normann, J. and Wagner, E. (2008). Short-term effects of Benzalkonium Chloride and Atrazine on *Elodea canadensis* using a miniaturised microbioreactor system for an online monitoring of physiologic parameters, *Ecotoxicology and Environmental Safety.* **69**: 254-262.

[75] Gimbun, J., Radiah, A. B. D. and Chuah, T. G. (2004). Bioreactor design via spreadsheet-a study on the monosodium glutamate, *Food Engineering*. **64**: 277-283.

[76] Assael, M. J., Antoniadis, K. D. and Wu, J. (2008). New measurments of the thermal conductivity of PMMA, BK7, and Pyrex 7740 up to 450K, *International Journal of Thermophysics*. **29**:1257-1266.

[77] Shin, Y. S., Cho, K., Lim, S. H., Chung, S., Park, S. J., Chung, C., Han, D. C. and Chang, J. K. (2003). PDMS-based micro PCR chip with Parylene coating, *Micromechanics and Microengineering.* 13: 768-774.

[78] Liu, L., Peng, S., Niu, X. and Wen, W. (2006). Microheaters fabricated from a conducting composite, *Applied Physics Letters*. **89**:223521.

[79] Yamamoto, T., Nojima, T. and Fujii, T. (2002). PDMS-Glass hybrid microreactor array with embedded temperature control device. Application to cell-free protein synthesis, *Lab on a Chip.* **2:** 197-202.

[80] van Leeuwen, M., Heijnen, J. J., Gardeniers, H., Oudshoorn, A., Noorman, H., Visser, J., van der Wielen, L. A. M. and van Gulik, W. M. (2009). A system for accurate on-line measurement of total gas consumption or production rates in

microbioreactors, *Chemical Engineering Science*. **64**: 455-458.

[81] Isett, K., George, H., Herber, W. and Amanullah, A. (2007). Twenty-four-well plate miniature bioreactor high-throughput system: Assessment for microbial cultivations, *Biotechnology and Bioengineering*. **98**: 1017-1028.

[82] PreSens (2009). Noninvasive pH probes. http://www.presens.de/products/brochures/category/sensor-probes/brochure/non-invasive-ph-sensors.html. Accessed 9 March 2009.

[83] Microsens (2009). Ion-Sensitive Field-Effect Transistor. http://www.microsens.ch/products/chemical.html. Accessed 9 March 2009.

[84] John, G. T., Goelling, D., Klimant, I., Schneider, H. and Heinzle, E. (2003). pH-Sensing 96-well microtitre plates for characterization of acid production by dairy starter cultures, *Dairy Research.* **70**: 327-333.

[85] Krommenhoek, E. E., Gardeniers, J. G. E., Bomer, J. G., Li, X., Ottens, M., van Dedem, G. W. K., van Leeuwen, M., van Gulik, W. M., van der Wielen, L. A. M., Heijnen, J. J. and van den Berg, A. (2007). Integrated electrochemical sensor array for on-line monitoring of Yeast fermentations, *Analytical Chemistry*. **79**: 5567-5573.

[86] Buchenauer, A., Hofmann, M. C., Funke, M., Büchs, J., Mokwa, W. and Schnakenberg, U. (2009). Microbioreactors with microfluidic control and a user-friendly connection to the actuator hardware, *Biosensors and Bioelectronics.* **24**: 1411-1416.

[87] Wu, M. H., Urban, J. P. G., Gui, Z. and Cui, Z. F. (2006). Development of PDMS microbioreactor wih well-defined and homogenous culture environment for chondrocyte 3-D culture, *Biomedical Microdevices.* **8**: 331-340.

[88] Applikon Biotechnology (2009). Micro 24 Bioreactor, Netherlands. http://www.applikon-bio.com/cgi-bin/applikonbio/basis-micro-bioreactor-u24. Accessed 9 March 2009.

[89] Fleger, M. and Neyer, A. (2006). PDMS microfluidic chip with integrated waveguides for optical detection, *Microelectronic Engineering*. **83**: 1291-1293.

[90] Ferstl, W., Klahn, T., Schweikert, W., Billeb, G., Schwarzer, M. and Loebbecke S. (2007). Inline analysis in microreaction technology: A suitable tool for process screening and optimization, *Chemical Engineering Technology*. **30**: 370-378.

[91] Ulber, R., Frerichs, J.-G. and Beutel, S. (2003). Optical sensor systems for bioprocess monitoring, *Analytical and Bioanalytical Chemistry*. **376**: 342-348.

[92] Cervera, A. E., Petersen, N., Lantz, A. E., Larsen, A. and Gernaey, K. V. (2009). Application of Near-infrared spectroscopy for monitoring and control of cell culture and fermentation, *Biotechnology Progress*. **25**: 1561-1581.

CHAPTER 3

Embedded resistance wire as heating element for temperature control in microbioreactors

CHAPTER 3

Embedded resistance wire as heating element for temperature control in microbioreactors

---

Abstract

This chapter presents the technical realization of a low-cost heating element consisting of a resistance wire in a microbioreactor, as well as the implementation and performance assessment of an on/off controller for temperature control of the microbioreactor content based on this heating element. The microbioreactor (working volume of 100 μL) is designed to work bubble-free, and is fabricated out of the polymers poly(methylmethacrylate) (PMMA) and poly(dimethylsiloxane) (PDMS). The temperature is measured with a Pt 100 sensor, and the resistance wires are embedded in the polymer such that they either surround the reactor chamber or are placed underneath it. The latter allows achieving an even temperature distribution across the reactor chamber and direct heating of the reactor content. We show that an integrated resistance wire coupled to a simple on/off controller results in accurate control of the temperature of the reactor (± 0.1 ^{o}C of the setpoint value) and provides a good disturbance rejection capability (corrective action for a sudden temperature drop of 2.5 ^{o}C at an operating temperature of 50 ^{o}C takes less than 30 s). Finally, we also demonstrate the workability of the established temperature control in a batch *Saccharomyces cerevisiae* cultivation in a microbioreactor.

This chapter has been published as Zainal Alam, M. N. H., Schäpper, D., and Gernaey, K. V. (2010). Embedded resistance wire as heating element for temperature control in microbioreactors. *Journal of Micromechanics and Microengineering*. DOI: 10.1088/0960-1317/20/5/055014.

3.1 Introduction

Microbioreactors have the promise of offering cheap experimentation under well-controlled conditions, a feature that is highly desirable in the bioprocess engineering field. The fundamental idea underlying the microbioreactor concept is (1) to fabricate a reactor that operates with very small volumes (< 1 mL), thus allowing for high-throughput experimentation; and (2) to develop a micro-scale reactor platform that performs similarly to a bench scale bioreactor (V = 0.5 – 5 L). Miniaturization of experiments obviously leads to a significant cost reduction for substrates and utility consumption. However, it imposes many challenges as well, particularly in establishing a tight control over the culture conditions (temperature, pH, dissolved oxygen concentration, etc.).

In this paper we focus on the establishment of a simple and cheap temperature control scheme in disposable polymer-based microbioreactors. A cheap temperature control system is essential to keep the cost per microbioreactor as low as possible. Such microbioreactors are fabricated specifically to facilitate biological processes, e.g. fermentations [1-6], bioconversion via enzymes [7-8], or cultivations of mammalian cells in perfusion systems [9]. Accurate temperature control is crucial because the reaction rates are temperature-dependent [10].

Ideally, a well-functioning microbioreactor temperature control loop should allow rapid temperature set point tracking as well as providing adequate disturbance rejection throughout its operation [10,11]. However, it should be emphasized here that the relevant time scales in a microbioreactor are considerably larger compared to for example the fast temperature step changes that have been demonstrated in e.g. microfluidic polymerase chain reaction (PCR) chips [12], where heating rates up to 175 $^{o}C.s^{-1}$ have been reported [13]. For fermentation experiments in microbioreactors, for example, it is sufficient if temperature step changes can be achieved within a couple of minutes. With respect to practicality, installation and final assembly of the components of the microbioreactor temperature control loop, the main design requirement is that embedding of the temperature sensor and actuators should neither complicate the reactor microfluidics connections nor compromise the leak-free operation of the system. In our application aiming at development of disposable single-use microbioreactors, the fabrication cost of the temperature control loop has to be kept as low as possible in order to keep the total running cost per experiment low.

In microbioreactors, several technical and heat transfer-related issues have to be tackled before a tight temperature control scheme can be realized. First of all, only limited space is available for insertion of temperature sensors and integration of heating elements as actuators for temperature control. As a consequence, the temperature sensor and the micro-heater have to be positioned within a reasonable thermal distance from each other, such that the temperature measurement – and thus also the heater that usually functions as an actuator in a feedback loop for temperature control – responds according to the change of the temperature of the reactor content (the object being heated) and not the change of the temperature of the heating element. Secondly, microbioreactors have a very high surface area to working volume ratio (S/V) compared to bench scale reactors. Since microbioreactors are typically not thermally insulated, the high S/V ratio leads to significant and inevitable heat dissipation to the surroundings by natural convection; typically at a rate of 20 $W.m^{-2}.{}^{o}C^{-1}$ [9]. On the one hand, this might impose some technical challenges because heat losses to the surroundings need to be compensated with a corresponding heating of the reactor such that the temperature of the reactor contents can

be maintained at a desired set point. One also has to ensure adequate heater power such that sufficient heat can be transferred to induce desired temperature changes. On the other hand, the high S/V ratio is also advantageous because it implies that this type of reactor has a very fast thermal response. This means that only a small amount of heating power is required to raise the temperature of the reactor significantly [14]. Note also that typically only a heating element is required to regulate the microbioreactor temperature. Indeed, the optimal temperature of most fermentation, for example, is typically above room temperature (20 ^{o}C). Finally, another point that needs to be taken into account is the uniformity of the local heating of the microbioreactor. It is critically important that the heating element is placed such that an even heat distribution in the reactor chamber is achieved. Uniform temperature of the microbioreactor contents can also be promoted by guaranteeing sufficient mixing in the reactor and by appropriate design of the reactor.

Potential solutions for temperature control in microbioreactors have been recently reviewed by Schäpper *et al.* [11]. As summarized in Table 3.1, potential solutions include temperature controlled rooms or incubators [15], circulating thermostated water through the microbioreactor chamber base [2,3], and the integration of electrical micro-heaters [4-6,9,14]. As an alternative to already proposed temperature control methods in microbioreactors, we propose the use of resistance wires integrated in polymer-based microbioreactors as a suitable heating element that allows a tight temperature control. It is first described in detail how the resistance wires were embedded in the polymer, and how temperature control in such a polymer-based microbioreactor is achieved by means of a closed-loop circuit consisting of a Pt 100 temperature sensor, a simple on/off controller and a DC power supply connected to the resistance wires embedded in the polymer. The on/off temperature controller is subsequently tuned, and its performance will be characterized in terms of control accuracy, set point tracking and disturbance rejection capability. Furthermore the temperature distribution profile in the reactor chamber is evaluated and the proposed temperature control scheme is finally demonstrated on a batch *Saccharomyces cerevisiae* cultivation in a microbioreactor.

Table 3.1. State of the art temperature sensing and control in microbioreactors.

Source	Type of MBR	Working Volume (μL)	T sensor	Measurement approaches	Operating T (°C)	T regulation	Control precision
[15]	Loop reactor	150 – 650	Pt 100	*ex situ*	25	T Controlled room	± 1.5 °C
[2,3]	Stirred tank	50 – 150	Thermo-couple	*ex situ*	37	Reactor base heated with thermosted water	N/A
[4]	Micro well	250	Thermistor	*in situ*	25-55	Micro-heater	± 2 °C
[5]	Stirred tank	100	Pt 100	*ex situ*	37	Reactor base heated with foil heater	N/A
[9]	Perfusion	50	Thermistor	*in situ*	37	Micro-heater	± 0.26 °C
[6]	Micro well	200	Pt 100	*in situ*	30	Micro-heater	± 0.4 °C
[14]	Micro tank	1.25	RTD	*in situ*	20 -90	Micro-heater	± 0.4 °C
[This work]	Stirred tank	100	Pt 100	*in situ*	30-50	Resistance wire	± 0.1 °C

MBR=microbioreactor;T=temperature;N/A=data not available.

3.2 Materials and methods

3.2.1 Microbioreactor prototypes

Two different microbioreactor prototypes were fabricated to evaluate the workability of the proposed temperature control scheme. The first microbioreactor prototype (MBRT1) has a simple configuration and was only used for the proof-of-concept study. This includes tuning of the on/off controller and investigation of the controller accuracy, set point tracking and disturbance rejection capability. The second microbioreactor prototype (MBRT2) was fully equipped to allow fermentations with suspended micro-organisms. MBRT2 was thus used (1) to probe temperature uniformity in the reactor chamber and (2) to demonstrate the workability of the proposed temperature control scheme for a batch *Saccharomyces cerevisiae* cultivation.

3.2.2 Microbioreactor prototype 1 (MBRT1)

A scheme of the experimental setup for the MBRT1 prototype is illustrated in Figure 3.1a. MBRT1 consisted of a 3 mm thick poly(dimethylsiloxane) PDMS layer sandwiched in between two 5 mm thick poly(methylmethacrylate) PMMA layers (Figure 1a). Both PMMA layers and the mold for the PDMS layer (also made up from PMMA) were fabricated by using a computer-numerical-controlled (CNC) milling machine (CNC micromill, Minitech MiniMill 3/Pro, Minitech Machinery Coorporation, Norcross, GA, USA). The PDMS layer was fabricated by pouring liquid PDMS (Sylgard 184, Dow

Corning Corp., Midland, MI, USA. Mixing ratio of 10 parts silicone : 1 part curing agent) into the mold and subsequently curing at 70 °C for one hour. The cured PDMS layer was then removed from the mold. The top PMMA layer consists of four clearance holes with a diameter of 3.2 mm for M3 screws and two holes with a diameter of 1.5 mm for the fluidic connections. External fluidic connections were established by gluing standard perfluoroalkoxy (PFA) tubing with an outer diameter of 1.59 mm to these holes. The bottom PMMA layer contains four threaded holes for M3 screws. M3 stainless steel screws were used to press the three polymer layers together for a tight sealing. PMMA layers with a thickness of 5 mm were used because they do not bend significantly when clamped with screws at the desired maximum temperature (~50 ^{o}C) for the experiments. The middle PDMS layer serves as the main body of the MBRT1 prototype. It has a reactor chamber (centered in the middle of the PDMS layer) with a depth of 2 mm and a diameter of 8 mm, resulting in a total working volume of 100 µL. The reactor chamber is connected to the inlet and outlet ports (diameter = 1.5 mm) by two 0.5 mm deep x 1 mm wide micro-channels. These inlet and outlet ports together with the micro-channels function as the micro-fluidic connections for water replenishment and waste outflow, respectively. In the MBRT1 prototype, temperature is the only measured variable. It is measured with a Pt 100 sensor (PCA 1.2005.1L, JUMO GmbH & Co., Fulda, Germany), a resistance temperature detector made up from a platinum element with a nominal resistance of 100 Ohm at 0 ^{o}C [16]. The small size of the Pt 100 sensor (5x2x1.3 mm) enables it to be placed very close to the reactor chamber wall. When positioning the Pt 100 sensor, the sensor tip was fixed in perpendicular position to the reactor chamber (Figure 3.1b), such that it is located less than 1 mm ($\Delta x < 1$ mm) from the reactor chamber.

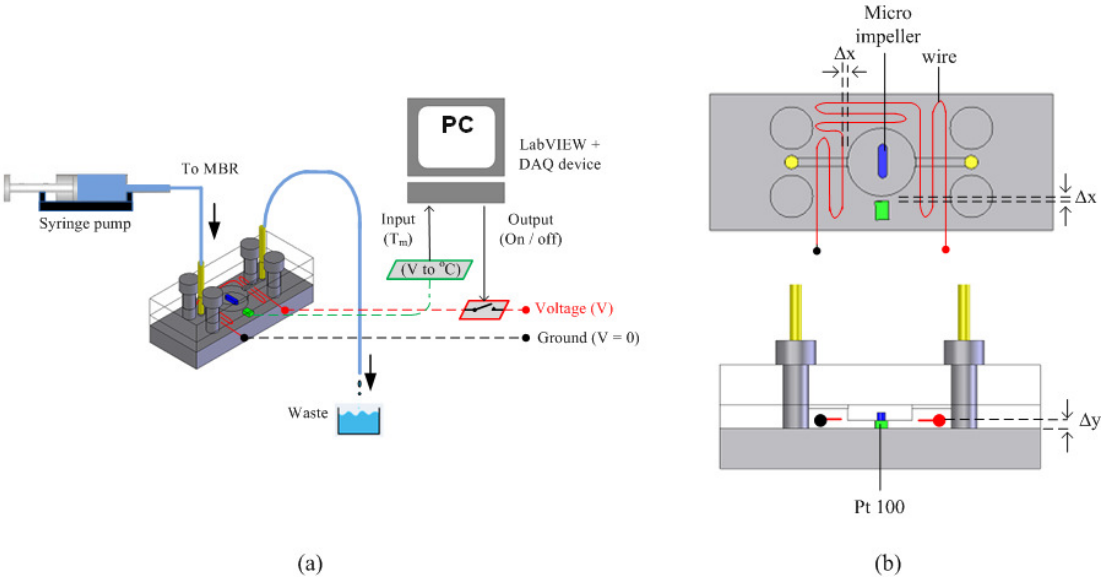

Figure 3.1. Schematic of experimental setup for the MBRT1 prototype. a) Overall setup with fluidic and temperature control connections, b) precise positioning of both the sensor and the heating wire in the reactor.

Kanthal A wire (AB Kanthal, Hallstahammar, Sweden) with an outer diameter of 0.085 mm and a resistivity of 243.2 $\Omega.m^{-1}$ is embedded in the polymer surrounding the reactor chamber. The total length of wire embedded is 14 cm. The wire was embedded in this way in order to achieve an even temperature distribution across the reactor chamber

(Figure 3.1b). The resistance wire was positioned right underneath the micro-channels (Δy = 1 mm) and the measured distance between the resistance wire and the edge of the reactor chamber was less than 1 mm (Δx < 1 mm). The resistance wires are connected to a direct current (DC) power supply (235W ATX Power Supply, DPS-200PB-101, Delta Electronics) and serve as the heating element (actuator) for the temperature control system. The power supply used is a regular ATX computer power supply converted into a DC power supply with 3.3, 5, and 7 volt outputs. Mixing of the MBRT1 reactor contents is achieved by means of a magnetic stirrer bar with a length of 3 mm and diameter of 1 mm that is located in the center of the reactor chamber. In all experiments with the MBRT1 prototype, the reactor chamber was completely filled with distilled water and placed on a magnetic stirrer such that constant mixing was provided at 500 rpm. Since the water evaporation rate in microbioreactors was found to be in the order of magnitude of 5 $\mu L.hr^{-1}$ (water at 37 ^{o}C, membrane with thickness of 100 µm and a diameter of 10 mm) [1], the reactor was continuously fed with distilled water at a flow rate of 10 $\mu L.hr^{-1}$ with a syringe pump (MA1 70-2211, Harvard Apparatus, Massachusetts, USA) to ensure that the reactor volume remains constant throughout the experiment.

3.2.3 Microbioreactor prototype 2 (MBRT2).

This microbioreactor (Figure 3.2a) is designed for the aerobic cultivation of microorganisms. It consists of two thick layers of PDMS and one PDMS membrane which were bonded together to form one single block of PDMS with outer dimensions of 5 x 25 x 40 mm (height x width x length). The bottom main layer (4 mm thickness) includes the reactor volume (cylinder with 9 mm diameter and 3 mm depth resulting in 190 µL volume), two PDMS windows for a pH (SP-pH-HP5-YOP-D4, PreSens - Precision Sensing GmbH, Regensburg, Germany) and a dissolved oxygen (DO) (SP-PSt3-NAU-D4-YOP, PreSens - Precision Sensing GmbH, Regensburg, Germany) sensor spot, a heating wire (copper wire with an outer diameter of 0.1 mm and length of 8.5 cm), a temperature sensor and the stirrer bar (3 mm length, 1.2 mm diameter). Two optical fibers are also cast into the PDMS material which then allows for the measurement of optical density (OD).

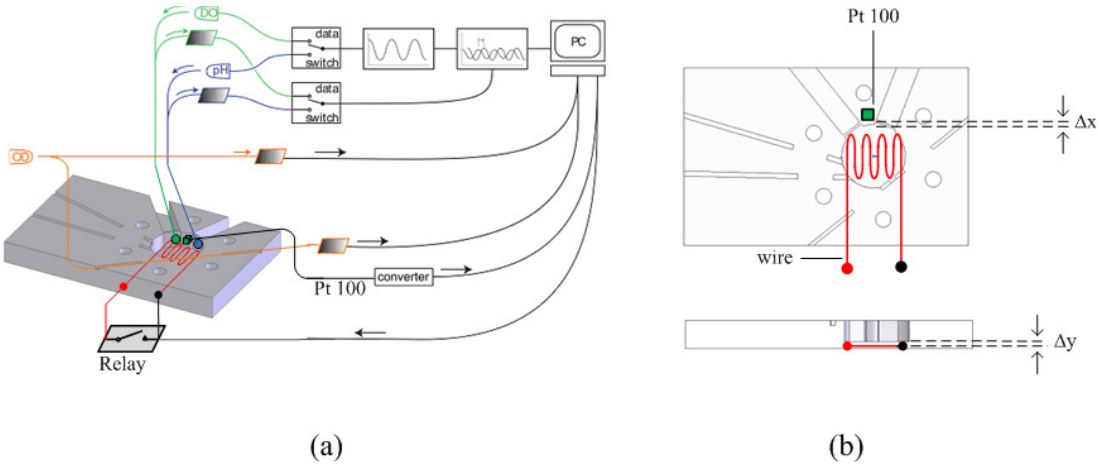

Figure 3.2. Schematic of experimental setup for MBRT2 prototype. a) Overall setup with optical (OD, DO and pH) and temperature control connections, b) precise positioning of both the sensor and the heating wire in the reactor.

For every PDMS layer a negative image was micromilled (CNC micromill, Minitech MiniMill 3/Pro, Minitech Machinery Coorporation, Norcross, GA, USA) into PMMA which then served as a mold. Liquid PDMS (Sylgard 184, Dow Corning Corp., Midland, MI, USA. Mixing ratio of 10 parts silicone : 1 part curing agent) was then poured into the mold and cured at 70 °C for one hour. Upon removal from the mold the two optical sensor spots were bonded onto their respective windows on the inside of the reactor using PDMS itself as the glue. In this manner no additional glue was used, hence eliminating the risk of chemical contamination of the culture. Finally, a magnetic stirrer bar was placed into the bottom (reactor) layer.

The 80 μm thick PDMS aeration membrane was spin-coated onto the bottom of the upper main layer (1 mm thickness) which only serves as a carrier for the aeration membrane. These two main layers were then bonded by applying liquid PDMS to the contact surface and curing for an hour at 70 °C to form one single block of PDMS.

Tight temperature control was achieved by casting the temperature sensor into the PDMS. In this reactor, the temperature sensor was positioned in the side wall of the reactor (Figure 3.2b). Distance between the temperature sensor and the reactor chamber was measured to be less than 0.1 mm ($\Delta x < 0.1$ mm). The heating wire was cast into the floor of the reactor chamber in a meandering shape so that the floor is as evenly heated as possible (Figure 3.2b). The average parallel distance between wire loops is < 2 mm, and the distance to the culture broth is < 0.2 mm ($\Delta y < 0.2$ mm). Good mixing additionally minimizes the risk of temperature gradients both in the reactor material itself and the cultivation broth.

3.2.4 Temperature control scheme

The temperature of the reactor content was controlled by an on/off controller which was implemented in the LabVIEW™ v8.5 software (National Instruments, Austin, TX, USA). Operation of the temperature controller is illustrated in Figure 3.3.

The temperature measurements with the JUMO temperature sensor were converted into an analog voltage signal by means of a transmitter (JUMO dTRANS T04, JUMO GmbH & Co., Fulda, Germany). The output from the transmitter was logged on-line in the computer through a data acquisition (DAQ) card (NI USB-6229, National Instruments, Austin, TX, USA) where the analog voltage signal was linearly correlated with temperature. The LabVIEW program then computed the deviation (error) between the desired set point value T_{sp} and the measured value T_m. If the error is positive ($T_{sp} > T_m$), the heater is activated. In any other situation ($T_{sp} \leq T_m$) the heater will remain off. To ensure a stable operation and prevent rapid switching of the relay output, a time delay of 1 second was introduced before every temperature measurement. For example, if Tm is below Tsp, the heater will be on, for example for a pulse length of 4 seconds, and thus total cycle time would be 5s. When the heater is off, the total cycle time would only be 1 s.

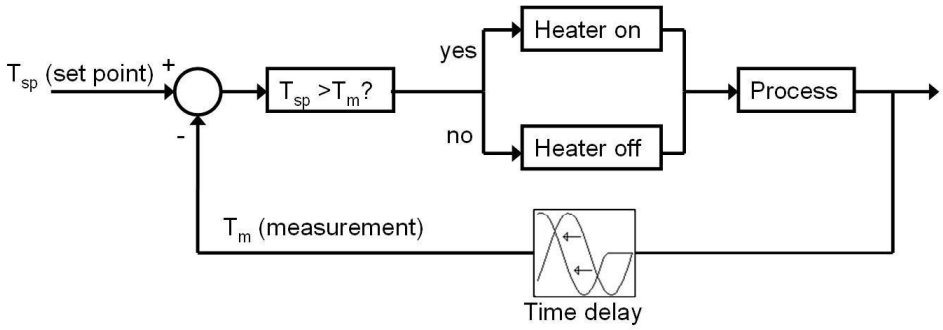

Figure 3.3. Block diagram of the on/off temperature controller.

Heating is achieved by passing an electrical current at fixed voltage through the resistance wire embedded in the microbioreactor. A latching relay was used to connect the voltage supply (235W ATX Power Supply, DPS-200PB-101, Delta Electronics) for heating. When heating is on, the controller will only heat up the system for a short period of time before turning the heater back off. The length of the period during which the heater is on (pulse length) is one of the controller parameters that can be tuned. Other settings to be adjusted by the user are the voltage of the power supply which sets the power of the heating system (heat influx per time), and of course the temperature set point.

3.2.5 Mathematical model of heat transfer in the microbioreactor

Heat transfer in the microbioreactor can be described by the following energy balance equation [17]:

$$m_r c_p \frac{dT}{dt} = Q_{heat} - \left(Q_w + Q_f + Q_{loss} \right) \tag{3.1}$$

where m_r is the mass of water in the reactor chamber (kg), c_p is the specific heat capacity of water (4186 J.kg^{-1}.K^{-1}), T is the corresponding temperature (K), t is the time (hr), Q_{heat} is the heat generated by applying a voltage to the resistance wires (W), Q_w is the heat absorbed due to water evaporation through the thin gas-permeable membrane (thickness ~ 100 μm) covering the top surface of the microbioreactor (W), Q_f is the heat transfer due to the inflow of water into the reactor that was used to replace evaporated water and Q_{loss} is the heat loss to the surroundings by convection (W). Both m_r and c_p are assumed to be constant.

The heat generated by the heating system, Q_{heat}, is a function of the voltage, V across the resistance wire (V) and the current, I flowing through the resistance wire (A) which can be described as [18]:

$$Q_{heat} = VI \tag{3.2}$$

Heat transferred due to water evaporation through the membrane, Q_w is given by the following equation [19]:

$$Q_w = J_w L_v = \theta_w \rho_w L_v \tag{3.3}$$

where J_w is the rate of mass loss due to the water evaporation through the membrane (kg.s^{-1}), L_v is the latent heat of water vaporization, calculated as 2247 kJ.kg^{-1} at 37 ^{o}C [11], ρ_w is the water density (1000 kg.m^{-3}) and θ_w is the water evaporation rate in microbioreactors which was reported to be in the order of magnitude of 5 µL.hr^{-1} (water at 37 ^{o}C, membrane with thickness of 100 µm and a diameter of 10 mm) [1]. In our own evaporation rate experiments, a rate of 1 µL.hr^{-1} for water at room temperature (~23 ^{o}C) was determined.

Heat transferred due to the inflow of water into the reactor to replace evaporated water, Q_f is described as follows [17]:

$$Q_f = \dot{m}_f c_p \left(T_r - T_f\right) \tag{3.4}$$

where $\dot{m}_f$ is the feed flow rate (µL.hr^{-1}), T_f is the feed temperature (^{o}C) and T_r is the reactor temperature (^{o}C).

Heat loss due to natural convection in the microbioreactor was modeled in a similar way as heat transfer by conduction. It was assumed that heat dissipates only through the side wall (wall thickness ~ 12 mm) and through the top surface of the microbioreactor. The floor of the reactor is assumed to cool down at the same speed as the reactor contents. The heat transfer rate through the side wall, Q_{side} and through the top surface of the microbioreactor, Q_{top} is described as follows [16]:

$$Q_{loss} = Q_{side} + Q_{top} = \alpha_{side} A_{side} \left(T_r - T_{amb,side}\right) + \alpha_{top} A_{top} \left(T_r - T_{amb,top}\right) \tag{3.5}$$

where *side* and *top* denote the reactor side wall and top surface, respectively. α_i is the heat transfer coefficient (W.m^{-2}.K^{-1}), A_i is the heat transfer area (m^2), and $T_{amb,i}$ is the temperature of the surroundings (K). By substituting Equations (3.2), (3.3), (3.4) and (3.5) into Equation (3.1), we obtained:

$$m_r c_p \frac{dT_r}{dt} = \underbrace{VI}_{Q_{heat}} - \left[\begin{array}{l} \underbrace{\alpha_{side} A_{side} \left(T_r - T_{amb,side}\right)}_{Q_{side}} + \underbrace{\alpha_{top} A_{top} \left(T_r - T_{amb,top}\right)}_{Q_{top}} + \underbrace{\theta_w \rho_w L_v}_{Q_w} \\ + \underbrace{m_f c_p \left(T_r - T_f\right)}_{Q_f} \end{array} \right] \tag{3.6}$$

The main unknowns here are the heat transfer coefficients of the reactor side wall, α_{side} and the top surface, α_{top} which can be estimated with a cooling down experiment. To this purpose, the MBRT2 microbioreactor was first heated up to a temperature of 35^{o}C (T_r = 308 K) before turning off the heater (Q_{heat} = 0). Since the microbioreactor prototype was not thermally insulated, it immediately cooled down due to heat loss by natural convection until it reached room temperature. Heat transferred due to the inflow of water into the reactor, Q_f was neglected because the experiment was too short and the amount of water

that flows into the reactor to replace evaporated water was too small to influence the value of the heat transfer coefficients, α_{side} and a_{top} ($Q_f = 0$).

In order to determine α_{side} and α_{top} two different experiments were set up (Table 3.2). By placing a temperature controlled air chamber above the microbioreactor the surrounding temperature on the top surface, $T_{amb,top}$ could be set at different desired set points. The model parameters (α_{side} and α_{top}) were then estimated by fitting Equation (6) to the experimental data points by the least squares method implemented in Matlab v7.0 (The Mathworks, Natick, MA, USA) software.

Table 3.2. Experimental conditions for the cooling down experiment.

	Test 1	Test 2
$T_{amb,side}$	Room temperature (~25 ^oC)	Room temperature (~25 ^oC)
$T_{amb,top}$	Room temperature (~25 ^oC)	30 ^oC
T_r	35 ^oC	35 ^oC

3.2.6 Batch *S. cerevisiae* fermentation in MBRT2

Batch fermentations were carried out with *S. cerevisiae* (wild strain type CEN.PK 113-7D). The inoculum was prepared by using a YPD medium containing 10 g/L yeast extract (Lab M, UK), 20 g/L peptone (Lab M, UK), 20 g/L glucose monohydrate (Sigma, US) and 50 µg/L of streptomycin (Sigma, US). pH of the medium was adjusted to a pH of 5.5 with 2M hydrochloric acid. The medium was then autoclaved at 121 ^oC for 20 minutes. Glucose was sterilized separately to avoid caramelization, and was then combined aseptically with the rest of the medium. Streptomycin was added after the medium was autoclaved. A single yeast colony from the stock culture plate was transferred into the prepared medium as inoculum. The medium was incubated overnight on an orbital shaker (700 rpm) at 30 ^oC until the culture reached the exponential phase (optical density ~ 1). Optical density (OD) measurements were done every 2 hours with blank YPD medium as the reference measurement. All experimental work was carried out aseptically and no antifoam or any other substance was added to this inoculum prior to introduction into the microbioreactor.

Before inoculating the reactor with cells, the microbioreactor (MBRT2) was flushed with 70%(v/v) of ethanol to ensure sterility. Then, distilled water was filled into the microbioreactor to wash out the ethanol. For inoculation, a sterile needle was pierced through the PDMS layer of the microbioreactor until the tip of the needle reached the microbioreactor cultivation chamber. A 1 mL sterile syringe was used to transfer 100 µL of the *S. cerevisiae* cultures from the shake flask into the microbioreactor to initiate the fermentation process. The inoculum was injected with care to avoid any introduction of air bubbles into the microbioreactor. One of the inlet channels was then connected to an elevated water reservoir to passively replenish water that evaporated through the thin gas-permeable PDMS layer; thus keeping the reactor volume constant during experimentation. The temperature was controlled at 30 ^oC and oxygen was supplied to the reactor chamber by diffusion of oxygen from the ambient air through a gas-permeable PDMS layer. Mixing was provided by a constant agitation at 600 rpm. The fermentation was monitored by measuring the optical density of the culture broth (OD_{600}) until the cells reached stationary phase.

3.3 Results and discussions

3.3.1 Tuning of the on/off temperature controller

The on/off controller was tuned (with microbioreactor prototype MBRT1) to generate sufficient heat input via the resistance wire for a satisfactory performance over the temperature range of interest. In our application, the operating temperature range of interest is between 30 ^{o}C and 50 ^{o}C, as this is a highly relevant range for cultivation of mesophilic microorganisms (e.g. *Escherichia coli,* 37-42 ^{o}C [10] and *S. cerevisiae,* 30-37 ^{o}C [20]) and mammalian cells (~37 ^{o}C) [21], and for most enzymatic reactions as well [10]. When a voltage is applied to the embedded wire, a current will flow through the wire and thus increase its temperature [18]. The power input by the heater, P is a strong function of the voltage supplied, V (V) and the current, I (ampere). Heat supplied to the system (reactor content) is measured as the energy generated (or dissipated) by the flowing current over a certain period of time. It is a function of heater power input, P (W) and the total heating time, t and was calculated as $E\ (Joule) = V*I*t$.

Figure 3.4a illustrates the response of the on/off controller for a set point value T_{sp} = 50 ^{o}C, when the power input was increased gradually from 0.32 W to 1.43 W. As shown in Figure 3.4a, it can be seen that an increase of the heater power input accelerates the heating process (rise time, t_r, shortened from 5 minutes to 2.55 minutes when the power input was increased from 0.73 W to 1.43 W), as expected, and thus the temperature of the reactor content rises faster. It was also found that sufficient heating was not provided when the heater power input was set at 0.32 W. This behavior is explained because the heater (resistance wire) will only provide a fixed rate of heat input during each pulse (on/off controller), while the rate of heat loss from the system increases as temperature rises. In order to compensate for the heat loss at a higher operating temperature, it is necessary to increase the heat input, E (either by prolonging the heater pulse length, PL or by supplying a higher voltage, V). Any combinations of voltage and time should in the end yield similar total amounts of heat input. This is shown in Figure 3.4b. Regardless of power input supplied (0.73 W or 1.43W) or total heating time (actual heating time was 80% of the rise time, t_r because there was a delay of 1 s for every heating cycle); to reach the temperature setpoint of 50^{o}C, the same amount of heat input, E was provided which was 176.85 J (area under curve). A practical constraint is that the maximal power input is limited according to the type of resistance wire as too large a current will overheat the wire. The wire current handling capacity is depending on its length, L, cross-sectional area, A, wire resistivity, r and the heating time. Also, care has to be taken at high heating power as the controller reacts more aggressively which can lead to overshoot.

However, as demonstrated here, optimal settings (supplied power and pulse length) can be determined with a couple of short dedicated experiments. Moreover, it should be emphasized that these optimal settings are not limited to a certain operating temperature range. Indeed, if one would want to work at a higher operating temperature range where more heat is needed; the wire length or type of wire embedded in the polymer can be modified such that sufficient heating can be provided. This is one example of the flexibility offered by this temperature control method where the resistance wire embedded in the polymer can always be changed to best fit the specific application in mind. Once the optimal settings for each required temperature set point are determined, and assuming that a similar reactor is used for future experiments, the obtained optimal temperature settings can be programmed in the software controlling the setup, such that settings are changed

automatically when the temperature set point is modified. So, all in all the proposed system for microbioreactor temperature control is very user-friendly.

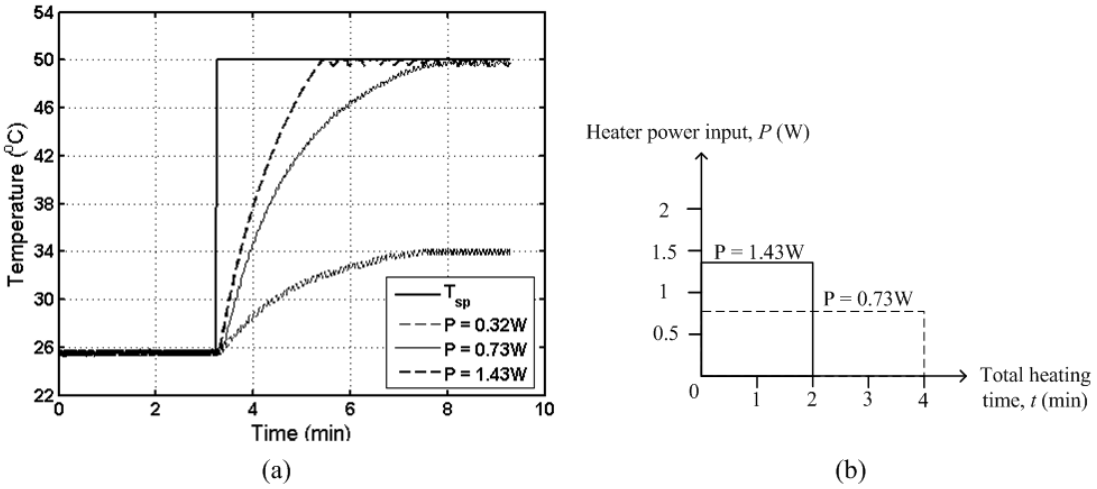

Figure 3.4. a) Response of the on/off controller when different power input was supplied (0.32 W, 0.73 W and 1.43 W) at T_{sp} = 50 ^{o}C. b) Relation between heater power input, P(W) and total heating time, t (min) .Area under curve represents total amount of heat input to the system, *E* (J).

3.3.2 Performance of the on/off temperature controller

The basic functionality was evaluated with microbioreactor prototype MBRT1 and its performance was characterized in terms of its accuracy, set point tracking and disturbance rejection capability. Depending on the characteristics of the controller chosen (power input, heater pulse length and the desired temperature set point), the temperature can be controlled to within $\pm$0.1 ^{o}C of the set point value. This is shown in Figure 3.5a. The results further demonstrate the fast set point tracking capability of the controller for a series of upward step changes in the temperature set point. Almost no delay was observed when temperature was regulated from one set point to another, which is probably due to the high surface area to volume ratio, *S/V* (1500 m^{-1}) in the microbioreactor allowing for a fast thermal response. The largest temperature step from room temperature (~23 ^{o}C) to the temperature set point of 50 ^{o}C only takes about 2.4 minutes. Whilst the heating process is fairly rapid (heating rate ~ 0.25 ^{o}C/s), cooling of the reactor is rather slow. This is because there is no active cooling foreseen on the reactor, and cooling thus merely depends on convective heat transfer to the surroundings. Room temperature is reached asymptotically as the driving force is the temperature difference itself.

The disturbance rejection capability of the controller was evaluated by deliberately perturbing the system from its steady-state at T_{sp} = 50 ^{o}C by injecting a pulse of distilled water at room temperature (~23 ^{o}C) at 15 mL/hr for 6 s. This disturbance (in which 25 % of the reactor content was flushed out) creates a sudden cooling of the reactor content, and a transient response is obtained when the controller drives the system back to the temperature set point (Figure 3.5b). At a temperature set point of 50 ^{o}C, the reactor temperature drops by 2.5 ^{o}C and it took less than 30 s to recover from this disturbance. The results obtained show good disturbance rejection capability of the proposed on/off temperature controller. This

experiment also indicates that positioning of the temperature sensor is close enough to detect any rapid temperature change of the reactor content with a minimal time lag.

Performance of the proposed microbioreactor temperature control system was demonstrated convincingly. The ability to shift the operating temperature is a very useful feature in conducting biological reactions. Such feature could for example be used to execute heat shock treatment to express heterologous protein production in inducible bacterial cultures [22]. Another potential application is for example the determination of the optimal operating temperature in biocatalysis microbioreactor applications to maximize product yield [7], which for a continuous reactor could be achieved by applying a series of temperature set points in the microbioreactor combined with measuring product concentration. It was thus concluded that – compared to method implemented by Maharbiz *et al.* [4], Krommenhoek *et al.* [6], Petronis *et al.* [9] and Yamamoto *et al.* [14] – the accuracy of the proposed temperature control system is as good or better compared to other microbioreactor temperature control schemes (see Table 3.1), and certainly sufficient to perform e.g. fermentation experiments [10,21].

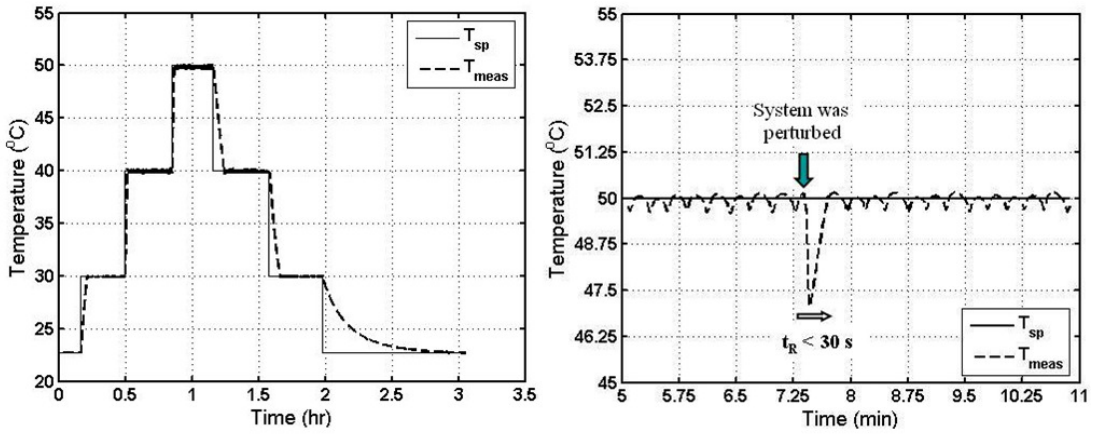

Figure 3.5. a) Response of the on/off controller for a series of step changes in the temperature set point. b) Response of the on/off controller towards a disturbance introduced at T_{sp} = 50 °C.

3.3.3 Temperature uniformity and mixing in microbioreactor prototype MBRT2

The temperature gradient in the reactor was investigated by measuring the temperature difference between the top and the bottom of the reactor chamber upon continuous heating at constant voltage supply of 0.6 V. Precise positioning of the temperature sensors for this experiment is illustrated in Figure 3.6a. Additionally, we also evaluated the quality of mixing in MBRT2 by using a fluorescent dye visualization technique. This was done by observing the mixing of a single drop of fluorescein green solution (DWYER Instruments, Inc. Michigan City, USA) in the reactor chamber at an agitation rate of 500 rpm. Results from both tests are presented in Figure 3.6.

Uniform colour spread of the fluorescent dye (homogenously mixed after approximately 1.2 seconds) indicates that the reactor contents are well-mixed. A slight temperature gradient ($\Delta T < 0.5^{o}C$) from the bottom to the top of the reactor chamber was probably due to a direct exposure of the top of the reactor to the surroundings resulting in

greater heat loss due to natural convection. This corresponds very well with our simulation results where the values of the heat transfer coefficient, α were predicted to be 3 and 59 $W.m^{-2}.K^{-1}$ for the side (α_{side}) and the top (α_{top}) respectively –suggesting a greater heat loss at the air-liquid interface. Furthermore, a comparison of the heat needed to heat up 100 µL of water by 25 °C (177 J) with the energy input through the heating system (0.15 W) and the heat lost through the side and the top of the reactor (0.0775 W using the calculated α values) consistently shows that the system has more than 50% heating loss. This is to be expected as the heating wires dissipate heat both upwards (towards the reactor) as well as downwards (to the surface on which the reactor is lying). In theory, the heat lost could of course be reduced by insulating the bottom of the reactor, but the results presented here convincingly demonstrate that this is not essential to achieve accurate temperature control in the microbioreactor.

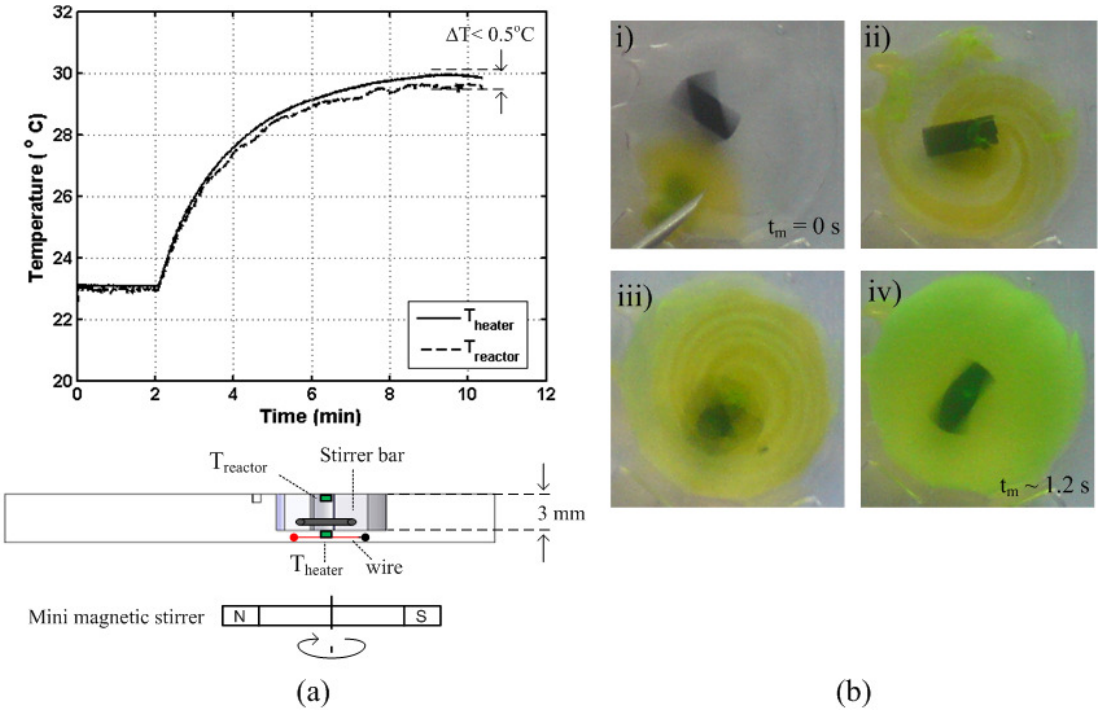

Figure 3.6. a) Positioning of the temperature sensors for temperature uniformity test (*bottom*) and transient response when the reactor was heated up continuously at voltage supplied of 0.6 V (*top*). b) Mixing test at 500 rpm show complete mixing after 1.2 secs.

3.3.4 Temperature controller performance in a *S. cerevisiae* fermentation

The performance of the proposed temperature control system consisting of the embedded resistance wires and an on/off control scheme was tested in a batch *S. cerevisiae* cultivation performed in MBRT2. Here the temperature was controlled at 30 °C which is the optimal growth temperature for the yeast strain used. After a startup phase the cells grow exponentially (Figure 3.7) for approximately eight hours during which time they completely deplete the dissolved oxygen in the culture broth. Temperature control held the culture at 30 ±0.2 °C which is sufficient to allow for undisturbed growth at rates which are comparable to larger scale (e.g. shake flask or bench-scale reactors) cultivations [10,21].

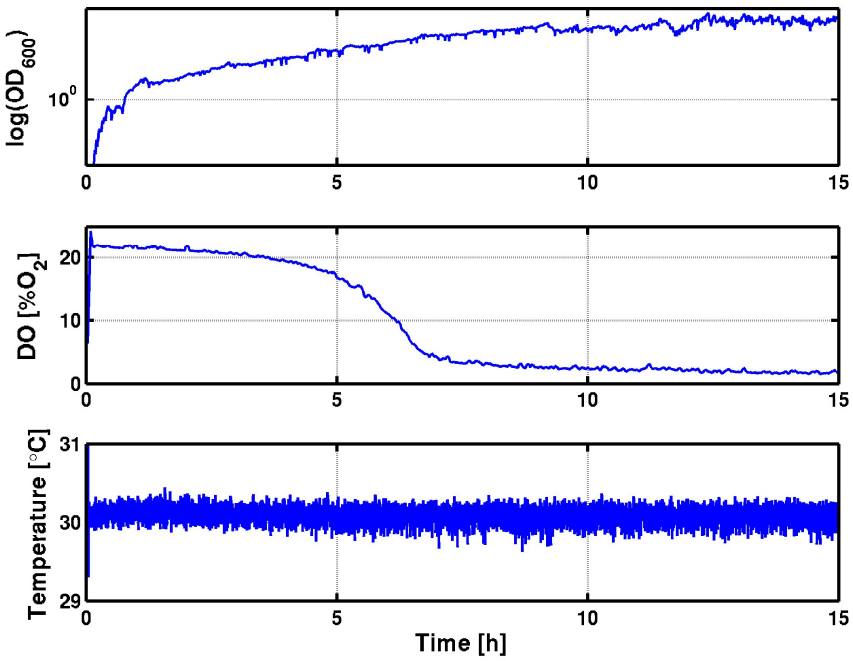

Figure 3.7. Batch cultivation of *S. cerevisiae* at a constant temperature of 30 °C.

3.4 Conclusion

A low-cost temperature control method relying on the use of resistance wires as heating element for polymer-based microbioreactors has been developed. It was shown that a simple on/off temperature controller applying a voltage to resistance wires embedded in the polymer results in accurate control of the temperature of the reactor ($\pm$ 0.1 ^{o}C of the set point value) and provides a good disturbance rejection capability (corrective action for a sudden temperature drop of 2.5 ^{o}C at an operating temperature of 50 ^{o}C takes less than 30 s). The controller is user-friendly as controller performance can be tuned by simply adjusting the supplied power input and the heating pulse length.

The proposed temperature control method fits nicely with the single-use microbioreactor concept, since the cost for the heating wire is negligible (only a few centimeters of resistance wires required per reactor) and the temperature sensor (which is produced in bulk quantities) is inexpensive as well. Despite the low-cost design, microbioreactor temperature control performs very well, as was demonstrated for a batch *S. cerevisiae* cultivation in which the reactor content temperature was controlled tightly at 30 $\pm$0.2 °C throughout the entire cultivation. The method has the additional advantage that it also offers the possibility to be implemented for either a single microbioreactor system or for parallel microbioreactor operations at different temperature set point values.

3.5 References

[1] Boccazzi, P., Zhang, Z., Kurosawa, K., Szita, N., Bhattacharya, S., Jensen, K. F. and Sinskey, A. J. (2006). Differential gene expression profiles and real-time measurements of growth parameters in *Saccharomyces cerevisiae* grown in microliter-scale bioreactors equipped with internal stirring. *Biotechnology Progress* **22:** 710-717.

[2] Zanzotto, A., Szita, N., Boccazzi, P., Lessard, P., Sinskey, A. J. and Jensen, K. F. (2004). Membrane-aerated microbioreactor for high-throughput bioprocessing. *Biotechnology and Bioengineering*. **87**: 243-254.

[3] Szita, N., Bocazzi, P., Zhang, Z., Boyle, P., Sinskey, A. J. and Jensen, K. F. (2005). Development of a multiplexed microbioreactor system for high-throughput bioprocessing. *Lab on Chip*. **5:** 819-826.

[4] Maharbiz, M.M., Holtz, W. J., Howe, R. T. and Keasling, J. D. (2004) Microbioreactor arrays with parametric control for high-throughput experimentation. *Biotechnology and Bioengineering* **85**: 376-381.

[5] Lee, H. L., Bocazzi, P., Ram, R. J. and Sinskey, A. J. (2006). Microbioreactor arrays with integrated mixers and fluid injectors for high throughput experimentation with pH and dissolved oxygen control. *Lab on chip*. **6:** 1229-1235

[6] Krommenhoek, E. E., van Leeuwen, M., Gardeniers, H., van Gulik, W. M., van den Berg, A., Li, X., Ottens, M., van der Wielen, L. A. M. and Heijnen, J. J. (2007). Lab-Scale fermentation tests of microchip with integrated electrochemical sensors for pH, temperature, dissolved oxygen and viable biomass concentration. *Biotechnology and Bioengineering*. **99**: 884 – 892.

[7] Swarts, J. W., Vossenberg, P., Meerman, M. H., Janssen, A. E. M. and Boom, R. M. (2008). Comparison of two-phase lipase-catalyzed esterification on micro and bench scale. *Biotechnology and Bioengineering*. **99**: 855-861.

[8] Muller, D. H., Liauw, M. A. and Greiner, L. (2005). Microreaction technology in education: Miniaturized enzyme membrane reactor. *Chemical Engineering Technology*. **28**: 1569-1571.

[9] Petronis, S., Stangegaard, M., Christensen, C. B. V. and Dufva, M. (2006). Transparent polymeric cell culture chip with integrated temperature control and uniform media perfusion. *BioTechniques*. **40:** 368-376.

[10] Shuler, M. L. and Kargi, F. (2002). *Bioprocess Engineering: Basic Concepts*, 2nd ed., (New Jersey Prentice Hall), pp. 169-170.

[11] Schäpper, D., Zainal Alam, M. N. H., Szita, N., Lantz, A. E., and Gernaey, K. V. (2009). Application of microbioreactors in fermentation process development: a review. *Analytical and Bioanalytical Chemistry*. **395**: 679-695.

[12] Zhang, C. and Xing, D. (2007). Miniaturized PCR chips for nucleic acid amplification and analysis: latest advances and future trends. *Nucleic Acid Research*. **35**: 4223-4237.

[13] Neuzil, P., Zhang, C., Pipper, J., Oh, S. and Zhuo, L. (2006). Ultra fast miniaturized real-time PCR: 40 cycles in less than six minutes. *Nucleic Acid Research.* **34**: e77 1-9.

[14] Yamamoto, T., Nojima, T. and Fujii, T. (2002). PDMS-Glass hybrid microreactor array with embedded temperature control device. Application to cell-free protein synthesis. *Lab on a Chip*. **2:** 197-202.

[15] Vervliet-Scheebaum, M., Ritzenthaler, R., Normann, J. and Wagner, E. (2008). Short-term effects of Benzalkonium Chloride and Atrazine on *Elodea canadensis* using a miniaturised microbioreactor system for an online monitoring of physiologic parameters. *Ecotoxicology and Environmental Safety*. **69:** 254-262.

[16] Maiti, T. K. (2006). A novel lead-wire-resistance compensation technique using two-wire resistance temperature detector. *Journal of IEEE Sensors*. **6**: 1454-1458.

[17] Perry, R. H. (1997). *Perry's Chemical Engineer's Handbook*, 6th ed. (New York: McGraw-Hill).

[18] Madsen, M. J. (2009). Ohm's law for a wire in contact with thermal reservoir. *American Journal of Physics*. **77**: 516-519.

[19] Qtaishat, M., Matsuura, T., Kruczek, B. and Khayet, M. (2008). Heat and mass transfer analysis in direct contact membrane distillation. *Desalination*. **219**:272-292.

[20] Arroyo-Lopez, F. N., Orlic, S., Querol, A. and Barrio, E. (2009). Effects of temperature, pH and sugar concentration on the growth parameters of *Saccharomyces cerevisiae, S. kudriavzevii* and their interspecific hybrid. *Journal of Food Microbiology*. **131:** 120-127.

[21] Chuppa, S., Tsai, Y., Yoon, S., Shackleford, S., Rozales, C., Bhat, R., Tsay, G., Matanguihan, C., Konstantinov, K. and Naveh, D. (1996). Fermentor temperature as a tool for control of high-density perfusion cultures of mammalian cells. *Biotechnology and Bioengineering*. **55**: 328-338.

[22] Razali, F., Moo-Young, M., Scharer, J. M. and Glick, B. R. (2007). Review: Over expression of protein under transcriptional regulation of Lambda r^L promoter system in *Escherichia coli*. Consequences and bioprocess improvement approaches. *Journal of Chemical and Natural Resources Engineering, FKKKSA, Universiti Teknologi Malaysia*. **1:** 22-39.

CHAPTER 4

Establishment of a gaseous pH control concept in microbioreactors

CHAPTER 4

Establishment of a gaseous pH control concept in microbioreactors

---

Abstract

Existing methods for pH control in bench-scale bioreactor systems often can not be directly adapted for microbioreactors. This is because microbioreactors are commonly designed to work with constant volumes, operate bubble-free and have no headspace, which technically rules out any possibility of adding acid/base solution for pH control in microbioreactors. This work reports on the establishment of a gaseous pH control concept in microbioreactors where pH control was achieved by dosing of ammonia (NH_3, 20 000 ppm) and pure carbon dioxide (CO_2) gases to respectively; increase and lower the pH of the reactor content. It encompasses the establishment of an optical pH measurement by means of a fluorescent sensor spot, realization of the necessary gas connections, mixing of gases, and gas-exchange via a thin semi-permeable poly(dimethylsiloxane) (PDMS) membrane. It was shown that addition of NH_3 and CO_2 gases coupled to a simple on/off controller results in a satisfactorily control performance (pH control accuracy = $\pm$ 0.1 of the set point value and system responses of a few minutes were achieved) within the dynamic measuring range of the optical sensor spot which is between pH 6 and 8.

4.1 Introduction

A microbioreactor is a microfabricated reactor (volume typically less than 1 mL) developed as potential substitute to shake flasks and microtiter plates for high throughput and low cost bioprocessing under well-controlled conditions. Compared to conventional shake flasks and microtiter plates, advantages of microbioreactor operation include flexibility due to the possibility of running the microbioreactor in fed-batch or continuous (e.g. chemostat) operation, better mass and heat transfer as microbioreactors can be integrated with pumps, impellers and heaters, the capacity to acquire real-time experimental data which increases the amount of information gained per experiment, and finally, a superior degree of control over relevant experimental conditions – temperature, pH, dissolved oxygen (DO) concentration, etc. Additionally, due to their small size, microbioreactors also offer a number of cost reducing advantages for studying biological processes. These include significant reductions in running cost per experiment (low substrate and utilities consumption, low waste generation), less space required for parallel operation and the possibility of making the microbioreactor disposable to minimize reactor preparation efforts [1].

The basic functionality and usefulness of microbioreactors in running biological experiments (e.g. fermentation processes [2-6], tissue culture [7,8] and enzymatic reactions [9,10]) have been demonstrated. Feasibility for parallel operations with parallel sensing and control over key reactor variables (e.g. pH, temperature and dissolved oxygen concentration, etc.) have also been presented [3-5]. Indeed, the ability to fully control the main reactor variables in a microbioreactor is a necessity not only to obtain meaningful experimental results but also to enable data obtained in microscale to be extrapolated and compared under similar conditions applied in typical bench-scale bioreactors. Whilst methods to control reactor variables, namely temperature and dissolved oxygen concentration, do exist [2-6], suitable methods to control pH in microbioreactors are still in the development phase.

pH has a strong impact on the cell growth and production rate and is important in all enzyme-catalyzed processes as well. In fermentation processes, conversion of carbon sources typically results in a generation of acid and carbon dioxide. This increases the amount of protons (H^+) and thus, acidifies the reactor's content. Consequently, if pH is not controlled at its set point value, culture pH will decrease over time and may halt the cell growth rate due to the fact that the reactor pH shifts away from ideal culture conditions as a consequence of metabolic activity [11]. As for enzyme-catalyzed processes, it is of utmost importance to keep the pH of the reactor close to its optimum value to avoid any production of unwanted product or inactivation of the enzyme. This is because enzymes have a very narrow optimal pH band where they work at their optimal rate [11]. Given the importance of this variable, a tight pH control of the microbioreactor contents is indeed crucial for a successful microbioreactor experiment.

Table 4.1 summarizes currently existing pH control methods in microbioreactors as reviewed by Schäpper *et al.* [1]. The use of buffer is indeed the easiest way to control pH of the microbioreactor contents [2,3,12]. In addition, a buffered system simplifies reactor design. Thus, using buffered solutions eases the fabrication process and keeps cost per microbioreactor low. Despite its simplicity, the use of buffer is not always sufficient, for example due to a limited buffering capacity, where for example a pH drop by nearly 2 pH units has been reported in a buffered system due to the acidification during the

fermentation process [2,3]. This limitation can however be overcome by continuous feeding of freshly buffered medium to keep the pH level constant as demonstrated in Wu *et al.* [8] for a perfusion reactor system. Intermittently injecting base or acid – a typical pH control method for bench-scale bioreactor systems – has also been adapted for pH control in microbioreactors [5,6,13,14]. The limited microbioreactor chamber volume, however, prohibited the addition of sufficient amount of base/acid solution to maintain the pH level constant for a longer duration. Another viable alternative for pH control in microbioreactors is the addition of gas (e.g. ammonia, NH_3 and carbon dioxide, CO_2) through a semi-permeable poly(dimethylsiloxane) (PDMS) membrane [4,15,16]. The practical feasibility of this method has been successfully demonstrated in an industrial system [17] in a 24-well 4-6 mL plate (reactor system than is approximately 20 to 30 times larger in volume compared to a typical size of microbioreactor systems i.e 100-200 µL in volume). In this system, NH_3/CO_2 is sparged through the individual wells. Nevertheless, implementation in a microbioreactor with smaller volumes (< 1 mL) is not so straight forward as these types of reactors are generally designed to work under bubble-free conditions. Careful considerations have to be made for the necessary/additional fluidics connections for gas exchange and mixing. Additionally, the final design should also be feasible for scaling out in order to achieve parallel operation of multiple microbioreactors – all controlled by a feedback control loop to ensure that the desired set point value is met.

Table 4.1 State of the art pH sensing and control in microbioreactors.

Source	pH sensor	Measurement approach	pH regulation	Pros	Cons
[2,3]	pH optode	*in situ*	Buffered system	(1) Simple (2) Easy handling	(1) Limited buffer capacity (2) Scale-up: not feasible
[12]	External pH probe	*ex situ*			
[5,13, 14]	pH optode	*in situ*	Acid/base addition	(1) pH can be maintained longer (2) Scale-up: feasible	(1) Limited reactor volume (2) Concentrated acid/base leads to local high/low pH
[6]	pH ISFET	*in situ*			
[4,16,]	pH ISFET	*in situ*	Gas diffusion through PDMS membrane	(1) Not limited by reactor volume (2) Scale-up: feasible	(1) Complicated fluidics for gas supply
[This work]	pH optode	*in situ*			

In this chapter, we further develop the gaseous pH control concept for microbioreactors that was first introduced by Maharbiz *et al.* [4] and De Jong [16]. We propose the addition of either a gas mixture consisting of nitrogen gas containing 20000 ppm of ammonia or carbon dioxide gas, coupled with a simple on/off controller for pH control in microbioreactors. Introduction of these gases in the reactor was achieved through a thin semi-permeable membrane, thus keeping the microbioreactor volume constant. It is first described in detail how this gaseous pH control concept was achieved by means of a closed-loop circuit consisting of an optical pH sensor, the necessary gas connections, valves, and the on/off controller. The controller performance is then evaluated in terms of

control accuracy, response time and set point tracking capability. Practical issues, limitations and the potential for parallelization of microbioreactors are also discussed.

4.2 Materials and methods

4.2.1 Microbioreactor design and fabrication

The microbioreactor used consists of a disc-shaped reactor with 8 mm diameter and 2 mm height resulting in an operating volume of 100 µL (details of the design have been described elsewhere [18]). It contains a stirrer bar (3 mm long, 1.2 mm diameter) which can move freely inside the reactor. Aeration is achieved through a semi-permeable membrane at the top of the reactor. Gases can diffuse through the membrane and thus in/out of the cultivation broth. Bubble sparging for achieving improved gas transfer is not possible as already a few bubbles would completely fill the reactor (and thus push the liquid out). The aeration gas is led over the membrane by a meandering channel – this channel gives mechanical support to the membrane and also allows to flush any gas mixture over the membrane (Figure 4.1). It is also through this channel that the gas mixture for aeration and pH control is flushed.

Three optical measurements are integrated into the reactor: an optical transmittance measurement for the determination of cell mass (optical density), a fluorescent sensor spot (PreSens, Germany) for the measurement of dissolved oxygen and a second fluorescent sensor spot (PreSens, Germany) for the measurement of pH. All three measurements require no mechanical contact through the reactor wall as the material (PDMS) is transparent to light. Both the temperature measurement and the heating are done through the bottom layer of the reactor which also only consists of a thin membrane and thus does not offer a significant thermal resistance.

PDMS can be formed by first creating a mold – in this case by means of micromilling – which is a negative of the reactor geometry. A liquid PDMS mixture (Sylgard 184, Dow Corning Corp., Midland, MI, USA, 10 parts silicone : 1 part curing agent.) is poured into the mold and cured in the oven at 70 °C for an hour. The hardened PDMS can then be pulled out of the mold and the sensor spots and the stirrer bar are added. The same is done with the upper layer of the reactor which contains the aeration channel. Onto the bottom side of both layers a membrane (~100 µm thick) is attached. In a final step the two layers are bonded together (also with PDMS) and cured to form the final reactor.

The reactor was used for the characterisation of the pH control system by conduction of titration and set point tracking experiments.

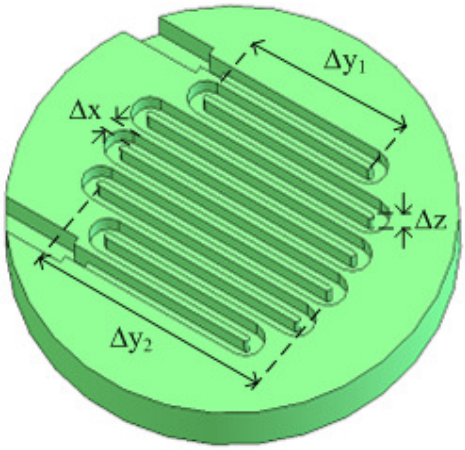

Figure 4.1. Meandering channel for aeration and pH control. Total membrane contact area with the reactor chamber is approximately 47.5 mm^2 with channel width, Δx, average length, Δy_{ave} and depth, Δz of 0.5 mm, 7 mm and 0.75 mm, respectively [18].

4.2.2 Gaseous pH control scheme

pH measurement

pH was measured by means of an optical measurement with the use of a fluorescent sensor spot. In every measurement, a sine-modulated light (44 kHz) from a blue LED (465 nm, NSPB500S, Nichia Corporation, Tokushima, Japan) was shone onto an optical sensor spot which was mounted on the inside of the reactor (in direct contact with the culture broth). This sensor spot in turn emitted fluorescent light at 520 nm peak wavelength, with the same frequency as the incoming light, but with a phase lag. The emitted light was then collected with a silicon detector (Thorlabs PDA36A, Thorlabs Inc., NJ, USA) and the resulting voltage was read by LabView. A lock-in amplifier programmed in LabView then measured the phase shift between the outgoing and the incoming signal, and this shift then translated directly to pH values. The optical pH sensor used has a measurement accuracy of about 0.01 pH units with a response time (t_{90}) of less than 90 s [1]. From our calibration data (data has been shown in [18]) the dynamic measurement range of the sensor spot is ranging between pH 5.5 to 8. Within this range, the sensor response is almost linear with a sensitivity of about 10^o phase angle per pH unit.

Gas connections

pH control was accomplished by dosing of either a gas mixture containing 20 000 ppm ammonia gas, NH_3 (the rest is nitrogen gas) or pure carbon dioxide gas, CO_2 respectively to increase and decrease the pH of the reactor content. The gas connections for the pH control are illustrated in Figure 4.2. Both gases were supplied from pressurized gas bottles equipped with two-stage gas regulators. A two-stage gas regulator ensures a more constant gas pressure, and therefore provides better stability for the process control than a single stage regulator would. The gas flow from the gas bottles was quantified by using mass flow meters (SHO-RATE, Brooks Instrument, Holland, Model 504-ES-22-F2B). For gas addition, 2-way Polyetheretherketone (PEEK) solenoid valves (Bio-Chem Valve,

Cambridge, UK, 038T2B12-32-5) were connected directly to each of the mass flow controllers (one for NH_3 and one for CO_2). Both valves were connected in parallel and remain closed unless a voltage supply is connected. An additional solenoid valve each was installed to depressurize the gas line prior to dosing of gas into the reactor. This additional valve is necessary because the continuous gas flow from the gas bottle causes the pressure in the tubing to increase when the solenoid valves are in the 'closed-position', until the whole tubing has the pressure which was adjusted at the regulator. Overpressure in the gas connections is not desirable because it may lead to an undesired overshoot in reactor pH.

The NH_3 and CO_2 gas lines were then joined together via a T-connector and introduced into the microbioreactor by connecting the gas line, F_1 to the top layer of the microbioreactor. During pH control, only one gas was dosed at a time. Part of the gas diffuses through the semi-permeable membrane and induces the desired pH changes. The remaining gas flows out through the outlet port, F_2 and is removed with the ventilation. All gas connections were established by standard Perfluoroalkoxy (PFA) tubing with an outer diameter of 3.175 mm using fittings from Upchurch Scientific.

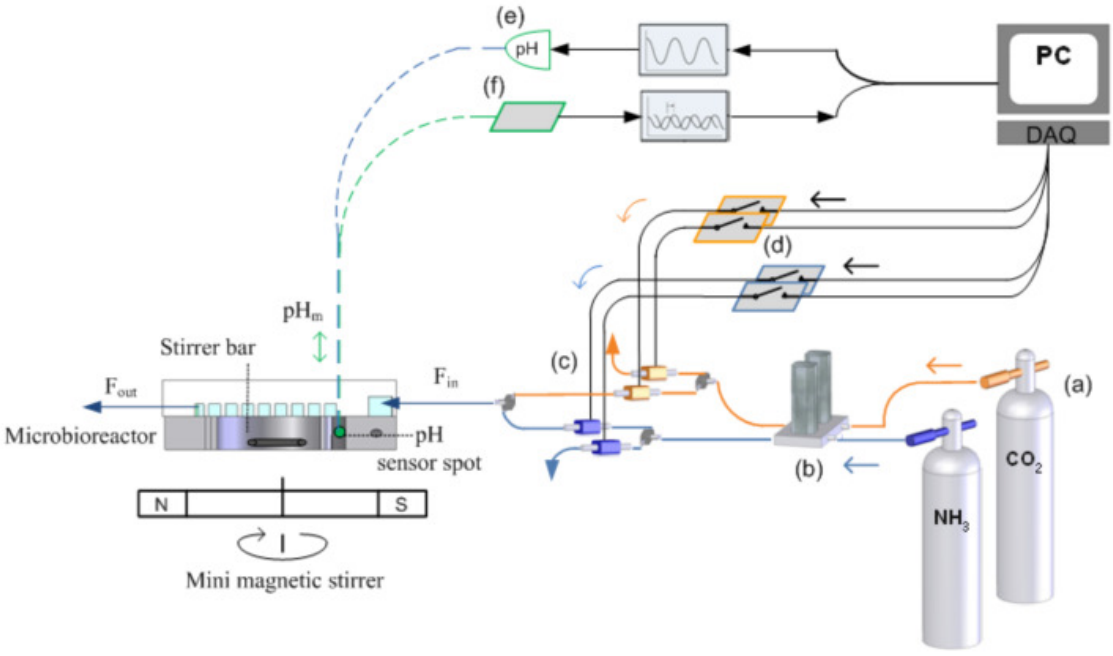

Figure 4.2. Schematic of the gas connections for the pH control. (a) NH_3 and CO_2 gas bottles (b) mass flow meters (c) solenoid valves (d) relays (e) LED (465 nm) (f) photo detector. Dashed lines (**--**), represent optical fibers, black solid lines represent electrical wiring (**-**), and blue/orange solid lines represent tubing for fluidics (**-**/**-**).

pH control algorithm

The pH of the reactor content was controlled by an on/off controller. The on/off controller was implemented in LabView™ v8.5 software (National Instruments Corporation, TX, USA), and interfaced with the reactor hardware using A/D cards (USB-6229 and PCI-4461, National Instruments Corporation, TX, USA). The operation of the pH control algorithm is schematically presented in Figure 4.3.

First, the LabView program will compute the deviation (error) between the desired set point value, pH_{sp} and the measured value, pH_m (pH measurements were done via the optical pH sensor as previously described). The controller was made to include a tolerance limit (dead band) around the set point. The dead band prevents the dosing valves from rapidly or continuously switching because the measured value never exactly fits the set point value when using an on/off controller in this type of systems. During pH control, no titration will take place if the pH deviation from the set point is within the tolerance limits. If the error is larger than the tolerance limit and positive ($pH_{sp} > pH_m$), NH_3 gas will be added and if the error is negative ($pH_{sp} < pH_m$), CO_2 gas will be added. A latching relay was used to control the state ('open' or remain 'closed') of the solenoid valve for gas addition. During addition of gas, the controller will first depressurize the gas connection (depressurizing period was set for 1 s) before opening up the dosing valve. Furthermore, the controller will only open the dosing valve for a very short period of time (pulse length of approximately 300 ms) before switching the valve back to its 'closed-position'. Thus the time needed for one dosing cycle is approximately 1.3 s.

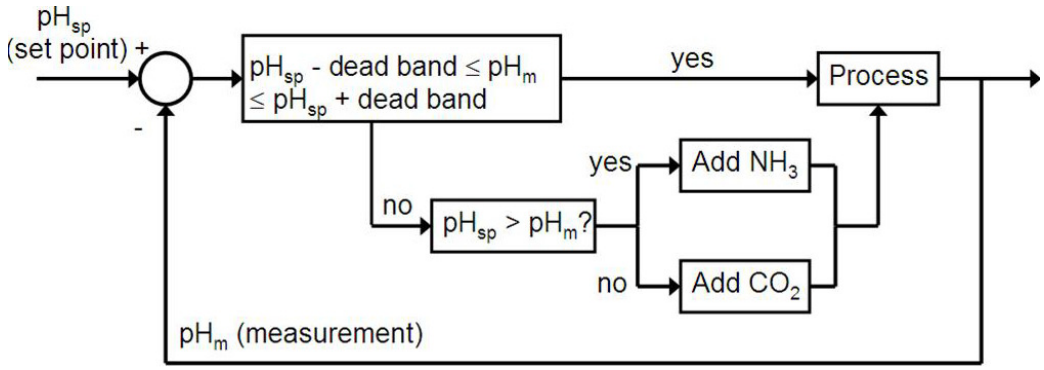

Figure 4.3. Block diagram of the on/off pH controller.

The period during which the dosing valve is open (pulse length) is one of the controller parameters that can be tuned. Other settings to be adjusted by the user are the gas bottle pressure (or the inflow gas flow rate via the mass flow controller) which determines the amount of gas diffusing through the membrane, the tolerance limits (dead band), and of course the pH set point. In this application, the on/off controller was tuned to give the smallest step change possible in both acidic and basic directions.

4.3 Results and discussions

4.3.1 System behavior and basic functioning of the on/off pH controller

Prior to tuning of the on/off controller, the system behavior was first evaluated by conducting two different sets of titration experiments (Figure 4.4). In the first titration experiment, CO_2 gas was dosed into a solution with a starting pH of 8 at a constant dosing pulse length of 1 s until the solution reached a final pH of about 6. In the second titration experiment, a reverse titration was made in which NH_3 gas was dosed into the reactor (initial pH of the solution is 6) at a constant dosing pulse length of 1 s until the solution pH reached an end value of about pH 8.2. For both experiments, tolerance limits of the controller were set to $\pm$ 0.1 of pH_{sp}, and the pressure of NH_3 and CO_2 gas bottles was regulated to 1 bar and 2 bar, respectively. At given operating pressures, NH_3 and CO_2 gas flow rates were measured to be 18 L/hr and 24 L/hr, respectively. The limited viable measuring range of the pH sensor spot does not permit to perform experiments beyond pH 6 and 8. This is because beyond this pH range (lower than pH 6 and higher than pH 8) the sensitivity of the sensor spot levels out [20]. The titration experiments were conducted in YPD medium (a common rich medium for *S. cerevisiae* cultivation [21]) consisting of 10 g/L yeast extract, 20 g/L peptone and 20 g/L glucose monohydrate at room temperature (T_m~25^oC). 1M hydrochloric acid, HCL and 1M sodium hydroxide, NaOH were used to adjust the pH of the solution to its desired starting pH value. By performing the experiment in YPD medium instead of distilled water, a more realistic and stable pH response from the process can be obtained due to the mild buffering capacity offered by the medium.

From the response obtained, it was seen that upon dosing of CO_2 gas; the pH of the reactor content drops significantly at a very fast rate (indicated by a steeper slope of the curve, $-dpH/dt_1$) until the solution pH reaches a pH value of about 6.5. From this point onward, the solution pH decreases slowly (indicated by the second slope of the curve, $-dpH/dt_2$) until it reaches a final pH value of about 6.2 to 6.3. This behavior is explained from the acid-base equilibrium of the system and the reactions that took place when CO_2 gas dissolved in the water. When CO_2 dissolves in water, it instantly reacts with OH^- ions from the water to produce hydrogen ions, H^+ and forms carbonic acid, H_2CO_3 which then rapidly dissociates into bicarbonate, HCO_3^- (pKa_1 at 25^oC = 6.36) and also into carbonate, CO_3^{2-} (pKa_2 at 25^oC = 10.32) [22]. This lowers the solution pH (pH = -log [H^+]). In the mild basic region of pH 7.5 – 8; due to the excess of hydroxyl ions, OH^-, and since the solution is not buffered (pH is nowhere near CO_2 pKa values), a sharp reduction in solution pH upon the addition of CO_2 was observed. However, in the slightly acidic region (~ pH 6 - 6.5), the solution pH is very close to the pKa of the first dissociation of H_2CO_3 (pKa_1 at 25^oC = 6.36). Around this pH the solution will be buffered and thus the rate of change of the pH decreases. On the contrary, NH_3 gas undergoes a much more straightforward reaction when it dissolves in water. It will react with the hydrogen (H^+) ions from the water forming ammonium ions, NH_4^+ and hydroxyl ions (OH^-) [23]. Further addition of NH_3 gas will consume more hydrogen (H^+) ions and thus, increase pH of the solution. Also, during the whole experiment, the working pH range (pH 6 to pH 8) was far away from the dissociation constant of ammonia (pKa_{NH3} at 25^oC = 9.25). This explains why the increase of solution pH following the dosage of NH_3 gas into the reactor only has one slope, dpH/dt_3.

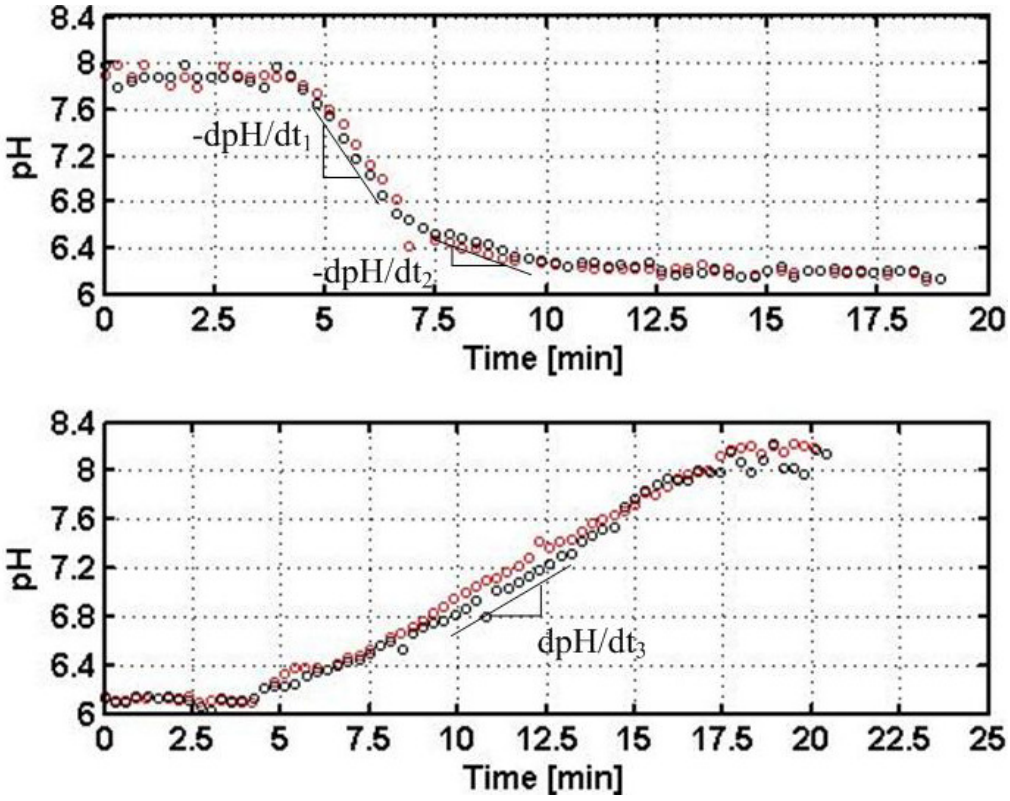

Figure 4.4. Responses from the titration experiments. Top: YPD medium (pH_o = 8) titrated with CO_2 gas (at 2 bar and 25°C) to a final pH of about 6.3. Bottom: YPD medium (pH_o = 6) titrated with NH_3 (20 000 ppm) – N_2 gas mixture (at 1 bar and 25°C) to a final pH of about 8.2.

Based on the results of the titration experiment, the on/off controller was tuned and a set point tracking experiment was performed to evaluate the controller performance in terms of its accuracy and response time. Since the values of pH_{sp}, tolerance limits, and the gas bottle pressures have already been set, the tuning steps required were simplified, leaving dosing pulse length of each gas as the only controller parameter to be tuned. In this application, the dosing pulse lengths of both gases were adjusted such as to induce pH changes that are as small as possible. This has the drawback that it may prolong the time needed to achieve the desired set point, especially if the pH set point is changed significantly. However, small step changes ensure a more stable operation in the sense that a large pH fluctuation around the set point due to dosing of gas for pH control can be avoided. Also, in cultivations of e.g. yeast or in enzymatic reactions the pH seldom changes very quickly, and thus a slower but more precise control is to be preferred.

During the experiment, the dosing pulse length of both gases was adjusted manually depending on the working pH region of interest. In the mild basic region (~pH 7.5 - 8), the dosing pulse lengths of CO_2 and NH_3 gases were set to 250 ms and 100 ms, respectively. The dosing pulse length of NH_3 gas was deliberately chosen to be a bit longer in order to counteract the sharp pH drop induced by the addition of CO_2 gas in this pH range. In the near neutral region ($6.5 < pH < 7.5$), dosing pulse lengths of both gases were set at 100 ms. For pH control around or below pH 6.5, NH_3 gas dosing pulse length was retained at 100 ms but CO_2 dosage pulse length was prolonged to 1000 ms. This is

necessary in order to dissolve more CO_2 such that the reaction equilibrium can be shifted to produce more carbonic acid, H_2CO_3 instead of bicarbonate, HCO_3^- ions. By implementing these settings, the set point tracking experiment was performed by adjusting the pH of the reactor content to reach three different pH set point values (pH_{sp} = 7.5, 6.8, and 6.3, respectively.). The results of the set point tracking experiment (Figure 4.5) demonstrate that the pH on/off controller has a fast set point tracking capability for a series of downward (pH 6.8 to pH 6.3) and upward (pH 6.8 to pH 7.5) step changes in the pH set point. The results also show that by only adjusting the gas dosing pulse length accordingly, a controller accuracy as high as $\pm$ 0.1 pH units around the pH_{sp} can be achieved. The largest pH step change made was from a pH set point of 6.3 to a pH set point of 7.5, and in this case the rising time was approximately 6.5 minutes (the rising time is the time the process output takes to first reach the new steady-state value [24]). During the pH step changes, only a short delay (less than a minute) was recorded. This is probably due to a high gas transport rate through the PDMS membrane and good mixing via the micro-impeller incorporated in the reactor which together allow for a fast response [18]. The responses obtained from the pH feedback control loop are comparable to the responses produced from a gaseous pH control system developed by De Jong [16] where a system delay time of approximately 60 seconds and a rising time of a few minutes have been recorded. In the current setup used for testing, adjustment of the dosing pulse lengths has to be done manually. However, optimal settings for the pulse length can be programmed in the software controlling the setup, such that the settings, and by this the controller gain, are changed automatically when the pH set point value is altered.

Although basic functioning of the on/off pH controller was successfully demonstrated, the preliminary experiments performed (titration and set point tracking experiments) do not entirely reflect the dynamic response of a real biological process. This is because in the preliminary experiments performed, there is no production or consumption of protons (H^+); as is to be expected when running a fermentation or a biocatalysis process.

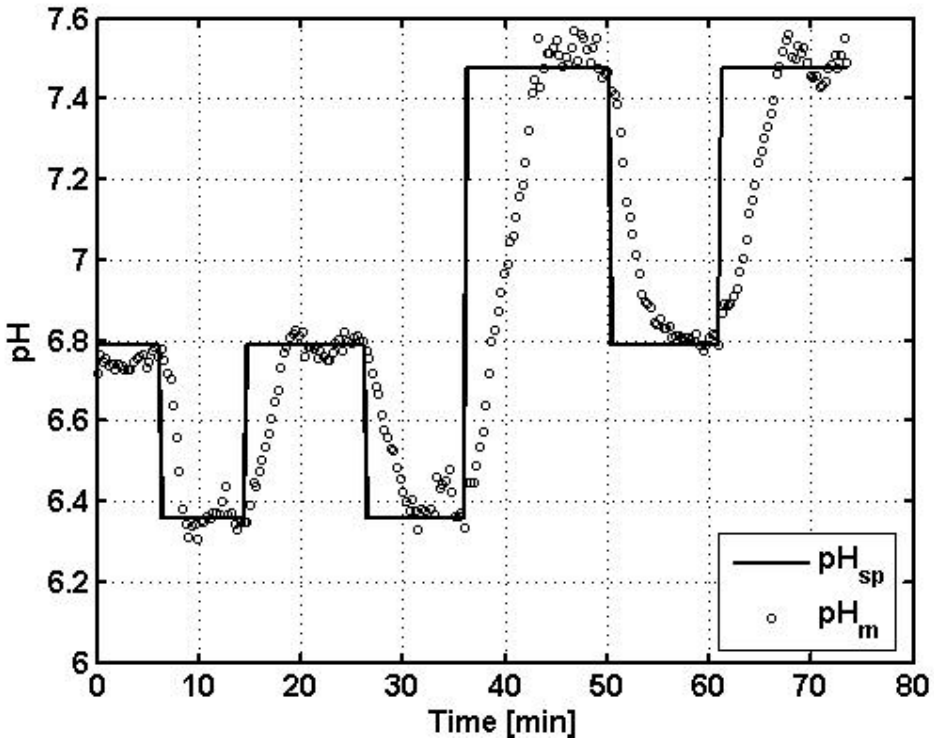

Figure 4.5. Closed loop response of the on/off pH controller for different set point values (pH_{sp} = 6.8, 6.3 and 7.5), starting from pH 6.8.

4.3.2 System limitations

One of the limitations of the proposed system is the limited viable measurement range of the pH sensor spot. Due to its poor resolution at low/high pH values (pH < 6 and pH > 8), even a large change in pH will only result in very little variation in phase shift. This makes process control very difficult, if not impossible in this pH range. The limited viable measurement range of the sensor spots also restricts its applicability and usage as most yeast, filamentous fungi and enzymatic reactions work best at pH 4-6 [1,11]. Alternatively, an ion sensitive field-effect transistor (ISFET) pH sensor chip can be used for pH measurement [1]. However, as this type of chip is very expensive the reactor design would have to be adapted such that the chip was removable and could be reused for several consecutive experiments. Different means of mixing would also have to be applied to avoid any complications for the integration of the reference electrode for the ISFET pH measurement. Another potential option is to use the pH measurement method established by Li *et al.* [25]. They developed a pH optode with a linear response (sensor response time is 120 s) over the pH range 2.17-10.3 by using 10-(4-Aminophenyl)-5,15-dimesitycorrole as the sensing material. Nevertheless, this sensor is not yet commercially available.

The other limitation of the proposed gaseous pH control concept is the low solubility of the CO_2 gas in the liquid. It depends on the CO_2 saturation constant, CO_2^* in the gas channel for a given CO_2 partial pressure and temperature (In our system, CO_2^* was calculated to be 0.07 mol/L at a partial pressure of 2 bar and temperature of 25°C) [26]. The low CO_2 gas solubility may cause difficulties for pH control especially for pH control at low pH levels (below pH 6) as large amounts of CO_2 are needed for further reduction of

pH. In this respect, longer dosing time can be implemented to increase the amount of CO_2 gas transferred per dosage. Nevertheless, when the saturation limit is reached (dissolved CO_2 (aq) = CO_2^* at given gas partial pressure), gas solubility will not increase any further with the increase of dosing time as explained by Henry's law [22]. In the pH control system that was described here – i.e. with the use of CO_2 gas near atmospheric pressure (1-2 bar) – it is not possible to reach for example a pH that is far below pH 6 due to the fact that the pKa of the first dissociation of H_2CO_3 is 6.36. There are several potential solutions to this limitation. One is to use a much stronger acidification agent, e.g. dilute sulfur dioxide gas, SO_2 or hydrochloric acid, HCL in vapor form. These gases certainly offer the possibility of working at low pH levels and are harmless to the microorganisms. Mendoza *et al.* [27] reported that dissolved SO_2 (up to 250 $mg.L^{-1}$) has little or no effect on the growth of a *S. cerevisiae* culture. These gases, however, are corrosive and may not be compatible with PDMS or PMMA (even in low concentration), the materials which are most commonly used for the fabrication of microbioreactors [1,28]. Another alternative solution is to work with a higher CO_2 gas partial pressure (greater driving force for gas diffusion) as this would increase the CO_2 solubility in the liquid. Maharbiz *et al.* [4] estimated that the lowest pH attainable corresponding to a saturated solution of CO_2 is 3.9. Higher gas pressure also promotes faster pH reduction per dosage. Operating at high pressure (e.g. above 5 bar) is however problematic for microbioreactor systems. This is because inflow of high pressure gas into the system could (1) compromise the leak-free operation of the reactor e.g. damage fluidics interconnects, and/or (2) result in a large pH overshoot in the non-buffering region (~pH 7 to 9), thus complicating reactor process control.

Finally, the workability of the proposed method was only tested in a single reactor system. However, the proposed method can be implemented for parallel microbioreactor operation using different pH set point values. This is one area that could be worth looking at to further improve the method. If these limitations can be addressed and resolved, it is believed that the proposed gaseous pH control concept can be measured up to the pH control capabilities of bench scale bioreactors.

4.4 Conclusion

A gaseous pH control method was developed and was demonstrated to provide satisfactory pH control performance in microbioreactor systems equivalent to the pH control method implemented in bench-scale systems (acid-base addition). The proposed method is very user-friendly and in depth knowledge of the microbioreactor system is not necessary to operate the pH controller. The necessary apparatus (mass flow meters, solenoid valves, and relays) to transport the gas into the microbioreactor and its basic functionality has been presented. It was shown that addition of NH_3 and CO_2 gases coupled to a simple on/off controller results in a satisfactorily pH control performance (pH control accuracy = $\pm$ 0.1 of the set point value and system response times of a few minutes were achieved) within the dynamic measuring range of the optical sensor spot which is between pH 6 to 8.

References

[1] Schäpper, D., Zainal Alam, M. N. H., Szita, N., Lantz, A. E. and Gernaey, K. V. (2009). Application of microbioreactors in fermentation process development: a review. *Analytical and Bioanalytical Chemistry.* **395**: 679-695.

[2] Zanzotto, A., Szita, N., Boccazzi, P., Lessard, P., Sinskey, A. J. and Jensen, K. F. (2004). Membrane-aerated microbioreactor for high-throughput bioprocessing. *Biotechnology and Bioengineering.* **87**: 243-254.

[3] Szita, N., Bocazzi, P., Zhang, Z., Boyle, P., Sinskey, A. J. and Jensen, K. F. (2005). Development of a multiplexed microbioreactor system for high-throughput bioprocessing. *Lab on a Chip.* **5**: 819-826.

[4] Maharbiz, M. M., Holtz, W. J., Howe, R. T. and Keasling, J. D. (2004) Microbioreactor arrays with parametric control for high-throughput experimentation. *Biotechnology and Bioengineering.* **85**: 376-381.

[5] Lee, H. L., Bocazzi, P., Ram, R. J. and Sinskey, A. J. (2006). Microbioreactor arrays with integrated mixers and fluid injectors for high throughput experimentation with pH and dissolved oxygen control. *Lab on a chip.* **6:** 1229-1235.

[6] Krommenhoek, E. E., van Leeuwen, M., Gardeniers, H., van Gulik, W. M., van den Berg, A., Li, X., Ottens, M., van der Wielen, L. A. M. and Heijnen, J. J. (2007). Lab-Scale fermentation tests of microchip with integrated electrochemical sensors for pH, temperature, dissolved oxygen and viable biomass concentration. *Biotechnology and Bioengineering.* **99**: 884 – 892.

[7] Petronis, S., Stangegaard, M., Christensen, C. B. V. and Dufva, M. (2006) Transparent polymeric cell culture chip with integrated temperature control and uniform media perfusion. *BioTechniques.* **40**: 368-376.

[8] Wu, M. H., Urban, J. P. G., Gui, Z. and Cui, Z. F. (2006). Development of PDMS microbioreactor with well-defined and homogenous culture environment for chondrocyte 3-D culture. *Biomedical Microdevices.* **8:** 331-340.

[9] Muller, D. H., Liauw, M. A. and Greiner, L. (2005). Microreaction technology in education: Miniaturized enzyme membrane reactor. *Chemical Engineering Technology.* **28**: 1569-1571.

[10] Swarts, J. W., Vossenberg, P., Meerman, M. H., Janssen, A. E. M. and Boom, R. M. (2008). Comparison of two-phase lipase-catalyzed esterification on micro and bench scale, *Biotechnology and Bioengineering.* **99**: 855-861.

[11] Shuler, M. L. and Kargi, F. (2002). *Bioprocess Engineering: Basic Concepts*, 2nd ed., (New Jersey Prentice Hall), pp. 169-170.

[12] Vervliet-Scheebaum, M., Ritzenthaler, R., Normann, J. and Wagner, E. (2008). Short-term effects of Benzalkonium Chloride and Atrazine on *Elodea canadensis* using a miniaturised microbioreactor system for an online monitoring of physiologic parameters. *Ecotoxicology and Environmental Safety.* **69:** 254-262.

[13] Zhang, Z., Perozziello, G., Boccazzi, P., Sinskey, A. J., Geschke, O. and Jensen, K. F. (2007). Microbioreactors for bioprocess development. *Journal of the Association for Laboratory Automation.* **12**: 143-151.

[14] Buchenauer, A., Hofmann, M. C., Funke, M., Büchs, J., Mokwa, W. and Schnakenberg, U. (2009). Microbioreactors with microfluidic control and a user-friendly connection to the actuator hardware. *Biosensors and Bioelectronics.* **24:** 1411-1416.

[15] Isett, K., George, H., Herber, W. and Amanullah. (2007) A Twenty-four-well plate miniature Bioreactor high-throughput system: Assessment for microbial cultivations. *Biotechnology and Bioengineering.* **98:** 1017-1028.

[16] de Jong, J. (2008). Application of Membrane Technology in Microfluidic Devices. (Ph.D. thesis). University of Twente, Twente.

[17] Applikon Biotechnology 2009 Micro 24 Bioreactor, Netherlands. http://www.applikon-bio.com/cgi-bin/applikonbio/basis-micro-bioreactor-u24. Accessed 9 March 2009.

[18] Schäpper, D., Stocks, S. M., Szita, N., Lantz, A. E. and Gernaey, K. V. (2010). Development of single-use microbioreactor for cultivation of microorganisms. *Chemical Engineering Journal*. **160**: 891-898.

[19] Fiaux, J., Cakar, Z. P., Sonderegger, M., Wu¨thrich, K., Szyperski, T. and Sauer, U. (2003). Metabolic-flux profiling of the yeasts *Saccharomyces cerevisiae* and *Pichia stipitis Eukaryotic Cell.* **2**: 170-180.

[20] John, G. T., Goelling, D., Klimant, I., Schneider, H. and Heinzle, E. (2003). pH-Sensing 96-well microtitre plates for characterization of acid production by dairy starter cultures. *Journal of Dairy Research.* **70:** 327-333.

[21] Chen, C. W., Lei, B. C., Yeh, K. W. and Duan, K. J. (2003). Recombinant sweet potato sporamin production via glucose/pH control in fed-batch cultures of *Saccharomyces cerevisiae. Process Biochemistry.* **38:** 1223-1229.

[22] Roosen, C., Ansorge-Schumacher, M., Mang, T., Leitner, W. aand Greiner, L. (2007). Gaining pH-control in water/carbon dioxide biphasic systems *Green Chemistry.* **9:** 455-458.

[23] Clegg, S. L. and Brimblecombe, P. (1989). Solubility of ammonia in pure aqueous and multicomponent solutions. *Physical Chemistry.* **93:** 7237-7248.

[24] Seborg, D. E., Edgar, T. F. and Mellichamp, D. A. (2004). *Process Dynamics and Control,* 2nd ed. (New Jersey John Wiley & Sons), pp. 103-127.

[25] Li, C. Y., Zhang, X. B., Akermark, B., Sun, L., Shen, G. L. and Yu, R. Q. (2006). A wide pH range optical sensing system based on a sol-gel encapsulated amino-functionalised corrole. *The Analyst.* **131:** 388-393.

[26] Frahm, B., Bank, H. C., Cornand, P., OelBner, W., Guth, U., Lane, P., Munack, A., Johannsen, K. and Portner, R. (2002). Determination of dissolved CO_2 concentration and CO_2 production rate of mamalian cell suspension culture based on off-gas measurement. *Journal of Biotechnology.* **99:** 133-148.

[27] Mendoza, L. M., De Nadra, M. C. M., Bru, E. and Farı´as, M. E. (2009). Influence of wine-related physicochemical factors on the growth and metabolism of non-*Saccharomyces* and *Saccharomyces* yeasts in mixed culture. *Industrial Microbiology and Biotechnology.* **36:** 229-237.

[28] Becker, H. and Gartner, C. (2008). Polymer microfabrication technologies for microfluidic systems. *Analytical and Bioanalytical Chemistry.* **390:** 89-111.

CHAPTER 5

A continuous membrane microbioreactor system for development of integrated pectin modification and separation processes

CHAPTER 5

A continuous membrane microbioreactor system for development of integrated pectin modification and separation processes

---

Abstract

Evaluation of novel enzyme reactions and reactor systems is often hampered by costs related to obtaining sufficient amounts of enzymes. In this respect, it will be advantageous to assess new enzymatic processes in microbioreactors designed to resemble genuine reactor systems. In this work, we present a continuous membrane microbioreactor prototype for development of enzyme catalyzed degradation of pectin. Membrane reactors are becoming increasingly important for the novel 'biorefining' type of processes that either require product removal to avoid product inhibition or rest on partial hydrolysis of the substrate to obtain e.g. value-added oligosaccharides from complex biopolymers. The microbioreactor prototype was fabricated from poly(methylmethacrylate) (PMMA) and poly(dimethylsiloxane) (PDMS) and designed as a loop reactor (working volume approximately 190 μL) integrated with a regenerated cellulose membrane for separation of low molecular weight products. The main technical considerations and challenges related to establishing the continuous membrane microbioreactor are discussed. The workability of the prototype was validated by comparing the process data at microscale to those obtained using a lab-scale membrane reactor system. The prototype presented here is easy to handle, has a low complexity – thus a relatively simple fabrication process – and can be used to study extended enzymatic reactions.

This chapter has been submitted as Zainal Alam, M. N. H., Pinelo, M., Samantha, K., Jonsson, G., Meyer, A., and Gernaey, K. V. (2010). A continuous membrane microbioreactor system for development of integrated pectin modification and separation processes. *Chemical Engineering Journal*. – under review.

5.1 Introduction

Assessing the performance of new enzymes under various process conditions is a fundamental base for successful development of novel enzyme catalyzed processes. However, when evaluating new enzymes, the high costs related to obtaining sufficient amounts of enzymes or specific types of substrate molecules are often a limit. This limitation becomes more pronounced in case a large amount of experimental data is required, e.g. screening of new enzyme processes at a range of reaction conditions or on different substrate stocks. Therefore, to significantly reduce running cost per experiment, preliminary kinetic studies or screening of new enzyme processes are often performed wih very small volumes of substrates and enzymes (typically µg or µL-mL range) [1-3]. In addition, scaling down experiments greatly increases throughput for elucidating enzyme behaviour under various conditions in one single run [4,5].

At present, micro-tubes (1 – 1.5 mL) and the microtiter plate (96 or 384 wells plate) are the most commonly used research tools for assessing novel enzyme processes [1-3]. However, reactor design related information gained with a micro-tube or microtiter plate experiment is very limited. The impact of fundamental engineering aspects such as mixing and transport phenomena (mass and heat transfer) on the reactions can often not be assessed properly. Evaluation of such data or immediate provision of reaction conditions that resemble more genuine reactor system conditions are crucial, especially for the type of agro-industrial biomass reactions where impure, partially reactive substrates are to be upgraded enzymatically and/or where the process requires only partial enzymatic modification as for example for production of specific oligosaccharides from biomass [6]. In addition, the inability to run experiments otherwise than in batch mode is a severe limitation of microtiter plates since this prevents removal of inhibitory products during an experiment.

These bottlenecks have driven researchers to explore other possibilities, and most recently, the development of microbioreactors. Microbioreactors, typically with a working volume less than 1 mL, hold several distinct advantages over a microtiter plate system [7]. First, and perhaps the most obvious one, is the ability of running experiments in fed-batch or continuous mode [8-10]. Secondly, microbioreactors can be fabricated to have an in-line micro-pump, integrated micro-heaters and micro-impellers. These will then significantly improve heat and mass transfer rates achievable in the system. Moreover, microbioreactors offer a superior degree of control over relevant experimental conditions such as temperature and pH, where parallel experiments with parallel sensing and control can be realized [7]. Finally, the ability to integrate membranes into microfluidics devices [11] offers the technology to fabricate membrane microbioreactors. This would then allow for recirculation of enzyme and continuous separation of reaction products and/or low-molecular inhibitory compounds.

Various types of enzyme-based microbioreactors have been developed to facilitate enzymatic reactions in micro-scale. One of the most commonly designed systems is the immobilized micro enzyme reactor [12-15], where enzymes are typically immobilized physically or covalently on a specific support which is packed inside a column with predefined length – similarly to a configuration of a classic packed-bed reactor [16]. Micro-channel reactors are commonly used as well [9,17,18], and their operation is based on a simple loading of substrate and enzyme into separate inlets via syringe pumps and often integrated with passive mixing methods – T shaped mixer [9], Y shaped mixer

[17,18] or a combined serpent-like and staggered herring-bone mixers [17]. Finally, the loop reactor – a simple reactor system that is generally realized with standard chromatography tubing and fittings – has also been used [10,19].

The aim of the present work was to develop a continuous membrane microbioreactor that performs similarly to typical membrane reactors run at bench scale. Mono-enzymatic degradation of pectin with pectin lyase was chosen as the model system because pectic substances are abundant in agro-industrial waste streams and significant research efforts are currently directed toward converting these low-value waste streams into high value product, especially considering that these surplus pectic substances consist of suitable starting materials for obtaining bioactive carbohydrates with potential health benefits [6,20]. Firstly, the main technical challenges related to establishing the continuous membrane microbioreactor will be described, together with the technical solutions that were implemented. Secondly, experimental results obtained with the continuous membrane microbioreactor will be presented, demonstrating the workability of the reactor. Finally, validation of the results obtained in the microbioreactor will be demonstrated by comparing the data obtained to those of similar experiments conducted in a lab-scale membrane reactor.

5.2 Materials and Methods

5.2.1 Microbioreactor fabrication

The microbioreactor was fabricated from poly(methylmethacrylate) (PMMA) (Plexiglas GS, Klar 233, Nordisk Plast, Auning, Denmark) and poly(dimethylsiloxane) PDMS. Fabrication of the reactor's PMMA layers was done by using a computer-numerical-controlled (CNC) milling machine (CNC micromill, Minitech MiniMill 3/Pro, Minitech Machinery Coorporation, Norcross, GA, USA). As for the reactor's PDMS layer, a negative image of the PDMS layer was micro-milled into PMMA which then served as a mold. After machining, resistance wires with predefined length and a temperature sensor were first placed into the mold [21]. Next, liquid PDMS (prepared by mixing ten parts silicone to one part curing agent, Sylgard 184, Dow Corning Corp., Midland, MI, USA) was poured into the mold and cured at 70 °C for two hours. Finally, the cured PDMS layer was removed from the mold and 2-pin electrical connectors were soldered to the resistance wire and temperature sensor to establish electrical connections for heating and temperature measurement, respectively.

5.2.2 Operation of reactors

Figure 5.1 shows the 2-D schematics of the membrane microbioreactor and the lab-scale membrane reactor experimental setup. Both reactors were realized as a loop reactor consisting of a dosing pump, reactor unit, recirculation pump, and the membrane filtration unit as the main components of the loop. All experiments conducted in both scales were done in a similar manner. Substrate solution was continuously fed into the loop by the dosing pump at predetermined flow rates, F_{in}, and circulated by means of the recirculation pump. During the course of reaction, enzyme and un-reacted substrate solutions were retained in the system by the membrane while low molecular weight product (< membrane

molecular weight cut-off) was continuously removed. Permeate flux is measured at the outflow, F_{out}, a measurement which was done discontinuously every 30 minutes. In both scales, a regenerated cellulose membrane (PLGC06210, Millipore, Billerica, MA, USA) with molecular weight cut-off (MWCO) of 10 kDa was used for separation.

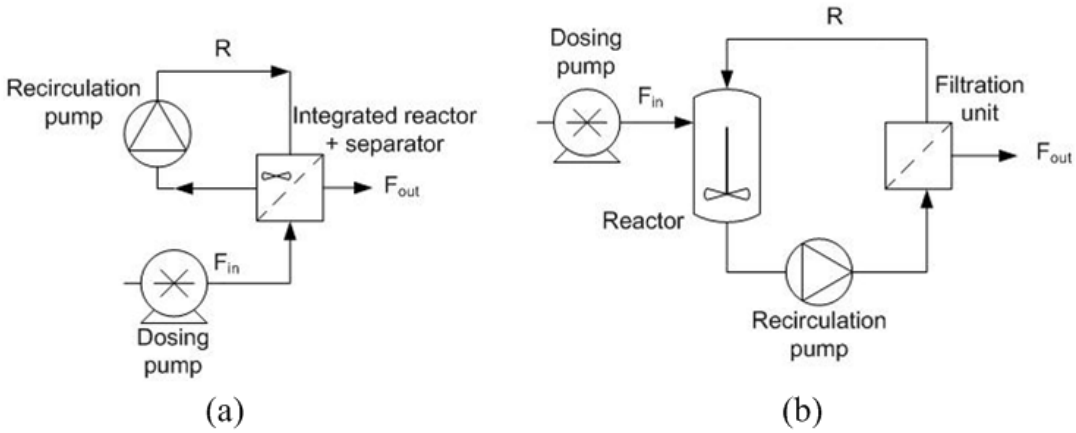

Figure 5.1. 2-D schematics of (a) membrane microbioreactor and (b) the lab-scale membrane reactor experimental setup.

For starting-up the reaction in the membrane microbioreactor, the reactor was first filled with enzyme solution to purge bubbles out of the system. Bubbles are not desirable because their relatively large size – compared to the size of the microbioreactor channels – would easily clog the micro channels. Once all bubbles were removed, the temperature was set at its desired set point value and the reaction was initiated by starting the feeding of the substrate solution. Similar steps were also followed for starting-up the reaction in the lab-scale membrane reactor except that in the lab-scale system, purging of bubbles was not necessary. Two different types of feeding strategy were implemented; (1) Substrate was fed for 1 hour (batch loading) and then the system was flushed continuously with buffer solution. (2) Continuous operation, i.e. substrate was fed continuously. Operating conditions applied in all experiments (mixing test and hydrolysis reaction) for both reactors are given in Table 5.1.

5.2.3 Lab-scale membrane reactor

For validation of results obtained in the membrane microbioreactor, similar experiments were conducted in the lab-scale membrane reactor (Figure 5.1). The lab-scale membrane reactor consisted of a cylindrical jacketed tank connected to a cross-flow membrane filtration unit via a peristaltic pump (Model 7554-60, Cole Parmer Instrument, Illinois, USA). Agitation was achieved by placing the reactor unit on a magnetic stirrer (MR 3000, Heidolph Instrument GmbH & Co., Schwabach, Germany) and a peristaltic pump (Masterflex L/S,7554-95, Cole Parmer Instrument, Illinois, USA) was used as the dosing pump for the system.

Table 5.1. Operating conditions applied in membrane microbioreactor and in lab-scale membrane reactor

Parameters	Membrane microbioreactor	Lab-scale membrane reactor
Working volume, V	190 µL	350 mL
Feed flow rate, F_{in}	200 µL.hr^{-1}	175 mL.hr^{-1}
Recirculation rate, R	2700 µL.hr^{-1}	5.5 L.hr^{-1}
Residence time, τ	1 hr	2 hr
Stirring speed, N	500 rpm	300 rpm
Temperature, T	controlled	controlled
Pressure, P	measured	measured
pH	pH sensor not integrated	measured

5.2.4 Mixing test: Fluorescent dye visualization technique

A fluorescent dye visualization technique was used to evaluate the quality of mixing in our systems. For this purpose, distilled water and fluorescent solution were used. In order to mimic flow conditions of the actual enzymatic hydrolysis reaction in the system, the fluorescent solution was prepared by mixing a concentrated fluorescein green solution (DWYER Instruments, Inc. Michigan City, USA) with 10 g/L of sugar beet pectin solution at a mixing ratio of 1:1. The fluorescent solution was mixed with the substrate solution to obtain the necessary viscosity effects for the mixing test. The experiment was performed by first filling the reactor with distilled water, which was then followed by continuous addition of the fluorescent solution. Mixing effects were observed and images of dispersion of the fluorescent solution in the reactor were recorded by a digital camera (Kodak EasyShare C763).

5.2.5 Enzymatic hydrolysis of sugar beet pectin by pectin lyase

Sugar beet pectin with a degree of methylation of ~60% and a degree of acetylation of ~19% (Danisco A/S, Brabrand, Denmark) was used as a substrate. Pectin lyase used was supplied by Novozymes A/S (Bagsværd, Denmark). It was a monocomponent enzyme from *Aspergillus aculeatus* with an enzyme activity on citrus pectin of 0.0085 U·mg^{-1}. The activity is defined as production of 1 µmol of double bonds formed per minute at pH 4.5 and 50^{o}C. The pectin lyase used degraded the sugar beet pectin (substrate) into smaller fragments with a double bond on its non-reducing ends via a β-elimination mechanism [22]. 0.1 M sodium acetate buffer solution (pH 4.5) was used to prepare both the substrate and the enzyme solutions. The enzymatic hydrolysis reaction was performed with an enzyme [E] to substrate [S] ratio, E/S, of 0.2%(w/w), and an initial substrate concentration, $[S]_o$, of 10 g/L. the reaction was performed at pH 4.5 while temperature was controlled at 50^{o}C.

The progress of the hydrolysis reaction was monitored by measuring sample absorbance via a microtiter plate reader at 235 nm. Beer-Lamberts law ($A_{235} = l\varepsilon c$) was used to estimate the concentration of product fragments, c, generated from the hydrolysis

reaction. A molar absorption coefficient, ε, of 5500 M^{-1} cm^{-1} was used [23] for the estimation and the absorbance path length, l, was calculated to be about 0.45 cm (corresponds to a sample volume of 150 µL). The hydrolysis was monitored until the reaction reached a steady-state.

5.3 Results and Discussions

5.3.1 Membrane microbioreactor design

Mechanical design and reactor configuration

The membrane microbioreactor prototype (Figure 5.2a) was realized as a loop-type reactor with an integrated reactor and membrane separation unit as the main component of the loop. A loop-type reactor (normally operated with a high recycle to feed flow ratio) has a good residence time distribution and was reported to show identical flow behavior to ideal continuously stirred tank reactors [10]. The prototype was fabricated as a single reactor device with a total working volume of about 190 µL. It was designed to work with constant working volume, with no head space and under bubble-free conditions.

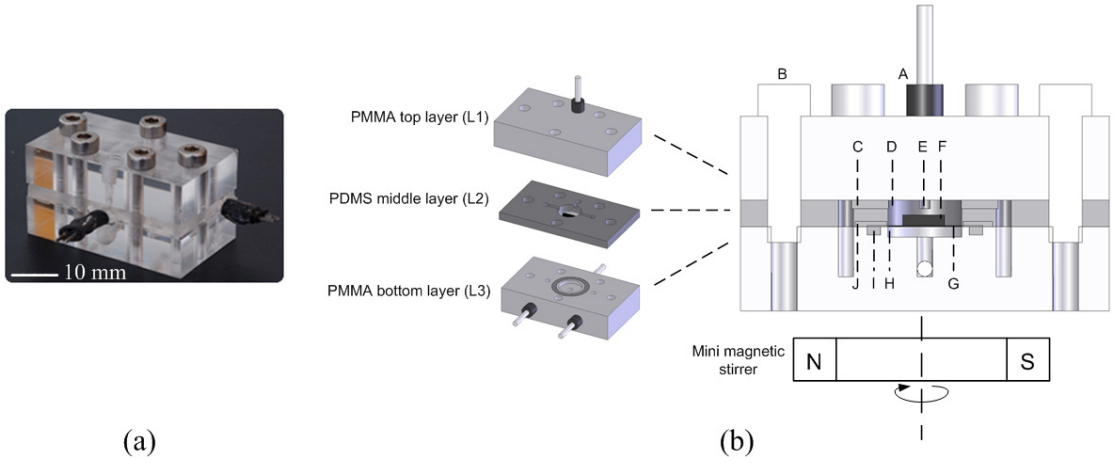

Figure 5.2. (a) Photograph of the membrane microbioreactor (b) Cross sectional view of the membrane microbioreactor; (A) 6-40 threaded port (B) M2.5 screw (C) location of microchannel connected to inlet/outlet ports of the recirculation line (D) reactor chamber (E) inlet feeding port (F) magnetic stir bar (G) regenerated cellulose membrane (H) permeate chamber (I) silicon O ring (J) resistance wire.

The prototype consisted of a 2.5 mm thick PDMS layer (L2) sandwiched in between two 8 mm thick PMMA layers (L1 and L3) as illustrated in Fig. 2b. PMMA layers with a thickness of 8 mm were used for two reasons. Firstly, they do not bend when clamped with screws at the desired maximum temperature (~50 ^{o}C) for the experiments. Secondly, they provide the required insertion depth for the tube-nut assembly which is 5 mm with an additional 3 mm for mechanical support. The top PMMA layer (L1) consists of five clearance holes with a diameter of 2.7 mm for M2.5 screws (B) and one 6-40 threaded port (A) with a diameter of 3.6 mm for the fluidic connection. This threaded port serves as the inlet port for the feeding solution.

The middle PDMS layer (L2) (Figure 5.2b) serves as the main body of the prototype. The middle PDMS layer also functions as a gasket layer to ensure water-tight sealing between the middle PDMS layer and the top and bottom PMMA layers. It has a reactor chamber (D) (centered in the middle of the PDMS layer) with a depth of 2.5 mm and a diameter of 7 mm, giving a volume of about 100 μL. A magnetic stirrer bar (F) with a length of 3 mm and thickness of 1 mm was placed on the reactor's floor for active mixing. When the PDMS middle layer is pressed between two PMMA layers with screws, the PDMS layers will be slightly deformed, especially if excessive pressure is applied. This may halt the stirring motion of the stirrer bar. Therefore, to prevent the stirrer bar from getting jammed due to excessive compression of the PDMS layer during the final assembly of the device, a reactor chamber height, to stirrer bar thickness ratio, H_T/h_i of 2.5 was selected. The reactor chamber is connected to the inlet feeding port (E) and to the inlet/outlet ports of the recirculation line (C) by 0.5 mm deep x 1 mm wide micro-channels. The reactor chamber design approximates the reactor design of Zhang *et al.* [8]. In their design, also with a similar active mixing scheme (a ring-shape magnetic stir bar with an arm length of 6 mm and a thickness of 0.5 mm was used); the depth of the reactor chamber was 2 mm – thus a H_T/h_i of 4.

The bottom PMMA layer (L3) (Figure 5.2b) formed the base for the reactor. It contains a permeate chamber (H) that is located on the upper part of the bottom PMMA layer. The permeate chamber (cylinder with 7 mm diameter and 1 mm height, resulting in about 38.5 μL volume) is aligned exactly under the reactor chamber. A groove was machined around the permeate chamber, and a silicon O ring (I) was fixed into that groove to prevent any overflow that might occur. When all the layers are pressed together during the final assembly, the silicon O ring was pressed between the bottom PMMA layer and the middle PDMS layer thereby creating water-tight sealing. The bottom PMMA layer also includes five threaded ports for M2.5 screws. Compress the layers together with screws has the advantage that the screws can also be used as a guide to ensure that all layers are properly aligned. A slight mis-alignment would indeed compromise the leak-free operation of the reactor.

Fluidic connections

External fluidic connections were established by standard perfluoroalkoxy (PFA) tubing (outer and inner diameters of the tube are 1.59 mm and 0.75 mm, respectively) with specialized connectors (M-644-03 headless nut, M-650 ferrule and stainless steel lock-ring were used) from Upchurch Scientific. This type of connections has a very low and defined dead volume and provided us with the plug-and-play solution for the fluidic connections of the microbioreactor system. Though this type of connection is relatively costly compared to tube-O rings or needle-diaphragm interconnects [7], it has the advantage that it can withstand a greater pressure build-up in the system. Pressure build-up in the reactor is to be expected from membrane bioreactor operation due to build-up of un-reacted substrate on the membrane surface.

Fluidic connections were required to supply feed into the reactor via the inlet port in the top PMMA layer and also for the recirculation line. External fluidic connections for the recirculation line were made on the side of the bottom PMMA layer (see Fig. 2b). The recirculation loop was established by connecting these side ports via PFA tubing to a micro gear pump (mzr 2905, HNP Mikrosysteme GmbH, Parchim, Germany) which serves as the recirculation pump for the system. The micro gear pump model mzr 2905 was chosen because it can guarantee a steady flow rate and has a low shear stress effect [10]. Total

volume of the recirculation loop (volume of the micro channels connected to the reactor chamber, additional PFA tubing used and dead volume in the micro gear pump) is calculated to be approximately 90 µL which accounts for 48% of the total volume of the reactor.

The membrane separation design

The micro-channels that are connected to the inlet/outlet ports of the recirculation line were positioned tangentially to the floor of the reactor where the regenerated cellulose membrane for separation (G) has been placed (membrane area, A_m is 38.5 mm^2, Fig. 2b). In this way the liquid could be pumped tangentially along the surface of the membrane, thus achieving a cross-flow mode membrane filtration operation. Pressure for the separation process was created by the feeding pump which forces the liquid in the reactor chamber through the membrane where it is collected at the permeate side. In our application, a syringe pump (MA1 70-2211, Harvard Apparatus, Massachusetts, USA) was used as the feeding pump due to its highly accurate flow, and due to the fact that it does not require any specialized tubing connection for operation.

Operation

In this prototype, there is no additional port nor is any small sample loop integrated for loading of the enzyme solution. Enzyme solution was loaded into the reactor by dis-connecting one of the inflow/outflow interconnects at the side of the bottom PMMA layer. Once the reactor is completely filled and all bubbles are removed, the loop is re-connected and the reaction is initiated. In this manner, reactor preparation efforts are reduced, and simpler reactor design eases the fabrication process. Additionally, a 4-port switching valve (V 101L, Upchurch Scientific) was installed in the feed line. This provided us with the options of operating the reactor in either batch, fed-batch or in continuous mode. With the use of the switching valve, handling errors and formation of undesirable bubbles in the system when re-distributing the flow in the system can be largely avoided.

Mixing

In microbioreactors, liquid flow is always in the laminar flow regime and mixing greatly relies on molecular diffusion which is in general, a very slow and time consuming process [7,19,24]. For our system, mixing is vital for circulation of substrates and enzymes within the loop, to increase enzyme and substrate contact times and also to promote uniform heat distribution for better heat transfer. An increase of the viscosity of the solution present in the reactor during the course of the enzymatic reaction makes the mixing in the reactor even more challenging.

In the membrane microbioreactor prototype presented here, mixing is achieved by means of a magnetic stirrer bar and the recirculation pump. The magnetic stirrer bar does not spin on a fixed rotational axis and was actuated by a mini magnetic stirrer (HI 190, Hanna Instruments, Rhode Island, USA) that was placed underneath the reactor. By positioning the reactor slightly off the center of the mini magnetic stirrer, the stirrer bar will then move and rotate irregularly all around the floor of the reactor, thus creating a chaotic tangential flow. This chaotic motion forces fluid to the reactor chamber wall and then circulates it around the reactor chamber, which prevents from having any ‘dead zones’ in the reactor chamber [21]. An additional means of mixing applied for the prototype is the recirculation pump. The use of a recirculation pump is the most straightforward way of transporting fluids in a loop reactor. It creates a convection flow that increases the concentration gradient for faster diffusion, hence better mixing [19]. Moreover, both the

magnetic stirrer bar and the recirculation pump create a combined sweeping action across the membrane surface. This would reduce the deposition of particles on the membrane surface (the concentration polarization effects) which are suspected to worsen as reaction proceeds [6].

Measurements and control
In this prototype, pressure measurements were done by means of a miniaturized pressure transducer (EPIH-37-1-3.5B, SensorONE Ltd., Rutland, UK). The pressure transducer was mounted in the feed line between the switching valve and the inlet feeding port. The sensor has a linear response of 16 mV/bar with accuracy of 0.01 bar over the measurement range from 0 to 3.5 bar. Pressure measurements were taken as a pressure difference between the actual pressure in the system and the ambient pressure (~1 bar).

The temperature of the reactor content was controlled by an on/off controller which is described in detail in Zainal Alam *et al.* [21]. Temperature measurements were done by using a Pt 100 temperature sensor. The Pt 100 sensor (5x1.5x1 mm) was positioned right underneath the inlet feeding port microchannel (E) and the sensor tip was fixed as close as possible to the reactor wall for a precise temperature measurement of the reactor content (the gap between the sensor tip and the reactor wall was measured to be less than 1 mm). Kanthal A resistance wire (AB Kanthal, Hallstahammar, Sweden) with an outer diameter of 0.085 mm and a resistivity of 243.2 $Ohm.m^{-1}$ was embedded in the middle PDMS layer such that the wire was surrounding the reactor chamber. The total length of wire embedded was 14 cm [21]. The wire was embedded in this way in order to achieve an even temperature distribution across the reactor chamber. In the on/off feedback temperature controller, anolog voltage signals received from the temperature sensor were linearized and converted to temperature values (^{o}C) via a transmitter (JUMO dTRANS T04, JUMO GmbH & Co., Fulda, Germany). Heating is achieved by passing an electrical current at fixed voltage supply through the resistance wire embedded in the microbioreactor. A latching relay was used to connect a direct current (DC) power supply (235W ATX Power Supply, DPS-200PB-101, Delta Electronics) for heating. With this temperature control system, temperature in the reactor content could be controlled accurately within $\pm$ 0.2 ^{o}C of the set point value [21].

All data collection and control routines were established in the LabVIEW^{TM} v8.5 software (National Instruments, Austin, TX, USA) interface using a NI USB-6229 data acquisition card (National Instruments, Austin, TX, USA).

5.3.2 Mixing quality

Evaluation of the mixing was facilitated by a fluorescent dye visualization technique. Images recorded are depicted in the series of snapshots in Figure 5.3. In the microbioreactor (Figure 5.3(a)), upon the addition of the fluorescent solution, the tangential flow created by random rotational motion of the magnetic stirrer bar instantly swept the fluorescent solution and dispersed it evenly through out the reactor chamber (uniform color was achieved in less than 30s). Uniform color distribution indicated that the reactor content was well-mixed without any “dead zones”. Whilst mixing in the reactor chamber was relatively fast; mixing in other parts of the reactor namely in the micro channels, and in the tubing was slow. This was observed from the slow dispersion of the fluorescent solution in the recirculation line which takes approximately 3 minutes and 15

seconds to be homogenously distributed. In the reactor chamber, the Reynolds number, N_{Re}, was calculated to be 75. However, in other regions of the reactor (i.e. in the microchannels and the recirculation line), N_{Re} was in the range of 0.15 to 0.3. This significant difference was most likely due to different mixing mechanism in different regions of the reactor. In the reactor chamber, the magnetic stirrer bar provided a larger interfacial area for molecular diffusion, and thus improved the mixing efficiency as compared to what has been achieved previously [24]. In the other parts of the reactor, mixing efficiency evaluation was merely based on the fluorescent solution concentration gradient which was driven by the recycle convection flow created by the recirculation pump [19].

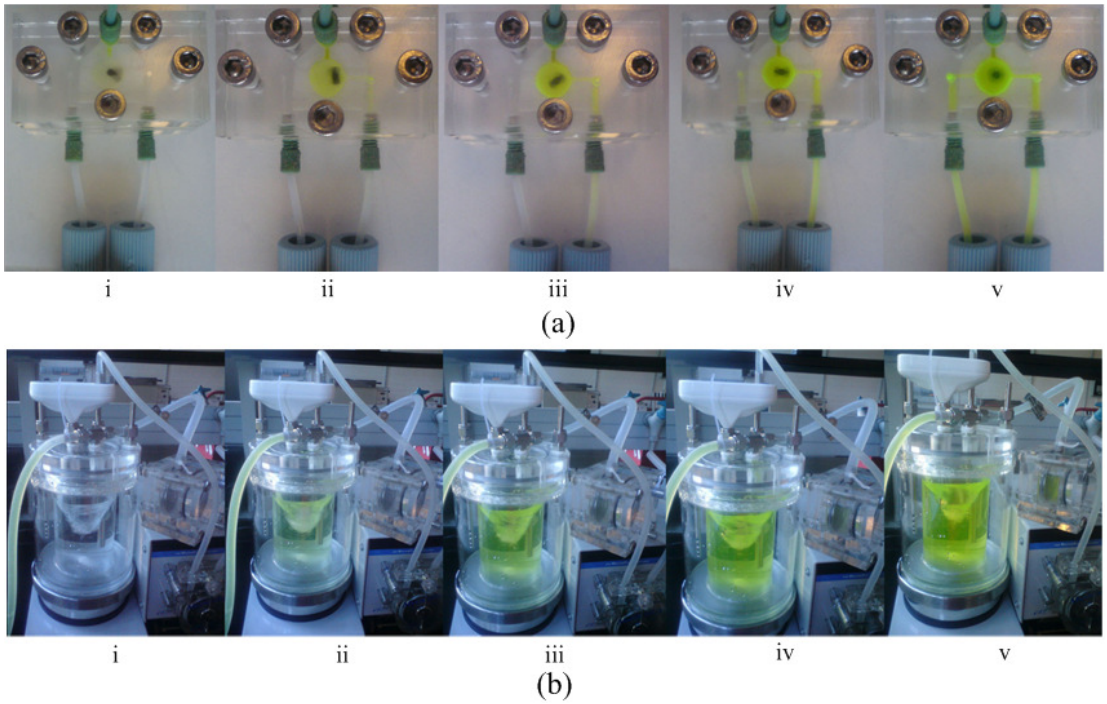

Figure 5.3. Images of mixing of the fluorescent solution in (a) membrane microbioreactor with stirring speed of 500 rpm i) Injection (t=0s) ii) 30s iii) 1 min iv) 2 min 10s v) 3 min 45s and in (b) lab-scale membrane reactor with stirring speed of 300 rpm i) Injection (t=0s) ii) 13s iii) 29s iv) 47s v) 1 min 15s.

Contrary to the mixing at the micro-scale, a more intense mixing was evident in the lab-scale membrane reactor (Figure 5.3(b)). This is due to the turbulent flow regime typically created in systems at this scale; N_{RE} in the reactor chamber was calculated to be 3 x 10^5. In the lab-scale membrane reactor, the centrifugal force generated by the spinning of the magnetic stirrer bar creates a vortex that helps to spread the fluorescent solution faster and evenly. Upon injection (at the surface of the liquid), it was seen that the fluorescent solution instantly unwound and spreads following the motion of fluid that swirls rapidly around the center of the reactor chamber. While the fluorescent solution was being mixed on the top compartment of the reactor chamber, the bottom portion of the reactor content was continuously displaced by the action of the recirculation pump. The displaced volume of fluid was passed into the membrane filtration unit and re-circulated back to the reaction chamber (N_{Re} = 40). The entire mixing process takes about 1 minute and 15 s for achieving complete mixing. As illustrated on the time-course images of mixing in both systems

(Figure 5.3), it can be concluded here that mixing in the lab-scale membrane reactor is faster (indicated by a shorter mixing time, t_m, which is a factor of 3 shorter) than the mixing in the membrane microbioreactor. However, it should be emphasized that mixing in the membrane microbioreactor was also relatively fast compared to other active mixing methods that have been implemented in different microbioreactor designs. Zhang *et al.* [8] for example use a magnetic stirrer for mixing and reported that it took 30 s to reach a well-mixed state for an agitation rate of 180 rpm. Li *et al.* [19] worked with a pressure based recycle flow mixing method, and mentioned that mixing time varies between 2 to 13 minutes depending on the combination of the recycle volume and the flow rate applied.

5.3.3 Enzyme-catalyzed degradation of sugar beet pectin

Operational modes: Semi-continuous and continuous

Enzyme-catalyzed sugar beet pectin degradation experiments performed in both micro and lab-scale membrane reactors were carried out in two different modes: (1) Semi-continuous mode, which consisted of a batch-wise load of substrate (substrate feed on for one hour) with subsequent flushing with buffer solution, and (2) Continuous mode operation. Results from both types of experiments are presented in Figure 5.4 and Figure 5.5, respectively. In the semi-continuous mode, upon switching from substrate loading to the flushing step (t = 1 h), concentration of pectin fragments in the permeate stopped increasing. A maximum concentration of 0.2 mM was reached. After the 1 hour mark, the concentration of pectin fragments in the permeate decreased asymptotically, indicating that all hydrolysis residues were being washed out as the reaction proceeded to completion. Only the enzyme and unreacted substrate remained in the system. A similar kinetic profile was also evident in Gallifuoco *et al.* [25]. In such operating mode, the reaction will never proceed to a steady-state, but a high removal of hydrolysis products can be facilitated [25]. On the contrary, in the continuous mode operation, the reaction came to a steady-state after approximately 5 hours of operation (Figure 5.5) i.e. five residence times. The final product concentration the permeate (yield ~ 0.5 mM), as calculated from the absorbance values, was also relatively higher than that observed for the semi-continuous mode of operation.

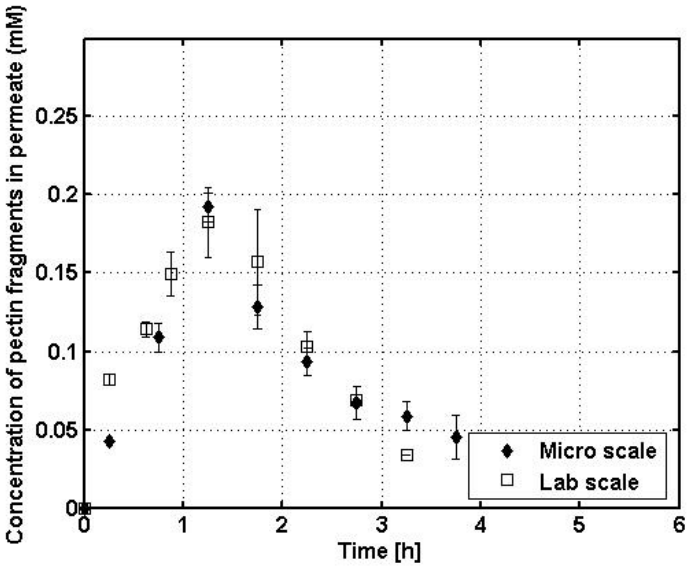

Figure 5.4. Comparison of enzymatic degradation of sugar beet pectin with pectin lyase in micro and lab-scale reactors (batch operation).

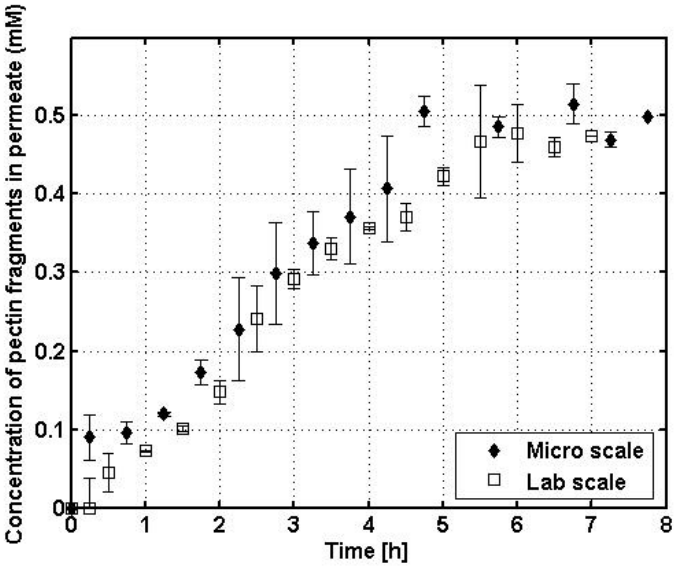

Figure 5.5. Comparison of enzymatic degradation of sugar beet pectin with pectin lyase in micro and lab-scale reactors (continuous operation).

In the continuous operation, whilst the concentration of enzyme in the reactor remained at a constant level, the substrate concentration increased progressively with time, as it was continuously fed into the system. Increasing substrate concentration in the reactor, increased the rate of the enzymatic reaction. This is in agreement with the Michaelis-Menten kinetics. As reaction proceeded, pectin lyase continued to catalyze the degradation also of partially degraded substrate generated a mixture of pectin fragments with a broad molecular weight distribution. Simultaneously, shorter pectin fragments (molecular weight < 10 kDa) continuously diffused through the membrane.

A steady-state was reached in the continuous operation. This could be due to two different facts:

(1) The concentration of substrate reached a level where the enzyme was saturated, i.e. zero-order kinetics. This implies that an increase of substrate concentration would not result in an increase of the enzymatic rate of reaction. This is in complete accordance with classical Michaelis Menten kinetics, i.e.substrate concentration for the zero-order maximum reaction rate is achieved relatively easy when the value of the Michaelis-Menten constant (K_M) is low compared to the substrate concentration. In our previous work, the Michaelis-Menten constant, K_M, for the breakdown of sugar beet pectin by pectin lyase from *Aspergillus niger* was found to be 2.66 g/L [26], which is relatively low as compared to the initial substrate concentration that was fed into the system, $[S]_o$, - 10 g/L.

(2) There was a balance between the amounts of substrate pumped into the system, the substrate degradation rate promoted by the enzyme, and the mass transport rate through the membrane. In this case, the conversion rate did not necessarily have to reach a maximum, as the level of substrate could be maintained at a low level. A similar profile of pectin concentration in the permeate was obtained during apple pectin hydrolysis in a free enzyme membrane reactor by Rodriguez-Nogales *et al.* [27], where the amount of reducing sugars increased during the first hour – corresponding approximately to the retention time of the reactor – and then the level remained constant.

The results attained also support the conclusion that the membrane microbioreactor prototype showed a comparable performance to other types of enzyme-based microbioreactors e.g. a microreactor system for enzymatic production of pectin-derived oligomers employing pectin lyase immobilized onto CIM discs (discs composed of methacrylate-based monolith matrices) [28]. Despite the simplicity of the proposed reactor design, the microbioreactor prototype has superior sensing and process control capability i.e. including active temperature control and mixing schemes. It is also important to address here that the size/volume of the proposed reactor design can easily be scaled-up to a larger scale of operation (e.g. milliliter range) whilst retaining most of the individual reactor components e.g. feeding strategy, mixing scheme, and membrane separation hybrid design.

Comparison of kinetics in lab-scale and micro-scale systems

Similar kinetic profiles - for both batch and continuous mode operation - were observed when the lab-scale reactor was operated at a residence time corresponding to two times the residence time in micro-scale reactor (Figure 5.4 and Figure 5.5). Assuming that the pectin fractions in the permeate produced from the enzymatic reaction in both configurations had a similar size distribution, it could be concluded that the efficiency in breaking-down the pectin polymers was higher in the laboratory-scale reactor. Differences in the reactor configurations might have influenced the efficiency in breaking-down the pectin polymer. In the hybrid design of the micro-scale configuration, the feeding solution came across the membrane immediately after being introduced into the reactor (Figure 5.3). On the other hand, a more thorough pre-membrane contact between enzyme and substrate probably took place in the reactor chamber of the laboratory-scale configuration (Figure 5.1) – thus allowing for a longer contact time between the substrate and the enzyme before separation occurs. In addition, better mixing in the lab-scale membrane reactor presumably promoted a more efficient contact between the enzyme and the substrate. As a result, a wider range of pectin polymer sizes might be expected in the reactor volume of the lab-scale reactor. Since no significantly higher levels of pectin fragments were seen (Figure 5.4 and Figure 5.5), the data signified that the enzymatic rate was at maximum in both the lab scale and the microbioreactor. In the case where the enzyme showed no preference for any specific substrate size, it would be difficult to predict or compare the concentration level of substrate inside the systems. Despite these differences, the ratio of enzyme to substrate concentration, [E]/[S] was the same in both systems.

We demonstrated here that the results obtained in the microbioreactor prototype are representative for the experimental results obtained in the lab-scale membrane reactor – a reactor system that is approximately 1750 times larger in volume compared to the size of the microbioreactor prototype i.e. ~ 200 µL in volume. The final aim of the proposed microbioreactor design is to convert it into a single use reactor concept. Indeed, the reactor materials, temperature control elements (i.e. few centimeters of resistance wires and a Pt 100 temperature sensor), stirrer bar and a small piece of membrane sheet used to construct the microbioreactor are all relatively inexpensive and disposable. Moving lab-scale membrane reactor experiments to a platform of disposable membrane microbioreactors is intended to minimize the cleaning efforts that are usually required for reusable lab scale reactors. Aside from the low running cost and the significant reduction in enzyme and substrate consumptions, these are all strong points supporting the idea of performing further experimental work for both research and process development studies at micro-scale.

Permeate flux and pressure build-up

In the lab-scale membrane reactor, the permeate flux followed the typical trend, declining intensely during the first phase of the process (~30%) and then decreasing in a less intense way (Figure 5.6). In both the batch and continuous experiments, an increase of the system pressure (increased until 1 bar) was observed, almost concomitantly with the decreasing permeate flux. The increasing pressure in the lab-scale operation was found to be due to the increased volume in the reaction chamber, caused by the continuous pumping of the feed solution. On the contrary, in the micro-scale operation, the working volume did not change with time ($dV/dt = 0$ and no head space). This resulted in a constant permeate flux because the volumetric feed inflow, F, into the system is equivalent to the volumetric permeate outflow, P (Figure 5.7a). Pressure build-up over time in the micro-scale operation for both the batch and continuous experiments are illustrated in Figure 5.7b. It can be seen here that, in the continuous operation, the pressure of the reactor continuously increased following the initiation of the reaction. When operating in batch mode (or semi-continuously), the pressure change reached a plateau at about 0.3 bar just after 1 hour.

The pressure increase and/or the permeate flux decrease were caused by the accumulation of un-reacted substrate in the membrane reactor system which increased the fouling on the membrane surface as reaction proceeded [29]. Despite the fact that fouling is the main drawback for utilization of membrane reactors, the advantages derived from a reduced product and substrate inhibition presumably counterbalance the negative effect of increasing retention and decreasing permeate flux. Alternatively, increase of pressure in a membrane reactor can be controlled by regulating the feed flow rate. It is recommended to operate at low pressures in order to maximize selectivity when saccharides are filtered [6]. At low pressures, the relationship between permeate flux and rejection increases in a linear way. When pressure overcomes a certain threshold value, the retention remains constant or decreases due to an increased concentration polarization [30].

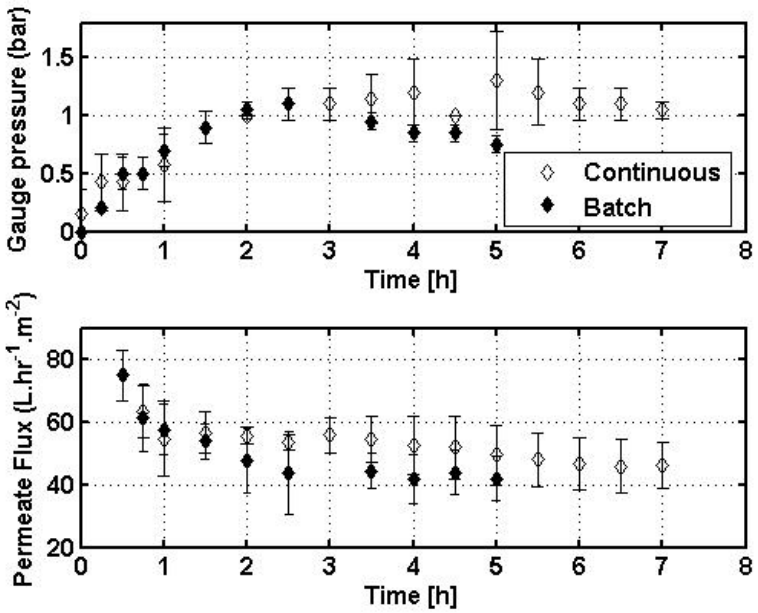

Figure 5.6. Pressure build-up (top) and permeate flux (bottom) measured in lab-scale membrane reactor during batch and continuous mode operation.

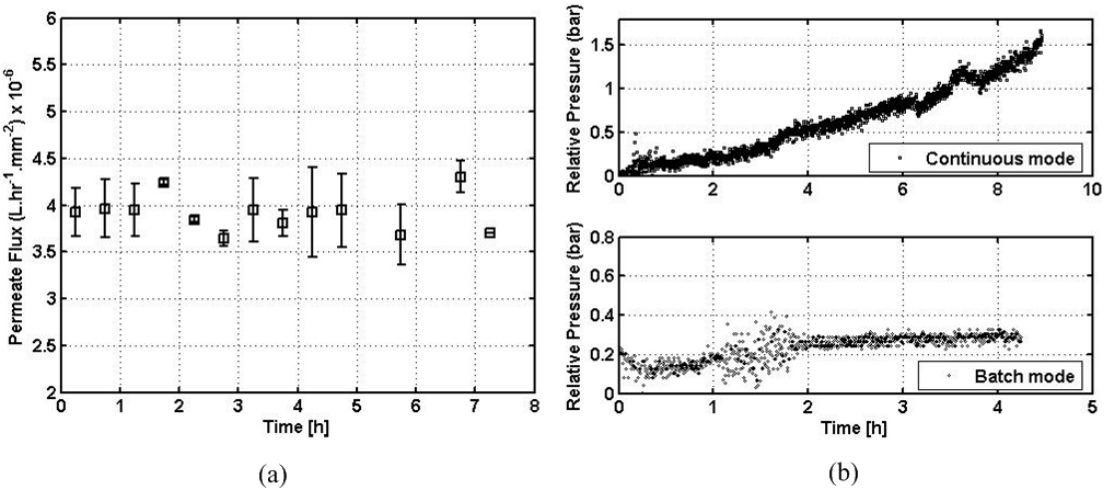

(a) (b)

Figure 5.7. (a) Permeate flux measured during experiments in membrane microbioreactor. (b) Pressure build-up measured in membrane microbioreactor during continuous (top) and batch (bottom) mode of operation.

Operation wise, the membrane microbioreactor prototype can run stable for hours (e.g. 10 - 15 hours) as long as the concentration polarization effects do not significantly reduce reactor product removal rate, and the enzyme activity remains considerably high. Those operational problems can be detected by a simultaneous and sharp increase of pressure build-up and a decrease in product absorbance values, respectively.

5.4 Conclusion

A continuous membrane microbioreactor prototype to facilitate enzyme-catalyzed degradation of pectin has been developed. The prototype was designed as a hybrid membrane microbioreactor system. A configuration that is geometrically identical to its macro-scale counterpart was adopted such that the reactor system could be amendable to scale-up. The prototype presented here is relatively easy to operate, has a low complexity – thus a relatively simple fabrication process. The micro-scale system was rather sensitive to pressure build-up within the system compared to its macro-scale counterparts. This feature might be useful as the reactor can be used as a system to get 'early' indications of for example pressure build-up caused from accumulation of un-reacted substrate in membrane reactors.

Despite differences in reactor configurations and residence time, similar kinetic profiles were achieved in both micro and lab scale operations. Comparable results achieved from both scales indicated that reaction conditions analogous to the lab scale membrane reactor had been successfully mimicked in the membrane microbioreactor. Advantages of the used setup are that hydrolysis products can be continuously removed – preventing e.g. product inhibition – and a low substrate concentration is maintained in the system at the beginning of the reaction thus avoiding a high viscosity and potential difficulties with mass transfer limitations.

The prototype membrane microbioreactor was only tested for one experimental condition. An extended study to further exploit the technology in assessing enzyme-catalyzed degradation of pectin under different experimental conditions (different type of substrates, different enzyme to substrate ratio, reactor residence time, etc.) will be conducted in the near future.

5.5 Supplementary data

Appendix A - Membrane microbioreactor: Mechanical drawings

Appendix B – LabView program

5.6 References

[1] Rosgaard, L., Pedersen S., Cherry, J. R., Harris, P., Meyer. A. S. (2006). Efficiency of new fungal celllulase systems in boosting enzymatic degradation of barley straw lignocellulose. *Biotechnology Progress* **22:** 493-498.

[2] Sørensen, H. R., Pedersen, S., and Meyer, A. S. (2007). Synergistic enzyme mechanisms and effects of sequential enzyme additions on degradation of water insoluble wheat arabinoxylan. *Enzyme Microbial Technology* **40:** 908-918.

[3] Arnous, A., and Meyer, A. S. (2010). Discriminated release of phenolic substances from red wine grape skins (*Vitis vinifera L.*) by multicomponent enzymes treatment. *Biochemical Engineering* 49: 68-77.

[4] Lye, G. J., Ayazi-Shamlou, P., Baganz, F., Dalby, P. A., and Woodley, J. M. (2003). Accelerated design of bioconversion processes using automated microscale processing techniques. *Trends in Biotechnology* **21:** 29-37.

[5] Rachinskiy, K., Schultze, H., Boy, M., BornScheuer, U., and Buchs, J. (2009). Enzyme Test Bench' a high-throughput enzyme characterization technique including the long-term stability. *Biotechnology and Bioengineering* **103:** 305-322.

[6] Pinelo, M., Jonsson, G., and Meyer, A. S. (2009). Membrane technology for purification of enzymatically produced oligosaccharides: Molecular and operational features affecting performance. *Separation and Purification Technology* **70:** 1-11.

[7] Schäpper, D., Zainal Alam, M. N. H., Szita, N., Lantz, A. E., and Gernaey, K. V. (2009). Application of microbioreactors in fermentation process development: a review. *Analytical and Bioanalytical Chemistry*. **395**: 679-695.

[8] Zhang, Z., Boccazzi, P., Choi, H., Perozziello, G., Sinskey, A. J., and Jensen, K. F. (2006). Microchemostat – microbial continuous culture in a polymer-based instrumented microbioreactor. *Lab on a chip* 6: 906-913.

[9] Swarts, J. W., Vossenberg, P., Meerman, M. H., Janssen, A. E. M. and Boom, R. M. (2008). Comparison of two-phase lipase-catalyzed esterification on micro and bench scale. *Biotechnology and Bioengineering*. **99**: 855-861.

[10] Muller, D. H., Liauw, M. A. and Greiner, L. (2005). Microreaction technology in education: Miniaturized enzyme membrane reactor. *Chemical Engineering Technology*. **28**: 1569-1571.

[11] de Jong, J., Lammertink, R. G. H., and Wessling, M. (2006). Membranes and microfluidics: a review. *Lab on a chip* **6:** 1125-1139.

[12] Miyazaki, M. and Maeda, H. (2006). Microchannel enzyme reactors and their applications for processing. *Trends in Biotechnology* **24:** 463-470.

[13] Urban, P. L., Goodall, D. M. and Bruce, N. C. (2006). Enzyme microreactors in chemical analysis and kinetic studies. *Biotechnology Advances* **24:** 42-57.

[14] Pijanowska, D. G., Baraniecka, A., Wiater, R., Ginalska, G., Lobarzewski, J. and Torbicz, W. (2001). The pH-detection of triglycerides. *Sensors and Actuators B*. **78:** 263-266.

[15] Gao, J., Xu, J., Locasscio, L. E., and Lee, C. S. (2001). Integrated microfluidics system enabling protein digestion, peptide separation, and protein identification. *Analytical Chemistry* **73:** 2648-2655.

[16] Diano, N., Grimaldi, T., Bianco, M., Rossi, S., Gabrovska, K., Yordanova, G., Godjevargova, T., Grano, V., C. Nicolucci, L. Mita, U. Bencivenga, P. Canciglia, D. G. Mita, Apple juice clarification by immobilized pectolytic enzymes in packed or fluidized bed reactors, Agricultural, Food and Chemistry, 56 (2008) 11471-11477.

[17] Kee, S., and Gavriilidis, A. (2009). Design and performance of a microstructed PEEK reactor for continuous Poly-L-leucine-catalysed chalcone epoxidation. *Organic Process Research & Development* **13:** 941-951.

[18] Znidarsic-Plazl, P., and Plazl, I. (2009). Modelling and experimental studies on lipase-catalysed isoamyl acetated synthesis in a microreactor. *Process Biochemistry* **44:** 1115-1121.

[19] Li, X., van der Steen, G., van Dedem, G. W. K., Van der Wielen, L. A. M., Van Leeuwen, M., Van Gulik, W. M., Heijnen, J. J., Krommenhoek, E. E., Gardeniers, J. G. E., van den Berg, A. and Ottens, M. (2008). Improving mixing in microbioreactors. *Chemical Engineering Science* **63:** 3036-3046.

[20] Nikolic, M. V., and Mojovic, L. (2007). Hydrolysis of apple pectin by coordinated activity of pectic enzymes. *Food Chemistry* **101:** 1-9.

[21] Zainal Alam, M. N. H., Schäpper, D., and Gernaey, K. V. (2010). Embedded resistance wire as heating element for temperature control in microbioreactors. *Journal of Micromechanics and Microengineering* DOI: 10.1088/0960-1317/20/5/055014.

[22] Yadav, S., Yadav, P. K., Yadav, D., and Yadav, K. D. S. (2009). Pectin lyase: A review. *Process Biochemistry* **44:** 1-10.

[23] van den Broek, L. A. M., den Aantrekker, E. D., Voragen, A. G. J., Beldman, G., and Vincken, J. P. (1997). Pectin lyase is a key enzyme in the maceration of potato tuber. *Science of Food and Agriculture* **75:** 167-172.

[24] Ryu, K. S., Shaikh, K., Goluch, E., Fan, Z., and Liu, C. (2004). Micro magnetic stir-bar mixer integrated with paralene microfluidics channels. *Lab on a chip* **4:** 608-613.

[25] Gallifuoco, A., Alfani, F., Cantarella, M., and Viparelli, P. (2003). New experimental procedure for monitoring molecular weight breakdown during enzymatic degradation of polygalacturonic acid in conctinuous membrane reactors. I*ndustrial & Engineering Chemistry Research* 42: 3937-3942.

[26] Silva, I. C. R. (2008). Characterization of *Aspergillus* enzymes for pectin modification. *MSc thesis* Center for BioProcess Engineering, Department of Chemical and Biochemical Engineering, Technical University of Denmark (DTU).

[27] Rodriguez-Nogales, J. M., Ortega, N., Perez-Mateos, M. and Busto, M. D. (2008). Pectin hydrolysis in a free enzyme membrane reactor: An approach to the wine and juice clarification. *Food Chemistry* **107:** 112-119.

[28] Mannheim, A. and Cheryan, M. Continuous hydrolysis of milk protein in a membrane reactor. *Food Science* **55:** 381-385.

[29] G. Jonsson (2004). Selectivity in membrane filtration in: J. K. Bungay, P. M. Bungay, H. K. Lonslade, M. N. Pinho (Eds.). *Synthetic Membranes: Science, Engineering and Applications,* Springer.

CHAPTER 6

Assessing enzymatic modification of pectin by application of a continuous membrane microbioreactor

CHAPTER 6

Assessing enzymatic modification of pectin by application of a continuous membrane microbioreactor

---

Abstract

This chapter presents the application of a membrane microbioreactor system for examining continuous enzyme-catalyzed degradation of pectin. The membrane microbioreactor prototype was fabricated from poly(methylmethacrylate) (PMMA) and poly(dimethylsiloxane) (PDMS) with a working volume of approximately 190 μL. The prototype also contained the necessary sensors and actuators, i.e. pressure transducer, temperature control and active mixing schemes. The functionality of the prototype was demonstrated by running a continuous enzyme-catalyzed degradation reaction of pectin for a range of reactor conditions: different membrane molecular weight cut-off (MWCO), enzyme to substrate ratio and substrate feeding rate were assessed. The MWCO influenced the evolution of the pectin degradation products in the permeate: the apparent rate appears to be higher with the higher MWCO membrane. At constant MWCO (10 kDa) the steady state concentration of pectin degradation products was higher at the lower substrate feed rate, presumably as a result of a higher extent of reaction due to the longer reactor residence time at the lower feed rate. The data thus signified that the microbioreactor could diagnose consequences of different process design options relevant for larger scale enzymatic pectin degradation reactions.

This chapter has been submitted as Zainal Alam, M. N. H., Pinelo, M., Arnuos, A., Jonsson, G., Meyer, A. S., and Gernaey, K. V. (2010). Assessing enzymatic modification of pectin by application of a continuous membrane microbioreactor. *Journal of Biotechnology and Bioengineering*. – under review.

6.1 Introduction

Existing fabrication methods for production of microfluidics systems offer the opportunity to design and operate low cost miniature size reactors, generally with working volume less than 1 mL [1-4]. An increasing number of microbioreactors have recently been deployed as support tools to evaluate different types of enzymatic reactions [5-9] as summarized in Table 6.1. Each of the studies included in Table 6.1 has addressed the potential use of enzyme-based microbioreactors either to evaluate reaction kinetics [9] test catalyst performance [8], evaluate scalability [9], or to study the effects of reactor operational variables (e.g. pH, T, residence time, etc.) on enzymatic reactions [6,7,9]. Several research projects [10-13] have successfully applied a membrane bioreactor for studying the enzymatic modification of pectin. Nonetheless, the use of continuous microbioreactors for evaluating process implications of process design choices, e.g. impact of feed flow rate or molecular weight cut-off (MWCO), has received limited attention.

In this chapter, the focus is on the development of a continuous membrane microbioreactor as a new research tool for assessing enzyme-catalyzed modification of pectin. Pectic substances can be found in fruits and vegetables, and are abundant in many different agro-industrial waste streams. Agro-industries are highly interested in converting these low-value waste streams into useful high-value products, for example into biofunctional oligosaccharides (carbohydrates containing between two and approximately 20 monomers; [14-15]). Such a conversion of pectin is possible through enzymatic reactions catalyzed by pectinolytic enzymes (typically of fungal origin), such as the pectin lyase (PL) (EC 4.2.1.10), pectinmethylesterase (PME) (EC 3.2.1.11), endo-polygalacturonase (PG) (EC 3.2.1.15) etc. [16-17].

Our hypothesis is that information gained from the experiments in a continuous membrane microbioreactor system could provide a better understanding of the enzyme-catalyzed reaction dynamics, i.e. product formation rate and yields, in response to the reactor and reaction design options, such as substrate feeding rate, enzyme dosage, and membrane weight cut-off etc. Such dynamics are indeed difficult to predict by kinetic modeling alone (because simple Michaelis-Menten kinetics equations do not suffice to describe the enzymatic degradation of pectin), whereas the description of the separation effect of the membrane usually leads to rather complicated mechanistic models. Knowledge on the reaction mechanism as well as on the membrane separation is crucial such that the enzymatic reaction can be controlled towards increased production of specific targeted oligomers produced in the reactor output [18].

In our previous work [19], the workability of the continuous membrane microbioreactor prototype was demonstrated. It was also shown that kinetic profiles achieved in micro-scale were congruent with those obtained in a bench scale setup. The workability of the prototype, however, was only tested for one experimental condition. In this chapter, we therefore aim to further demonstrate the functionally of the system: Experimental results obtained in the membrane microbioreactor prototype from a continuous β-elimination experiment of sugar beet pectin catalyzed by pectin lyase are reported. The experiments were performed under various experimental conditions, where membrane molecular weight cut-off (MWCO), substrate feeding rate F (μL/hr) and the enzyme to substrate (E/S) ratio were varied.

Table 6.1. Overview of various enzyme-based microbioreactors developed to assess different types of enzymatic reactions.

Ref.	Volume (μL)	MBR type	Operation mode	Reaction model system	Mixing	Controlled variables	Application
[9]	3.5	Chip type	Direct loading of [S] and [E] into separate inlets	Esterification of 1-butanol and propionic acid in a two-phase system	Y-shaped mixer	T, pH, and feed flow	Scalability, kinetic studies and T effect
[6]	615	Chip type	Direct loading of [S] and [E] into separate inlets	Poly-L-leucine-catalyzed chalone epoxidation	T-shaped and staggered-herringbone mixer	T, pH, and feed flow	T, [S], [E] and residence time effect
[7]	4.7	Immobilized	Direct loading of [S] into immobilized [E] in μ-channel	Hydrolysis of starch	Diffusion based (flow-through mode)	T, pH, and feed flow	Immobilization chemistry, buffer, T, pH, [S] and feed flow effect
[5]	340	Immobilized	Direct loading of [S] into immobilized [E] in monolithic disk	Enzymatic modification of pectin to produce oligosaccharide	Diffusion based (flow-through mode)	T, pH, and feed flow	Immobilized vs. free enzyme system, T and pH effect
[8]	200	Membrane loop reactor	Direct loading of [S] into reactor loop	Reduction of acetophenone to (S)-phenylethanol	T-shaped and pressure-based recycle flow mixer	pH and feed flow	Test catalyst performance

Ref.=reference; Vol.=volume; MBR=microbioreactor; [S]=substrate; [E]=enzyme; T=temperature.

6.2 Materials and Methods

6.2.1 Microbioreactor fabrication

The microbioreactor was fabricated from poly(methylmethacrylate) (PMMA) (Plexiglas GS, Klar 233, Nordisk Plast, Auning, Denmark) and poly(dimethylsiloxane) PDMS. Fabrication of the reactor's PMMA layers was done by using a computer-numerical-controlled (CNC) milling machine (CNC micromill, Minitech MiniMill 3/Pro, Minitech Machinery Coorporation, Norcross, GA, USA). As for the reactor's PDMS layer, a negative image of the PDMS layer was micro-milled into PMMA which then served as a mold. After machining, a Pt 100 temperature sensor (PCA 1.2005.1L, JUMO GmbH & Co., Fulda, Germany) was first placed into the mold. Next, liquid PDMS (prepared by mixing ten parts silicone to one part curing agent, Sylgard 184, Dow Corning Corp., Midland, MI, USA) was poured into the mold and cured at 70 °C for two hours. Finally, the cured PDMS layer was removed from the mold and a 2-pin electrical connector was soldered to the temperature sensor to establish an electrical connection for the temperature measurement.

6.2.2 Membrane microbioreactor prototype

A scheme of the experimental setup for the membrane microbioreactor is illustrated in Figure 6.1. The membrane microbioreactor prototype was realized as a loop-type reactor with an integrated reactor and membrane separation unit as the main components of the loop (as described in detail in [19]). It was designed to work with constant working volume (~190 μL), with no headspace and under bubble-free conditions.

The reactor consisted of a 2.5 mm thick PDMS layer sandwiched in between two 8 mm thick PMMA layers. The middle PDMS layer served as the main body of the prototype and included the reactor chamber (centered in the middle of the PDMS layer) with a depth of 2.5 mm and a diameter of 7 mm, giving a volume of about 100 μL. A magnetic stirrer bar with a length of 3 mm and thickness of 1 mm was placed on the reactor's floor for active mixing. The reactor chamber was connected to the inlet feeding port and to the inlet/outlet ports of the recirculation line by 0.5 mm deep x 1 mm wide micro-channels.

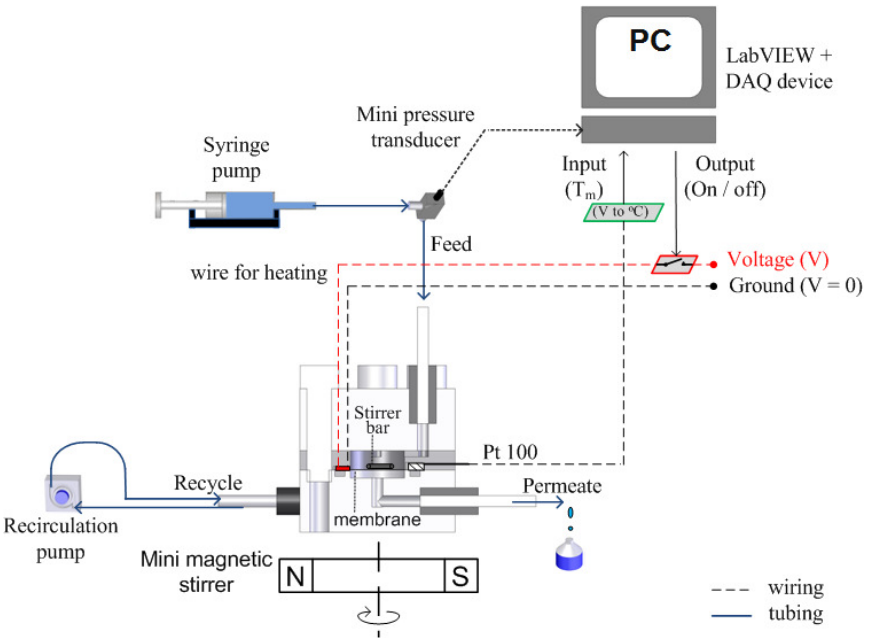

Figure 6.1. 2-D schematic of the membrane microbioreactor experimental setup.

The top PMMA layer had five clearance holes with a diameter of 2.7 mm for M2.5 screws and an inlet port for the feeding solution – a 6-40 threaded port with a diameter of 3.6 mm. The bottom PMMA layer formed the base of the reactor. It contained the permeate chamber (cylinder with 7 mm diameter and 1 mm height, resulting in about 38.5 µL volume) and side ports – also by using 6-40 threaded ports with diameter of 3.6 mm – for the recirculation line. The recirculation line was established by connecting these side ports via standard perfluoroalkoxy PFA tubing (outer and inner diameters of the tube are 1.59 mm and 0.75 mm, respectively) to a micro gear pump (mzr 2905, HNP Mikrosysteme GmbH, Parchim, Germany) which served as the recirculation pump for the system. The bottom PMMA layer also included five threaded ports for M2.5 screws.

The membrane for product separation was placed in between the reactor chamber and the permeate chamber (Figure 6.1); the membrane thus formed the reactor's floor (membrane area, A_m is 38.5 mm^2). Pressure for the separation process was created by the feeding pump which forces the liquid in the reactor chamber through the membrane where it was collected at the permeate side.

In this prototype, pressure measurements were done by means of a miniaturized pressure transducer (EPIH-37-1-3.5B, SensorONE Ltd., Rutland, UK). The pressure transducer was mounted in the feed line between the syringe pump and the inlet feeding port. The temperature of the reactor content was controlled by an on/off controller which is described in detail in Zainal Alam *et al.* [20]. Temperature measurements were done by using a Pt 100 temperature sensor – positioned right underneath the inlet feeding port microchannel – and a Kanthal A resistance wire (AB Kanthal, Hallstahammar, Sweden) with an outer diameter of 0.085 mm and a resistivity of 243.2 $Ohm.m^{-1}$ which was embedded in the middle PDMS layer for heating. Heating was achieved by passing an electrical current at fixed voltage supply through the resistance wire embedded in the microbioreactor. With this temperature control system, temperature in the reactor content

could be controlled accurately within $\pm$ 0.2 ^{o}C of the set point value [20].

All data collection and control routines were established in the LabVIEW^{TM} v8.5 software (National Instruments, Austin, TX, USA), which was interfaced to the experimental setup using a NI USB-6229 data acquisition card (National Instruments, Austin, TX, USA).

6.2.3 Starting-up and reactor operation

For starting-up the reaction in the membrane microbioreactor, the reactor was first filled with enzyme solution to purge bubbles out of the system. The enzyme solution was loaded into the reactor by disconnecting one of the inflow/outflow interconnects at the side of the bottom PMMA layer. Once the reactor was completely filled, the loop was re-connected. Then, the reactor's temperature was set at its desired set point value and the reaction was initiated by starting the feeding of the substrate solution.

Substrate solution was continuously fed into the reactor by using a syringe pump (MA1 70-2211, Harvard Apparatus, Massachusetts, USA) at predetermined feed flow rates, F_{in}, and circulated by means of the recirculation pump. During the course of reaction (which occurred in both the reactor chamber and the recirculation line), enzyme and un-reacted substrate solutions were retained in the system by the membrane while low molecular weight products (< membrane molecular weight cut-off, MWCO) were continuously separated from the system. A regenerated cellulose membrane with MWCO of 1 kDa and 10 kDa (PLGC06210, Millipore, Billerica, MA, USA) were used for separation.

6.2.4 Enzymatic depolymerization of sugar beet pectin by pectin lyase

Sugar beet pectin with a degree of methoxylation of ~60% and a degree of acetylation of ~19% (Danisco A/S, Brabrand, Denmark) was used as a substrate. The pectin lyase used in this study was supplied by Novozymes A/S (Bagsværd, Denmark). It was a cloned monocomponent enzyme from *Aspergillus aculeatus* with an enzyme activity on citrus pectin of 0.0085 U·mg^{-1}. One unit of activity (U) is defined as production of 1 µmol of double bonds per minute at pH 4.5 and 50^{o}C. 0.1 M sodium acetate buffer solution (pH 4.5) was used to prepare both the substrate and the enzyme solutions.

Several experiments were set up with the aim to demonstrate the workability of the membrane microbioreactor prototype (Table 6.2). For every experimental condition, the reaction was performed with initial substrate concentration, $[S]_o$ of 10 g/L, at pH 4.5 and temperature was controlled at 50^{o}C. The reaction was carried out until a steady-state was reached.

Table 6.2. Various experimental conditions tested in the membrane microbioreactor prototype.

	Parameters tested		
	Enzyme to substrate ratio, E/S	Substrate feeding rate, F	Membrane molecular weight cut-offs (MWCO)
Experiment 1	0.2% (g/g)	200 µL/hr	1 kDa and 10 kDa
Experiment 2	0.2% (g/g) and 0.4% (g/g)	200 µL/hr	1 kDa
Experiment 3	0.2% (g/g)	100 µL/hr and 200 µL/hr	10 kDa
Experiment 4	0.2% (g/g)	100 µL/hr	1 kDa and 10 kDa

6.2.5. UV absorption at 235 nm

The UV absorption analysis was performed in order to monitor the progress of the depolymerization reaction. This was done by measuring sample absorbance via a microtiter plate reader at 235 nm. Beer-Lamberts law ($A_{235} = l\varepsilon c$) was used to estimate the concentration of product fragments, c, generated from the depolymerization reaction. A molar absorption coefficient, ε, of 5500 M^{-1} cm^{-1} was used [21].

6.2.6 Mono and oligo- galacturonic acids electrochemical measurement via HPAEC-PAD

Identification and quantification of mono and oligogalacturonic acids in hydrolysates were performed using an ICS-3000 system coupled to an AS50 autosampler (Dionex Corp., Sunnyvale, CA). Separations were performed using a CarboPac™ PA20 (3 mm × 150 mm) analytical column (Dionex Corp., Sunnyvale, CA) according to the method of Arnous and Meyer [22]. All eluents were prepared from HPLC grade chemicals. The quantification of mono-, and di-galacturonic acids was carried out by use of external standards. Trigalacturonic acids were quantified by using the response factor of galacturonic acid. Data were collected and analyzed on computers equipped with Chromeleon 6.80 Sp8 software (Dionex Corp., Sunnyvale, USA).

6.3 Results and discussions

The kinetic profiles obtained with two different membranes with a molecular weight cut-off (MWCO) of 1 kDa and 10 kDa respectively (Figure 6.2) followed a general trend that is typical for continuous degradation of pectin substrate in a membrane reactor, where the concentration of the pectin fragments in the permeate increased progressively with time until a steady-state was reached [10-13]. A steady-state product formation level was reached when a balance between the feed flow rate, the kinetic conversion rate (i.e. the overall rate of the enzymatic reaction as measured from the product formation rate) and the membrane flux of the system was reached [19]. As expected, the membrane with a MWCO

of 1 kDa showed a higher membrane rejection at the beginning of the reaction compared to the membrane with MWCO of 10 kDa, resulting in an apparently lower product formation rate of pectin fragments (Figure 6.2). Theoretically, membrane rejection, R is defined as a function of the ratio between the solute concentration in the permeate, C_p and the solute concentration on the surface of the membrane, C_M (Equation 6.1) (The C_M is thus a function of the solute concentration in the reactor) [23].

$$R = 1 - \frac{C_p}{C_M} \tag{6.1}$$

From the relation given in Equation (1), a lower permeate concentration, C_p indicates a higher membrane rejection characteristic when C_M is constant. This is to be expected for a membrane with smaller pore size (i.e. 1 kDa) as larger fragments (i.e. molecular weights > 1 kDa) should be rejected by the membrane (i.e. retained in the system).

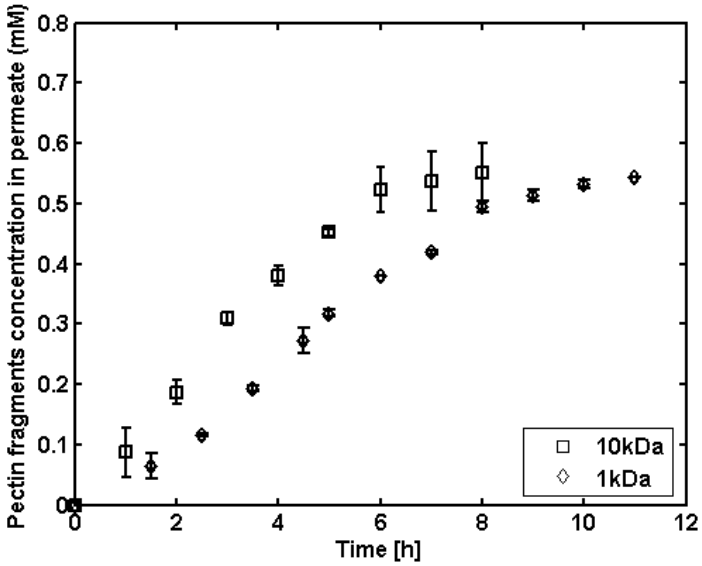

Figure 6.2. Pectin fragment concentration dynamics in the permeate (mM): comparison between membranes with molecular weight cut-off (MWCO) of 1 kDa and 10 kDa run at a feeding rate, F of 200 µL/hr with an enzyme to substrate, *E/S,* ratio of 0.2% (g/g).

Interestingly, when the enzymatic reaction came to steady-state (Figure 6.2), the final concentrations of pectin fragments in the permeate were comparable (yield ~ 0.55 mM) for both membranes (i.e. 1 kDa and 10 kDa). This result indicated that – as reaction proceeded to steady-state – the membrane pore size was no longer influencing the membrane rejection, despite the fact that the pore size of the membranes differed by a factor of 10. This observation may be due to increased viscosity and/or fouling resulting from the build-up of unreacted substrate in the reactor as well as at the membrane surface and/or be due to concentration polarization, increasing C_M and hence R of the 10 kDa membrane (Equation 6.1) .It was anticipated that the membrane with the lowest MWCO would have the highest membrane selectivity whilst removing pectin fragments from the reactor system, i.e. ,shorter fragments are to be expected when a membrane with smaller pore size (e.g. 1 kDa) is applied. The chromatographic profiles obtained confirmed the

presence of different sizes of pectin oligomers in the reactor permeate (data not shown), but based on the results of the HPAEC analysis (Figure 6. 3 and Table 6.3), it was found that similar types and relatively similar levels of low molecular weight pectin oligomers, i.e. galacturonic acid, *GalA,* monomers, dimers and trimers were recovered in the permeate for both membranes (the molecular weights of the dehydrated, methylated forms of the mono-, di- , and tri-galacturonic acids are ~190; 380; and 570 D, respectively). The oligomer concentration profiles for both membrane systems indicated a sharp increase of the oligomer concentration during the first 2 to 4 hours of reaction, before reaching a steady-state after a reaction time of about 4 hours (Figure 6.3). Although the concentrations of the recovered low molecular weight pectin oligomers in the permeate were slightly higher for the 10 kDa membrane system compared to the 1 kDa system (Figure 6.3 and Table 6.3), it can be concluded that the concentrations of these low molecular weight pectin oligomers were within the same order of magnitude for both membranes.

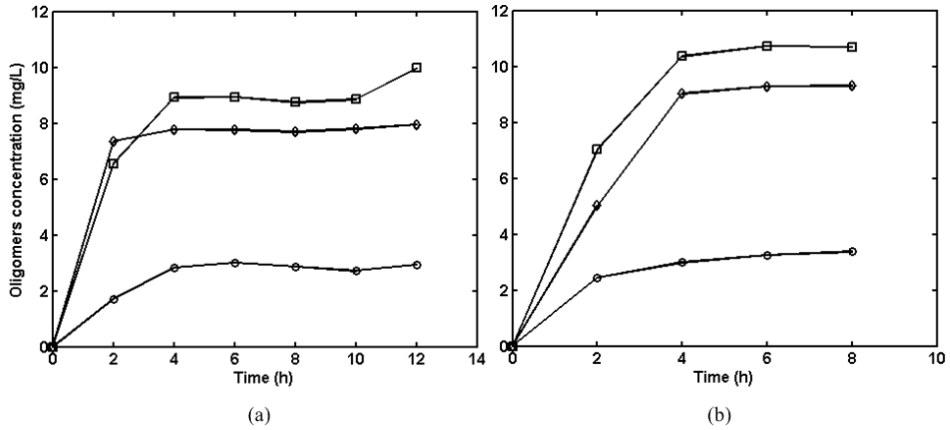

Figure 6.3. Concentration profiles of the pectin oligomers for membranes with different molecular weight cut-offs (MWCO) run at a feeding rate, *F*, of 200 µL/hr with enzyme to substrate, *E/S* ratio of 0.2%(g/g). (a) MWCO = 1 kDa. (b) MWCO = 10 kDa. - *GalA* monomers; ◊ - *GalA* dimers; ○ – *GalA* trimers.

Since the enzyme to substrate ratio, *E/S* was the same in both membrane systems – thus promoting a similar rate of catalytic activity – the product removal rate was strongly dependent on the membrane separation efficiency. This could be ascribed to concentration polarization phenomena. In our previous work [19], we reported that the system pressure increased gradually following the initiation of the enzymatic reaction. The pressure increase (i.e. relative pressure increases as high as 1.5 bar were registered) was believed to be caused by the accumulation of the unreacted substrate molecules in the system. The continuous increase of the concentration of unreacted substrates – presumably on the surface of the membrane – is assumed to lead to the formation of a gel layer on the membrane surface. Hence, it creates a concentration gradient between the substrate concentration in the bulk solution and the concentration on the membrane surface. The rejection capacity of the system can be greatly influenced by this additional gel layer on the membrane surface. Considering the typical diffusivity values of pectin molecules and a standard gel layer thickness (calculations not shown), it is possible to deduce that the concentration of pectin close to the membrane surface could be 7-10 times higher (~70-100 g pectin/L) than the concentration of pectin in the bulk solution. At this high concentration,

it is possible to hypothesize that the pectin layer could hinder the back diffusion of the small pectin fractions to the bulk solution, thereby neglecting the diffusivity term of the mass transfer balance of the solute across the membrane, (i.e. $dc/dx = 0$) as shown in Equation 6.2 [23]):

$$J.C_b + D\frac{dc}{dx} = J_p.C_p \qquad (2)$$

Where J is the flux to the membrane on the retentate side, D is the diffusivity, c the concentration of solute in a particular point of the retentate, x the distance between a point of the bulk solution and the membrane, and J_p the permeate flux.

Table 6.3. Concentration of oligomers (monomers, dimers, and trimers) in the retentate and in the permeate at steady state for the membranes used in the experimental work (a) MWCO of 1 kDa and (b) MWCO of 10 kDa.

(a)

At steady-state, t = 12 hr	GalA - monomers	GalA - dimers	GalA - trimers
[Retentate],C_b (mg/L)	8.03	4.5	2.2
[Permeate],C_p (mg/L)	10	8	2.9

(b)

At steady-state, t = 8 hr	GalA - monomers	GalA - dimers	GalA - trimers
[Retentate],C_b (mg/L)	8.5	4.6	2.3
[Permeate],C_p (mg/L)	10.7	9.3	3.38

In our particular continuous reactor system, the substrate feeding rate, F is equivalent to the permeate flux, J_p as the microbioreactor volume does not change with time (i.e. $dV/dt = 0$ and no headspace). Since J is the same as J_p, the pectin oligomer concentration in the bulk solution, C_b, can be assumed to be the same as the concentration of the pectin oligomers in the permeate, C_p (see Equation 6.2). The results from the HPLC analysis also supported the hypothesis of identical concentrations of small pectin fractions in the bulk solution and in the permeate. In the steady-state, comparable concentrations of *GalA* monomers, dimers and trimers were detected at both sides of the membrane (i.e. retentate and permeate) for both 1 kDa and 10 kDa membranes (as summarized in Table 6.3). Hence, based on this analysis, the apparent higher production rate of pectin fragments observed for the 10 kDa membrane as assessed by the amount of dehydrated reducing ends by UV absorbance (Figure 6.2), indicated that a higher amount of larger molecular weight pectin fragments (i.e. larger than tri-galacturonic acid) passed through the 10 kDa membrane than through the 1 kDa membrane during the first 8 hours of the reaction.

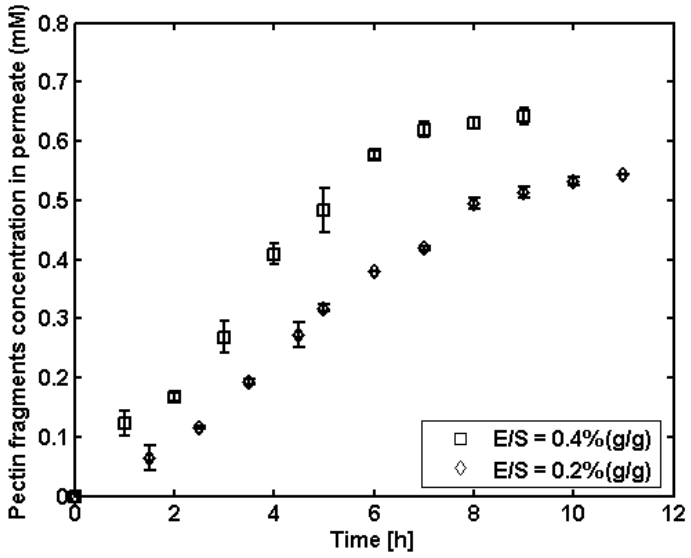

Figure 6.4. Concentration profiles of pectin fragments in the permeate (mM) for a membrane with molecular weight cut-off (MWCO) of 1 kDa operated under a different enzyme to substrate, *E/S* ratio (i.e. 0.2% (g/g) or 0.4% (g/g)) at a feeding rate, *F*, of 200 µL/hr.

To further evaluate the ability of the microbioreactor prototype to assess consequences of process operation choices, we tested the system by varying the enzyme to substrate ratio, *E/S*, as well as the substrate feeding rate, *F*. As suspected, an increase in the reaction rate was observed when the *E/S* ratio was increased (Figure 6.4). When the substrate feeding rate, *F* was lowered by 50% (i.e. system flux $\simeq$ 100 µL/hr), the apparent reaction rate increased and a significant increase in product yield (to ~0.8 mM) was observed (Figure 6.5). This result was expected since lowering of the substrate feeding rate, *F* by 50% in effect increased the reactor residence time from about 1 hour to about 2 hours The residence time, τ was defined as the reactor volume divided by the time period that the enzyme has the chance to catalyze the degradation of the pectin (i.e. substrate) before the degraded fragments were being removed from the system [24]. Additionally, a lowering of the system flux, apparently decreased the accumulation rate of the unreacted substrates on the membrane surface. In turn, this resulted in a higher product recovery rate as the concentration polarization effect was considerably reduced (and a less thick gel layer was formed on the membrane due to the lower flux rate). Olano-Martin *et al.* [12] also reported that an increase of residence time led to a higher product conversion of high methylated pectin into pectic-oligosaccharides in a continuous dead-end membrane reactor.

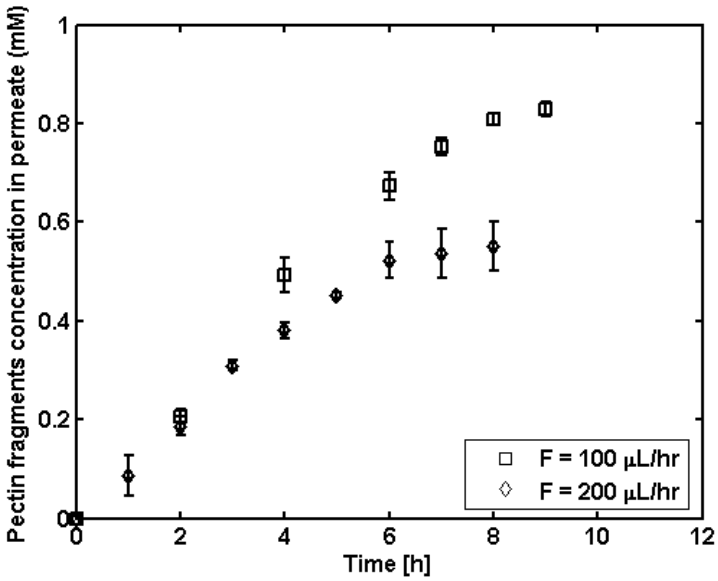

Figure 6.5. Concentration profile of pectin fragments in the permeate (mM) for a membrane with molecular weight cut-off (MWCO) of 10 kDa operated with different feeding rates (i.e. 100 µL/hr or 200 µL/hr) at an enzyme to substrate, E/S ratio of 0.2% (g/g).

Similarly, when the enzymatic reaction was performed under the same conditions as those reported in Figure 6.2, but with lower feeding rate (i.e. system flux $\underset{\sim}{}$ 100 µL/hr and residence time of 2 hours), a significantly higher product yield and recovery rate were observed (Figure 6.6). The apparent steady-state product formation level increased with longer residence time; i.e. up to approximately 0.8 mM and 0.65 mM for the 10 kDa and 1 kDa membrane, respectively (refer to Figure 6.6). Hence, the reactor residence time of 1 hour limited the apparent steady-state product formation levels (i.e. yield ~ 0.55 mM) when different membrane MWCO were evaluated (refer to Figure 6.2). The recorded effect of reactor residence time on the steady-state level product formation indicated that the apparent steady state product level could be controlled (at least within certain boundaries) by the feed rate that both controlled the substrate supply and the residence time. There was apparently plenty of substrate even at the low feed rate, which in turn must signify that the enzymatic rate in the reactor, i.e. at the apparent steady state, was running near maximum. Results attained in Figure 6.4, Figure 6.5, and Figure 6.6 highlight that the substrate feeding rate, *F* (i.e. system flux) is a critical variable that can dramatically alter the rejection profile of a membrane microbioreactor system.

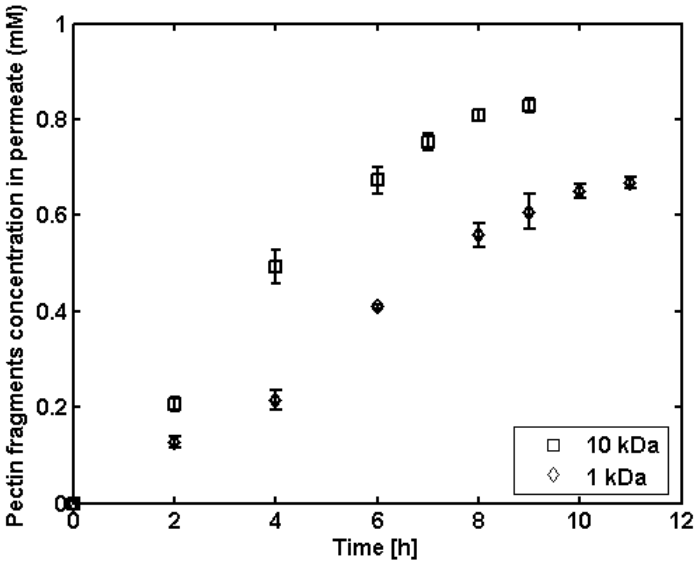

Figure 6.6. Concentration profile of pectin fragments in the permeate (mM) for membranes with molecular weight cut-off (MWCO) of 1 kDa and 10 kDa respectively, operated at a feeding rate, *F*, of 100 µL/hr with enzyme to substrate, *E/S* ratio of 0.2% (g/g).

6.4 Conclusion

A continuous β-elimination of sugar beet pectin catalyzed by pectin lyase has been successfully performed in a membrane microbioreactor prototype under various experimental conditions of membrane molecular weight cut-off (MWCO), substrate feeding rate, *F* (µL/hr) and enzyme to substrate (i.e. pectin), *E/S* ratio. The experimental data indicated that the concentration polarization phenomenon – an effect that is typically encountered in a membrane separation system – has a strong influence on the product removal rate of the reactor system. Whilst higher enzyme load increases reaction rates, the product recovery rate is highly governed by the system flux (i.e. feeding rate). Moreover, membrane molecular weight cut-off was also found to have little or no significant impact on membrane selectivity when concentration polarization became a limiting factor for product separation. Summarizing, the results demonstrate the potential use of the membrane microbioreactor prototype as a supporting tool for assessing novel 'biorefining' type of processes e.g. enzyme-catalyzed degradation of pectin.

6.5 References

[1] Betts, J.I., and Baganz. F. (2006). Miniature bioreactors: current practices and future opportunities. *Microbial Cell Factories*. **5:** 1-14.

[2] Lee, H. L., Bocazzi, P., Ram, R. J. and Sinskey, A. J. (2006). Microbioreactor arrays with integrated mixers and fluid injectors for high throughput experimentation with pH and dissolved oxygen control. *Lab on chip*. **6:** 1229-1235

[3] Schäpper, D., Zainal Alam, M. N. H., Szita, N., Lantz, A. E., and Gernaey, K. V. (2009). Application of microbioreactors in fermentation process development: a review. *Analytical and Bioanalytical Chemistry*. **395**: 679-695.

[4] Szita, N., Bocazzi, P., Zhang, Z., Boyle, P., Sinskey, A. J. and Jensen, K. F. (2005). Development of a multiplexed microbioreactor system for high-throughput bioprocessing. *Lab on Chip*. **5:** 819-826.

[5] Delattre, C., Michaud, P., and Vijayalakshmi, M. A. (2008). New monolithic enzymatic micro-reactor for the fast production and purification of oligogalacturonides. *Chromatography*. **861:** 203-208.

[6] Kee, S., and Gavriilidis, A. (2009). Design and performance of microstructured PEEK reactor for continuous Poly-L-leucine catalysed chalcone epoxidation. *Organic Process Research and Development*. **13:** 941-951.

[7] Melander, C., Tuting, W., Bengtsson, M., Laurell, T., Mischnick, P., and Gorton, L. (2006). Hydrolysis of maltoheptaose in flow through silicon wafer microreactors containing immobilized a-amylase and glycoamylase. *Starch*. **58:** 231-242.

[8] Muller, D. H., Liauw, M. A. and Greiner, L. (2005). Microreaction technology in education: Miniaturized enzyme membrane reactor. *Chemical Engineering Technology*. **28**: 1569-1571.

[9] Swarts, J. W., Vossenberg, P., Meerman, M. H., Janssen, A. E. M. and Boom, R. M. (2008). Comparison of two-phase lipase-catalyzed esterification on micro and bench scale. *Biotechnology and Bioengineering*. **99**: 855-861.

[10] Belafi-Bako, K., Eszterle, M., Kiss, K., Nemestothy, N., and Gubicza, L. (2007). Hydrolysis of pectin by *Aspergillus niger* polygalacturonase in a membrane bioreactor. *Food Engineering*. **78:** 438-442.

[11] Gallifuoco, A., Alfani, F., Cantarella, M., and Viparelli, P. (2001). Studying enzyme-catalyzed depolymerizations in continuous reactors. *Industrial and Engineering Chemistry Research*. **40:** 5184-5190.

[12] Olano-Martin, E., Mountzouris, K. C., Gibson, G. R., and Rastall, R. A. (2001). Continuous production of pectic oligosaccharides in an enzyme membrane reactor. *Food Science*. **66:** 966-971.

[13] Rodriquez-Nogales, J. M., Ortega, N., Perez-Mateos, M., and Busto, M. D. (2008). Pectin hydrolysis in free enzyme membrane reactor: An approach to the wine and juice clarification. *Food Chemistry*. **107:** 112-119.

[14] Ovodov, Y .S. (2009). Current views on pectin substances. *Russian Journal of Bioorganic Chemistry*. **35:** 269-284.

[15] Pinelo, M., Jonsson, G., and Meyer, A. S. (2009). Membrane technology for purification of enzymatically produced oligosaccharides: Molecular and operational features affecting performance. *Separation and Purification Technology*. **70:** 1-11.

[16] Nikolic, M. V., and Mojovic, L. (2007). Hydrolysis of apple pectin by coordinated activity of pectic enzymes. *Food Chemistry*. **101:** 1-9.

[17] Yadav, S., Yadav, P.K., Yadav, D., and Yadav, K. D. S. (2009). Pectin lyase: A review. *Process Biochemistry*. **44:** 1-10.

[18] Martin-Orue, C., Henry, G., and Bouhallab, S. (1999). Tryptic hydrolysis of κ-caseinomacropeptide: Control of the enzymatic reaction in a continuous membrane reactor. *Enzyme and Microbial Technology*. **24:** 173-180.

[19] Zainal Alam, M. N. H., Pinelo, M., Samantha, K., Jonsson, G., Meyer, A., and Gernaey, K. V. (2010a). A Continuous Membrane Microbioreactor system for Development of Integrated Pectin Modification and Separation Processes. – submitted to *Chemical Engineering Journal* on the 3rd March 2010 (under review).

[20] Zainal Alam, M. N. H., Schäpper, D., and Gernaey, K. V. (2010b). Embedded resistance wire as heating element for temperature control in microbioreactors. *Journal of. Micromechanics and Microengineering.* **20:** 055014. DOI: 10.1088/0960-1317/20/5/055014.

[21] van den Broek, L. A. M., den Aantrekker, E.D., Voragen, A. G. J., Beldman, G., Vincken, J. P. (1997). Pectin lyase is a key enzyme in the maceration of potato tuber. *Science of Food and Agriculture*. **75:** 167-172.

[22] Arnous, A., and Meyer, A. S. (2008). Comparison of methods for compositional characterization of grape (*Vitis vinifera* L.) and apple (*Malus domestica*) skins. *Food and Bioproduct Processing*. 86: 79-86.

[23] Mulder, M. (1996). *Basic principles of membrane technology*. London: Kluwer Academic Publishers.

[24] Lin, Y-W., Hsiao, Y-C., and Chiang, B-H. (2009). Production of high degree polymerized chitooligosaccharides in a membrane reactor using purified chitosanase from *Bacillus cereus. Food Research International.* **42:** 1355-1361.

CHAPTER 7

Summary and perspectives

CHAPTER 7

Summary and perspectives

The focus of this project has been on the development of a continuous membrane microbioreactor system. The membrane microbioreactor prototype presented here was specifically designed to accommodate an enzyme-catalyzed modification of pectin reaction. The establishment of the continuous membrane microbioreactor system was subdivided into several development phases.

In the early stage of the development, suitable materials for microbioreactor fabrication were investigated. PMDS and PMMA polymers were chosen owing to the advantages offered by these polymers (as reviewed in *Chapter 2*). The use of PMMA and PDMS as substrates for fabrication reduces time, cost and complexity for prototyping. PDMS and PMMA substrates are relatively cheap and fabrication can be done via micro-milling and casting fabrication methods, thus avoiding the need to access any specialized facilities e.g. a clean room facility. Due to the relatively inexpensive and rather straightforward fabrication method (i.e. micro-milling and casting), re-designing and fabrication of a new microbioreactor prototype (if at all necessary) is achievable in a very short period of time. This is indeed advantageous because development of such a microbioreactor prototype is an iterative process, where a series of refinements or adjustments of the prototype are often needed until the final design aim is achieved.

In the subsequent phase, a suitable temperature control method for microbioreactor systems was developed (*Chapter 3*). We utilized a miniaturized Pt 100 (5 x 2 x 1.3 mm) temperature sensor and embedded a resistance wire into the PDMS polymer which serves as the reactor heating element. Only a heating element is required to regulate the microbioreactor temperature as cooling is achieved by taking advantage of the heat losses to the surroundings by natural convection. Alternatively, it would also be feasible to mount a Peltier element or to install a very small mechanical fan as a cooling element on the prototype, for example at the base of the reactor. Such a cooling element on chip enables cooling down of the reactor content in a very short time (seconds, due to a significantly increased cooling rate capacity of the reactor). It is however completely unnecessary in our applications because at this reduced scale of operation (i.e. the reactor is not thermally insulated), the high surface to working volume ratio, *S/V* leads to significant and inevitable heat loss and thus provides sufficient cooling needed for the process as long as the reactor temperature is above the temperature of the surroundings. Furthermore, including an additional cooling element on chip may result in a more complex and costly prototype. Therefore, it was decided early on in the project that only a heating element would be installed. A resistance wire was chosen as the heating element as it is cheap and can be conveniently embedded into PDMS substrates. A simple and cheap temperature control system is imperative in order to keep the final fabrication cost of the reactor low. An inexpensive reactor could then be made disposable – thus saving time and reducing

microbioreactor preparation steps during the start up of an experiment. Positioning of the resistance wires together with a sufficient mixing guaranteed a uniform heat distribution in the reaction chamber. By coupling the embedded resistance wires with a simple on/off controller, a tight temperature control method (i.e. accuracy $\pm$ 0.2°C) was successfully established.

In the third phase of the development, a gaseous pH control strategy was established (*Chapter 4*). pH measurement was achieved by an optical measurement with the use of fluorescence sensor spots or pH 'optodes', and was controlled via the dosing of either pure CO_2 gas or an NH_3 (20 000 ppm) – N_2 gas mixture to respectively decrease and increase the pH of the reactor content. Here, the control loop algorithm and devices implemented for the temperature control were to a large extent reused – with only minor modifications – to establish a feedback pH control loop. PDMS properties were exploited to create a thin (~100 µm thickness) semi-permeable membrane (i.e. adhered on the ceiling of the reaction chamber) for diffusion of gases for pH control, thus keeping the reactor contents under bubble free conditions. The gaseous pH control capability was evaluated and its performance was found to be satisfactory (i.e. accuracy $\pm$ 0.1 pH units of pH_{sp} and system responses to change pH set point were in the order of minutes). Implementation and especially the practical usefulness of the pH control system, however, were hampered by the limited dynamic measurement range of the pH 'optode' used. The optimal pH range for the targeted application is between pH 4 and 5, which corresponds to the range where the pH optodes are rather insensitive. This makes pH control very difficult and inaccurate for the specific reaction studied (enzyme-catalyzed modification of pectin). The results clearly indicated that there is a need for an optical sensor spot that has a wider sensing range, preferably in the low pH range (pH 4 to 5, but also lower values). The limited measurement range is considered as one of the main limitations of the pH optodes for application in enzyme-catalyzed reactions as well as fermentation. An alternative solution was to utilize the ISFET pH sensor chip. However, pursuing this solution would require us to re-design most of the individual reactor components e.g. different mixing scheme, alter the membrane separation design, etc – which may increase the complexity of the reactor design. The use of ISFET technology also requires a reference electrode. When using such a reference electrode – which is relatively expensive – the idea of a disposable microbioreactor no longer holds. Since integrating the ISFET pH sensor chip into the microbioreactor system seemed to only impose complications rather than providing a simple solution, this implementation was given up.

In the last phase of the development, the membrane microbioreactor prototype design was finalized (*Chapter 5*). A loop reactor system was realized to operate in *cross flow* filtration mode, and was equipped with the necessary sensors and actuators (i.e. temperature control, and pressure transducer) and equipped with active mixing schemes (i.e. magnetically actuated stirrer bar combined with high velocity recirculation flow) to provide homogeneous mixing and a uniform heat distribution. The prototype has a relatively low complexity (i.e. minimal number of internal microfluidic inlet/outlet channels), which results in rather straightforward fabrication steps. The *clamp'n'play* reactor configuration and the *plug'n'play* fluidics interconnects design result in a modular prototype that is easy to use. Operation wise, integration of the multi-ports valve in the feed line proofed to be very useful. It prevents gas bubble formation when re-distributing different feeding solutions and allows the reactor to operate in semi-continuous mode – an alternating substrate-buffer feeding strategy – to facilitate a high product removal rate. Standardizing the reactor operating procedure (i.e. reactor assembly, enzyme loading, and

substrate feeding) was found to be a crucial step for a successful microbioreactor experiment. It ensures the least variation in initial reaction conditions and ensures an error-free operation (i.e. no bubbles formation, leak-proof, etc.). All of those elements are to be kept in mind, since they may to a certain extent affect the quality of the end results.

It was verified that the membrane microbioreactor prototype – in its current state – fulfilled all the basic requirements needed to facilitate the enzyme-catalyzed modification of pectin reaction (*Chapter 5 and Chapter 6*). It was demonstrated that the prototype is capable of running series of continuous pectin modification and separation experiments under well-controlled conditions (e.g. tight temperature control, good mixing, constant permeate flux, etc.). In addition, it was shown that conditions applied in micro-scale operation can be reproduced in a bench scale membrane reactor system (*Chapter 5*). This is a very important result since it proofs that results obtained at micro-scale are scalable, i.e. results at micro-scale can be extrapolated to larger scales of operation, for example to predict the effect of operational variables on the achieved process performance.

Already in the membrane microbioreactor prototype presented here, some technical problems – encountered during the development phase of the various reactor subcomponents – have been addressed and solved whilst some may still require future modifications. The following recommendations can be made for further improvement of the reactor design:

- Development of pH optodes that have a wider sensing range particularly at the mildly acidic pH region (pH 4-5).
- Construction of onboard micropumps as substitutes for the large – compared to the size of the prototype which has a characteristic footprint of 35 mm (length) x 20 mm (width) – and expensive syringe and recycle pumps used thus far. Onboard micropumps are also an elegant solution if one would pursue the multiplexing of the microbioreactor system to operate multiple reactors in parallel.
- Interface the permeate stream with a microfluidic detection chip to facilitate *on-line* measurement (e.g. UV absorption, Near infrared (NIR), Raman spectroscopy, etc.) of the product concentration. In the current design, samples were taken intermittently (e.g. every 1 to 2 hours) from the permeate stream such that the progress of the experiment performed in the prototype can be monitored continuously. This is a relatively simple solution, but in practice it can be very laborious and demanding for a lengthy reactor operation. If a microfluidic detection chip can be installed; it will eliminate the need for sampling and in principle a fully automated system (i.e. no human intervention during reactor operation) can be established. This is indeed an important feature if the prototype is to make its way to industrial applications and could be used for parallel reactor operation as well.
- With all the above-mentioned reactor subcomponents modified and in place, it is then worth to put a serious thought on parallel reactor operation. This is indeed a very challenging task as fluidic handling (e.g. feeding strategy), and local reactor monitoring and control become increasingly complex when the number of microbioreactors increases from one to many units.

Summarizing, in this thesis a continuous membrane microbioreactor prototype is presented, and it is demonstrated how this technology can be exploited to operate and study enzyme-catalyzed modification of pectin processes. The development of the prototype also encompassed establishment of feasible temperature and pH control

strategies for the reactor as they are key operational variables when running enzymatic reactions. The research objectives have been met, and the hypotheses formulated for the work have been confirmed as well. Indeed, the prototype presented here works fine in a laboratory environment and can readily be deployed as supporting tool for industrially relevant studies. Nevertheless, the prototype can still be improved as previously suggested to keep pushing the technology until satisfactory industrial standards are met. It is also important to emphasize here that employment of microbioreactors is not to completely replace current lab-scale reactor technology, but merely offers an alternative way to study this kind of processes at micro-scale with reduced consumption of enzyme.

APPENDIX A

Membrane microbioreactor: Mechanical drawings

Drawing A.1: Membrane microbioreactor prototype - top PMMA layer

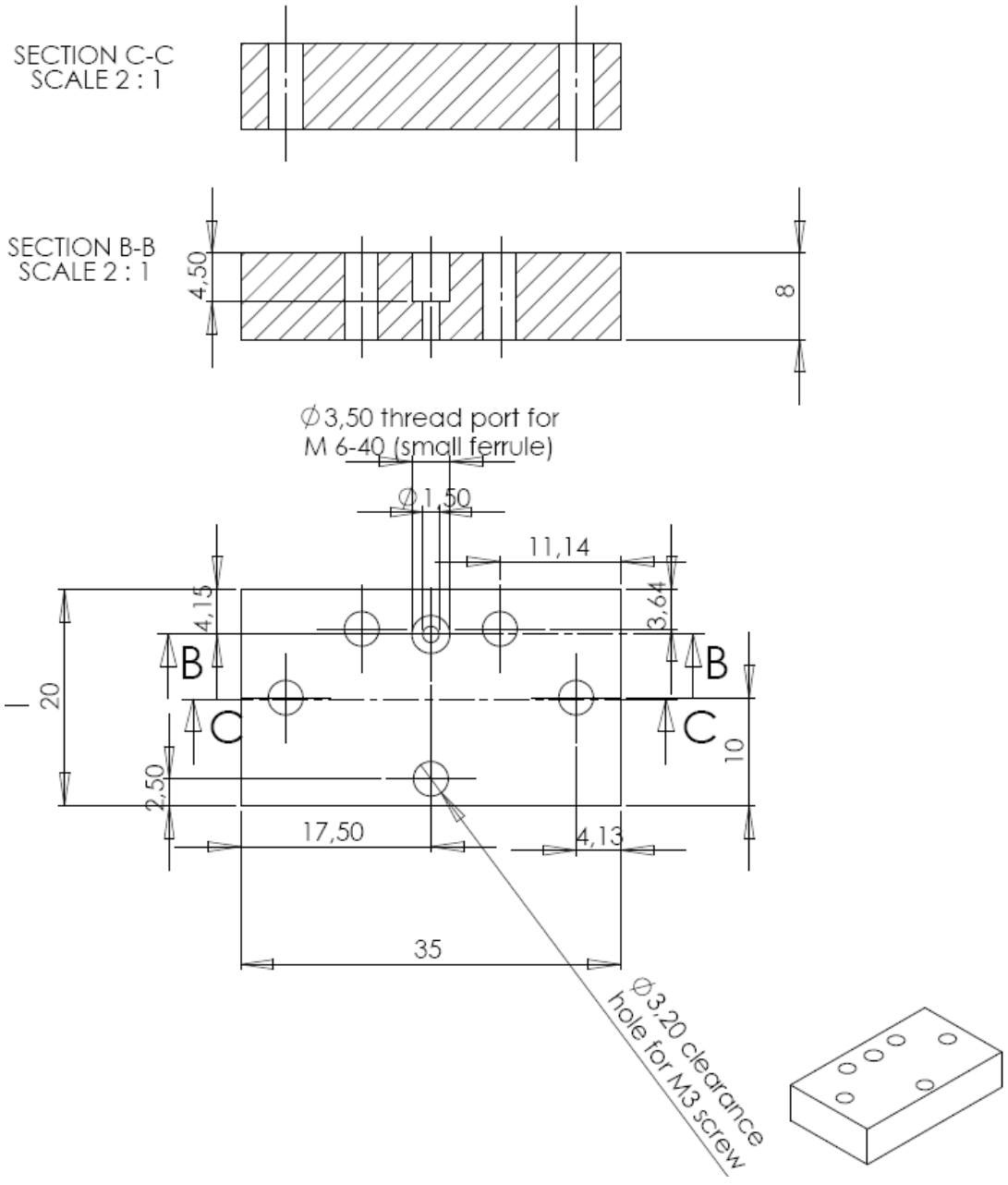

Drawing A.2: Membrane microbioreactor prototype - middle PDMS layer

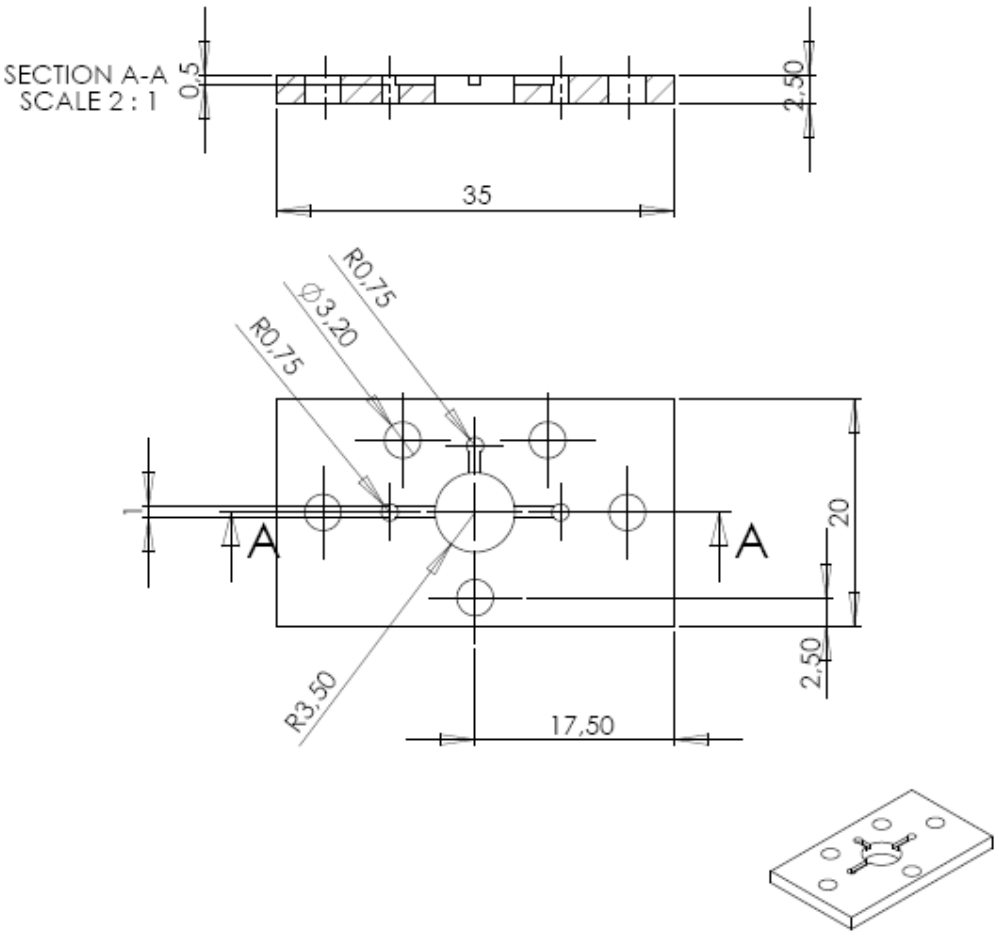

Drawing A.3: Membrane microbioreactor prototype - bottom PMMA layer

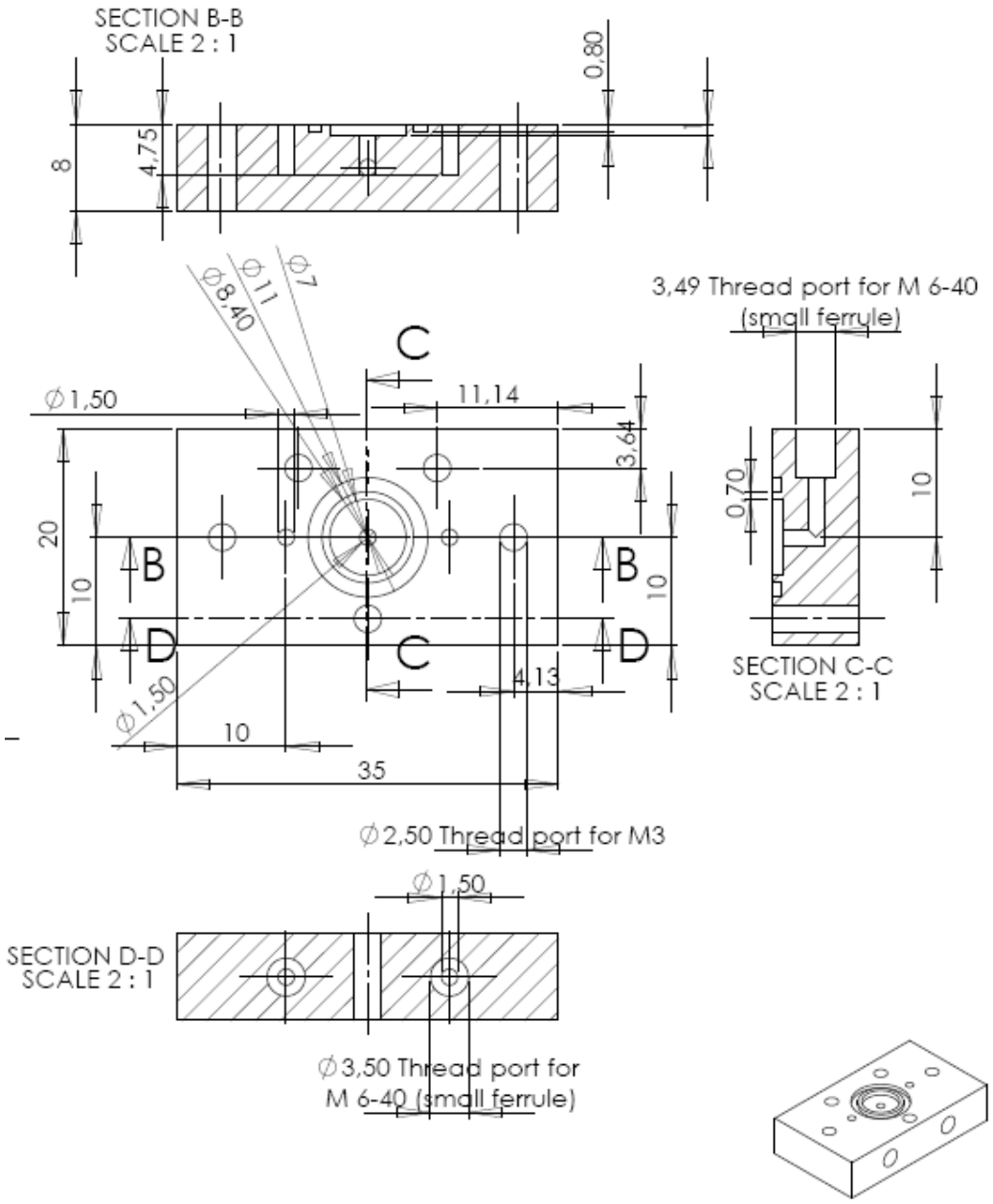

APPENDIX B

LabView program

Temperature control loop front panel

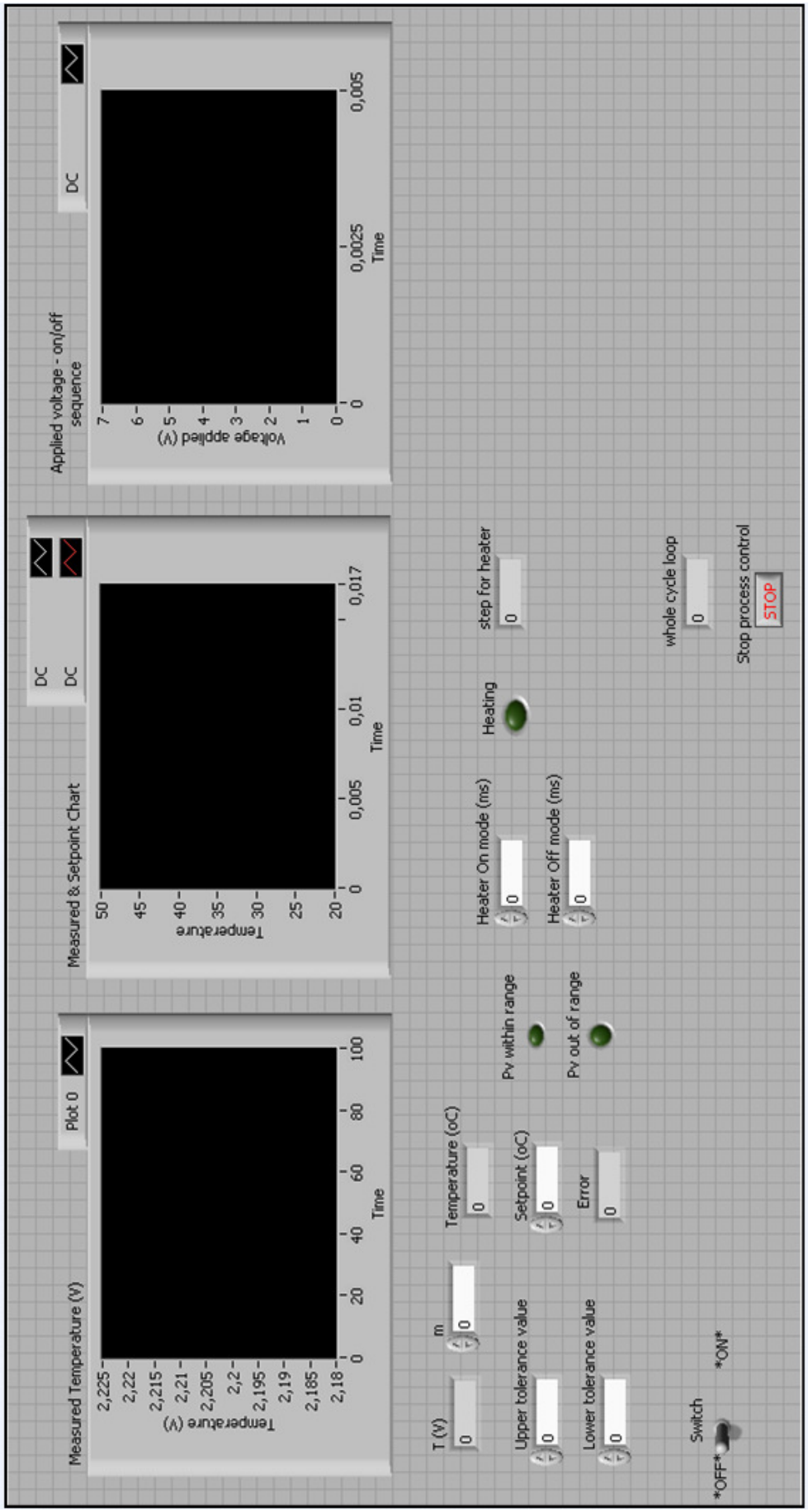

LabView programming B.1: Temperature control loop block diagram

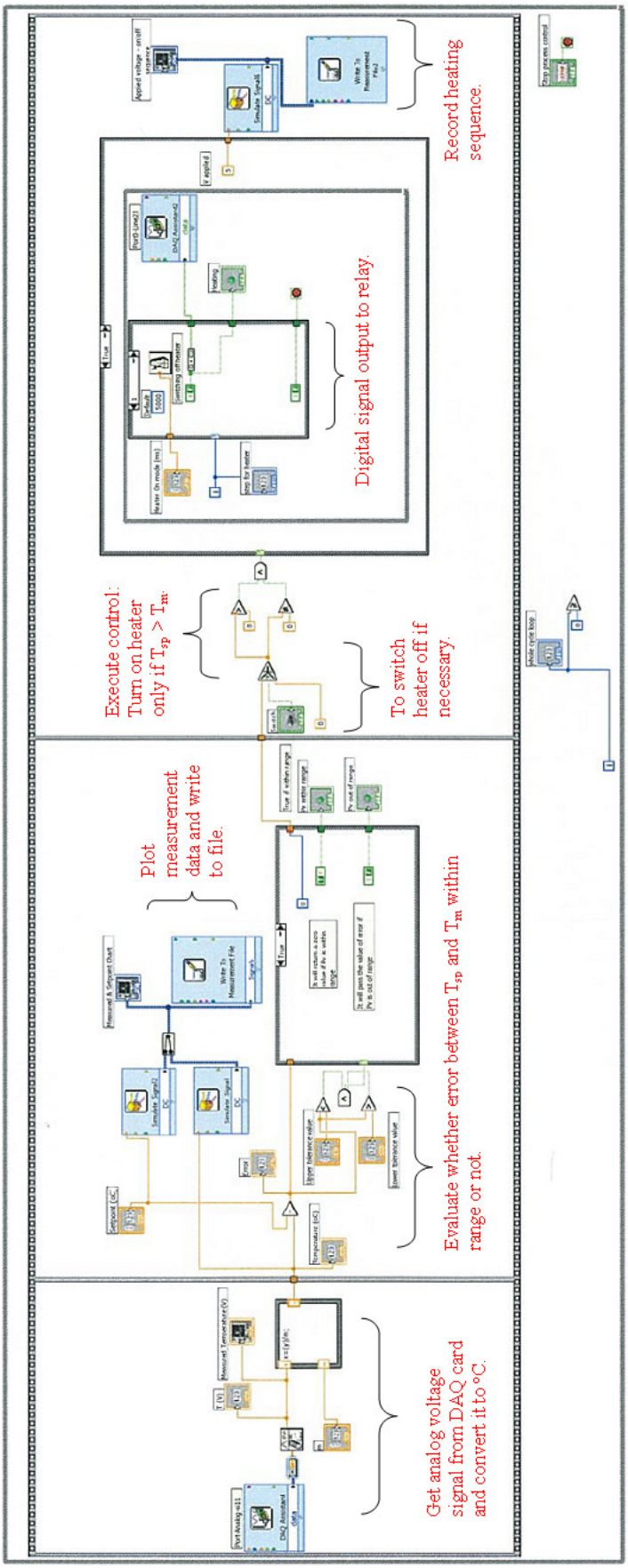

True/false statement – Evaluate whether error between T_{sp} and T_m within range or not.

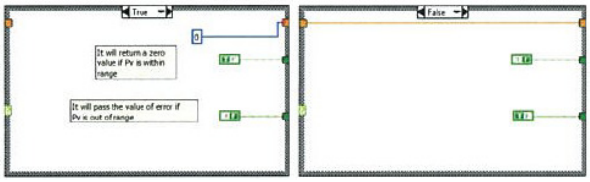

True/false statement – to turn on heater only and only if $T_{sp} > T_m$.

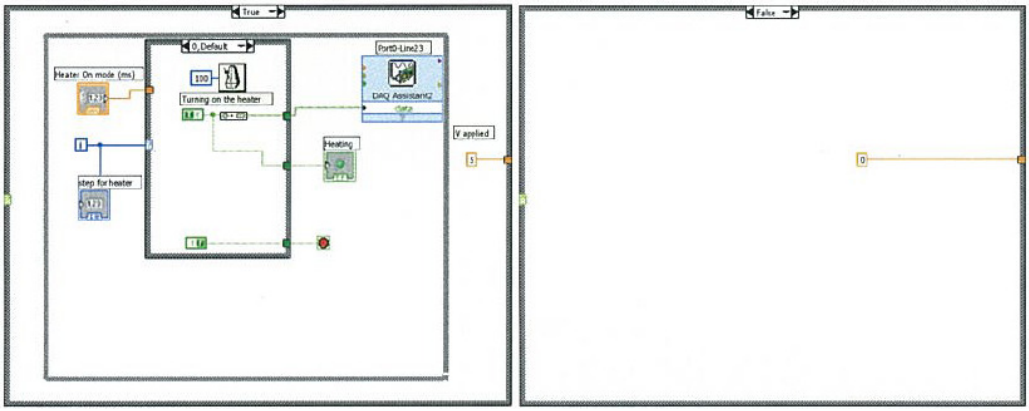

Case structure – heating pulse sequence.

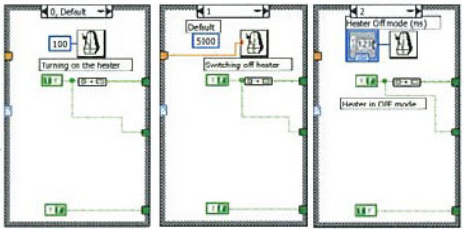

Pressure measurement loop front panel

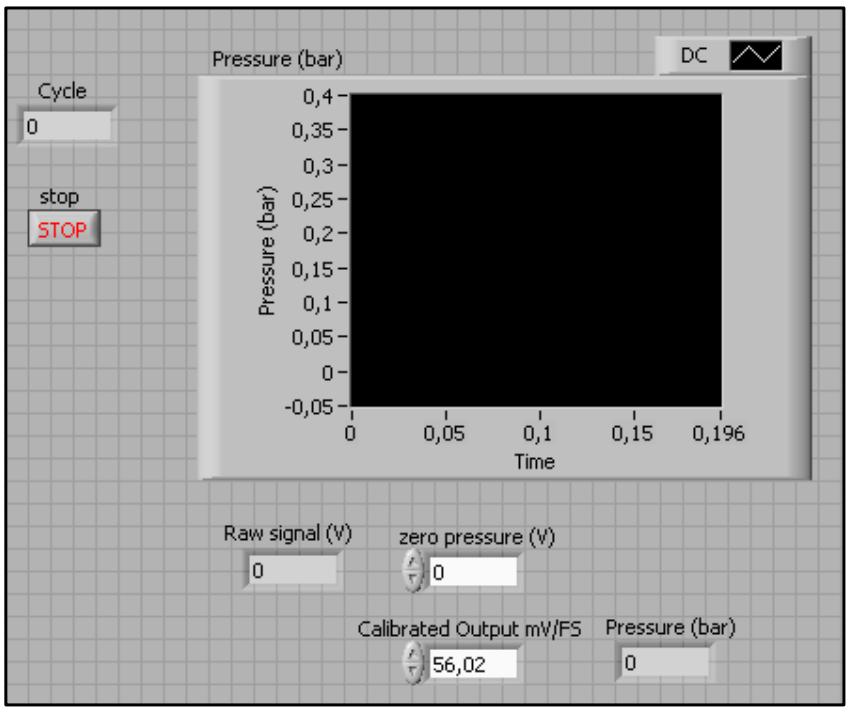

LabView programming B.2: Pressure measurement loop

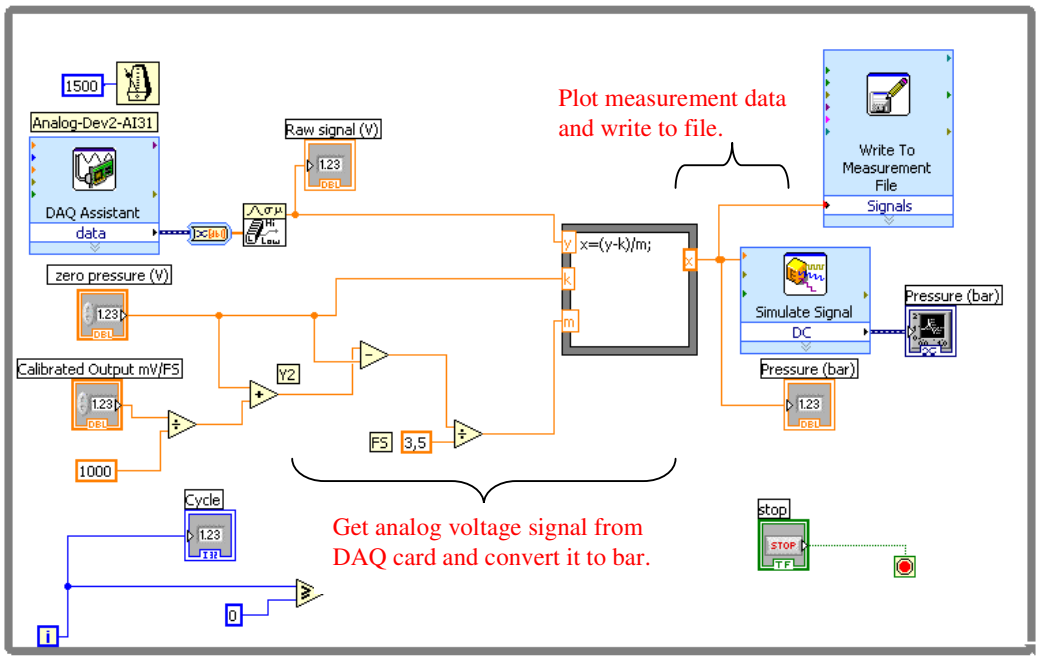

pH control loop front panel

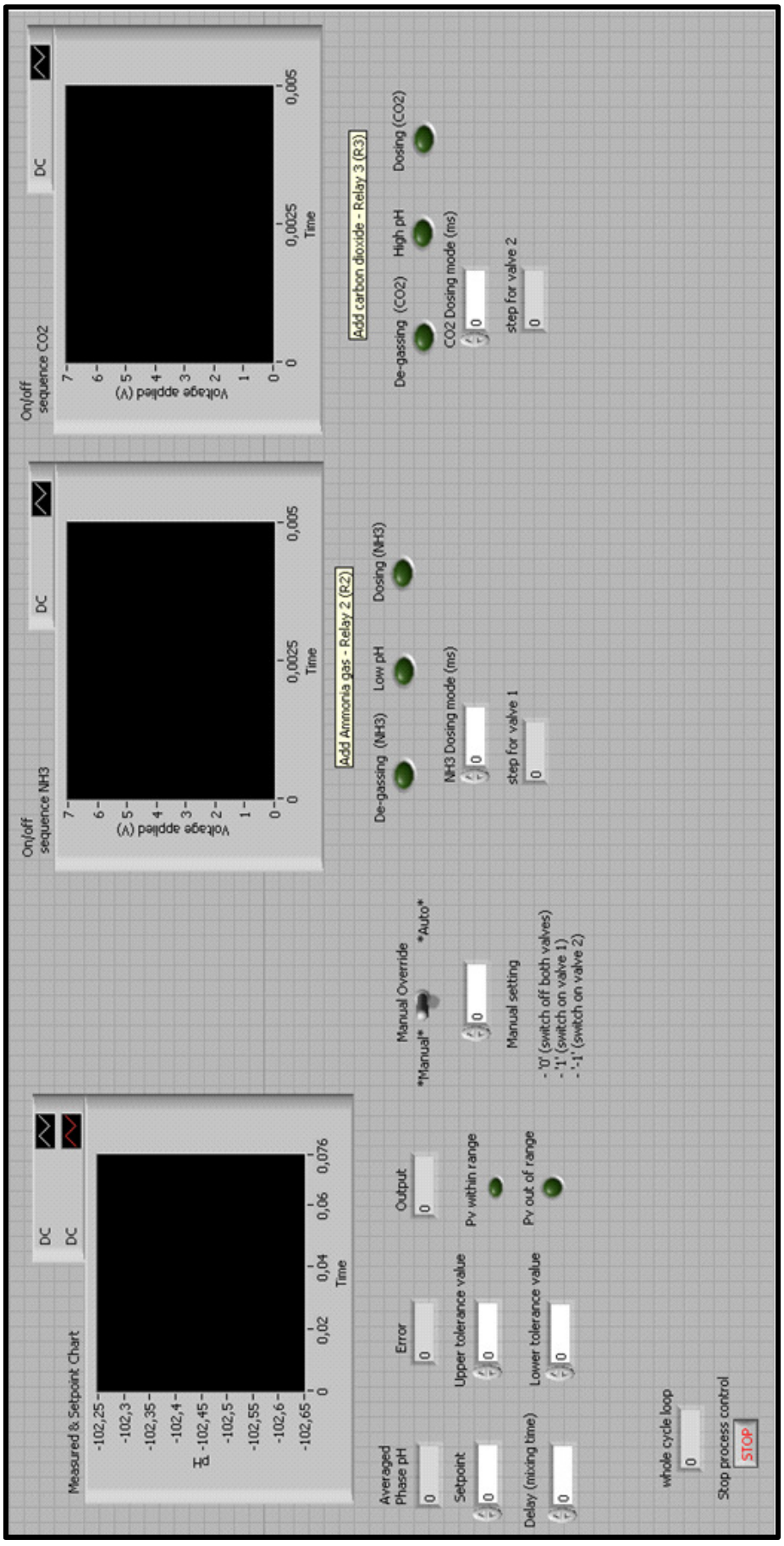

LabView programming B.3: pH measurement block diagram

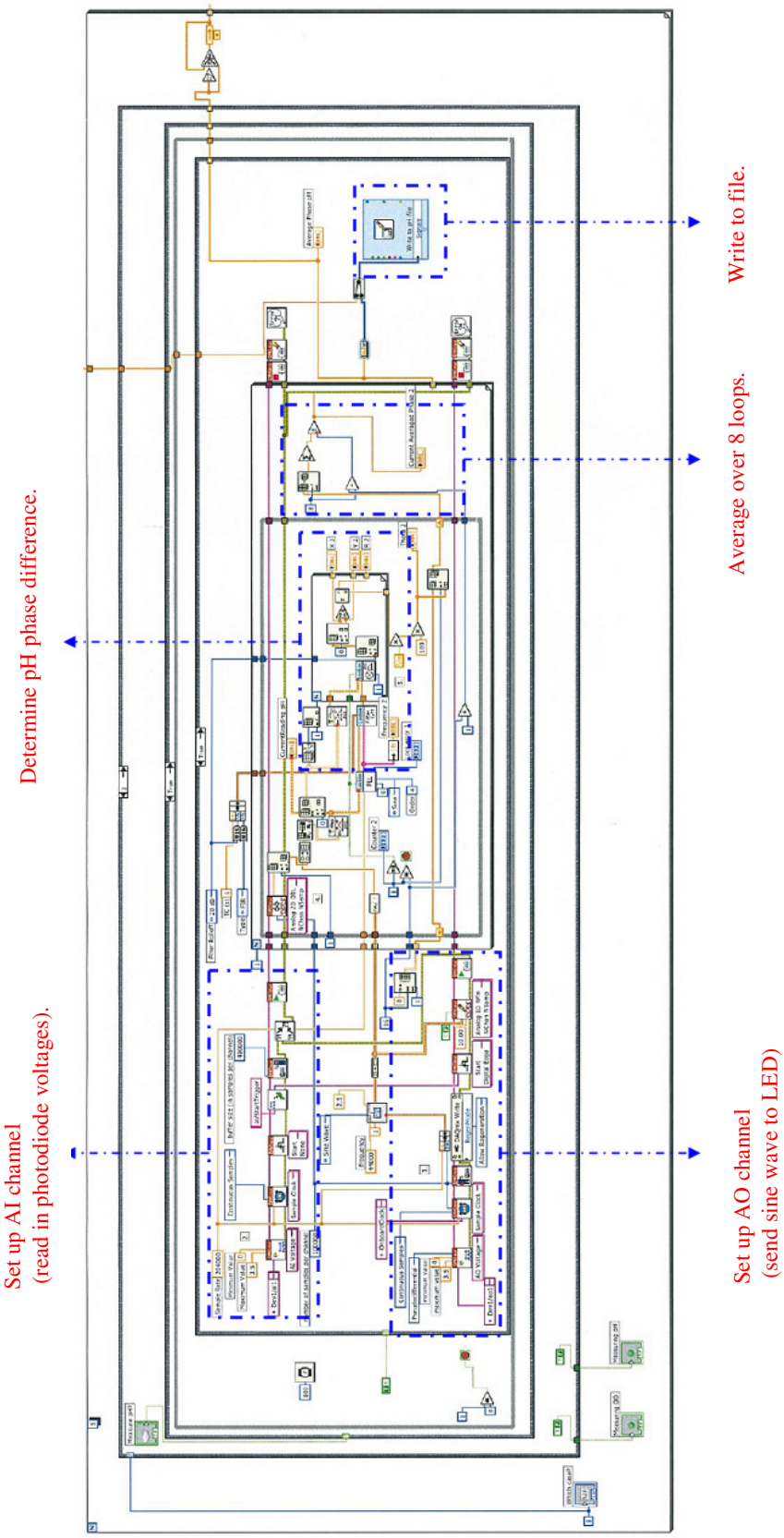

LabView programming B.4: pH control loop block diagram

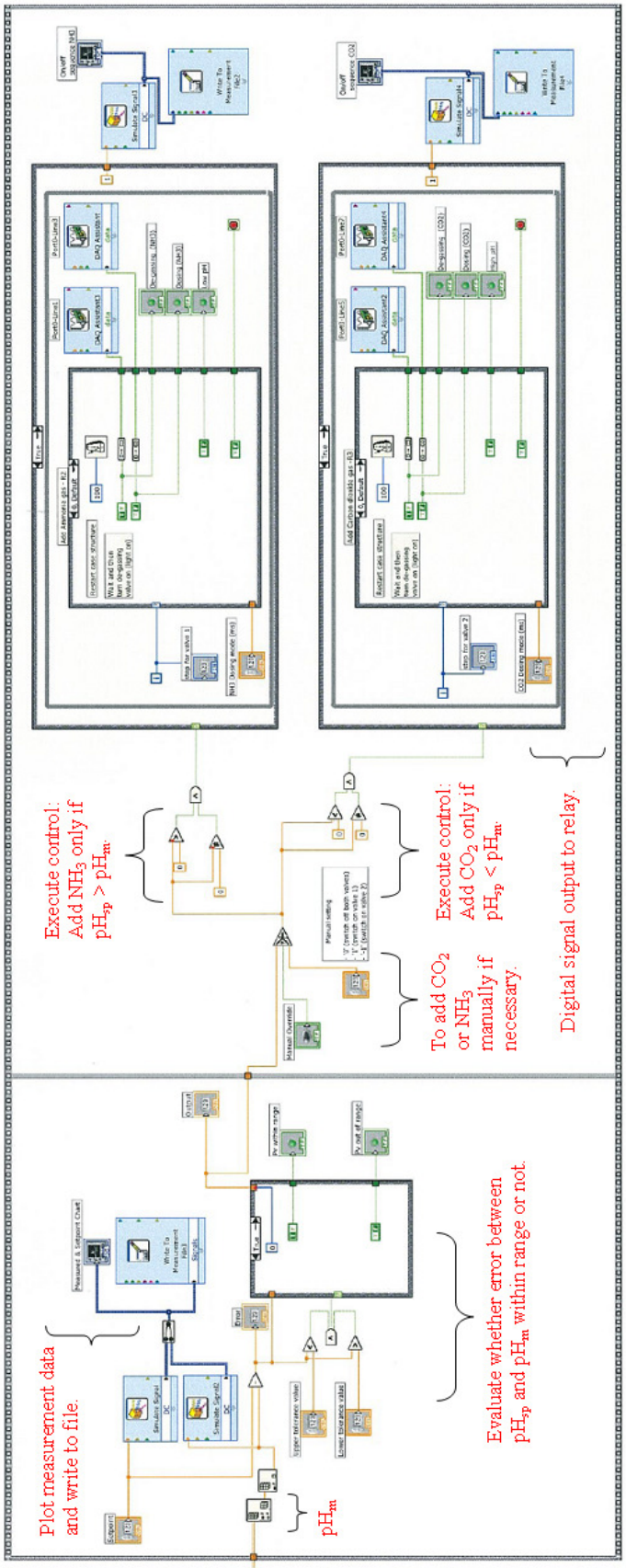

pH control main loop block diagram.

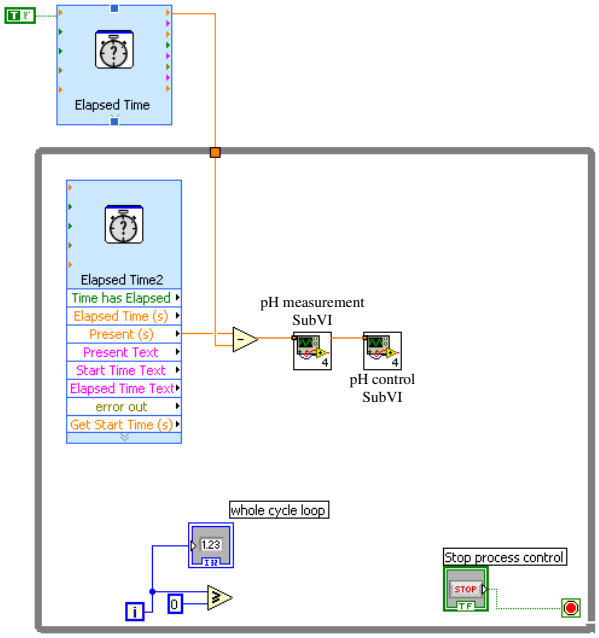

True/false statement – Evaluate whether error between pH_{sp} and pH_m within range or not.

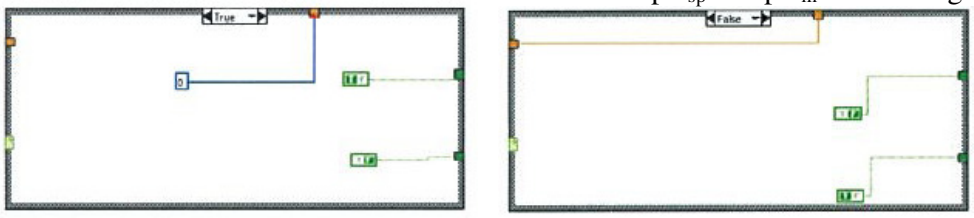

Case structure – De-pressurizing and gas (CO_2/NH_3) addition sequence.

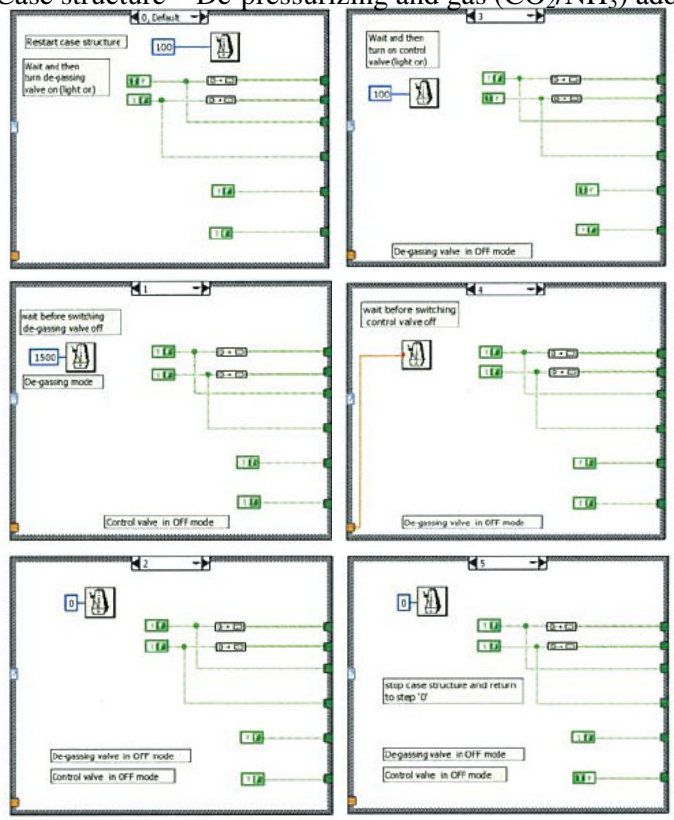

www.kt.dtu.dk

Center for Process Engineering and Technology (PROCESS)
Department of Chemical and Biochemical Engineering
Technical University of Denmark
Søltofts Plads, building 229
DK-2800 Kgs. Lyngby
Denmark

Tel: (+45) 45 25 35 00
Fax: (+45) 45 93 29 06
Email: kt@kt.dtu.dk